Design and development of a composite ventral fin for a light aircraft

JL Pieterse

26624966

Dissertation submitted in fulfilment of the requirements for the degree *Magister* in Mechanical Engineering at the Potchefstroom Campus of the North-West University

Supervisor: Dr J van Rensburg

April 2015

DECLARATION

I, Justin Lee Pieterse, hereby declare that the work contained in this dissertation was produced by myself and is my own, original and unaided work. Some of the information contained in this dissertation has been gained from various journal articles; text books etc, and has been referenced accordingly. The word herein has not been submitted for a degree at another university.

_____

Author: Justin Lee Pieterse

ABSTRACT

The AHRLAC aircraft is a high performance light aircraft that is developed and manufactured in South Africa by Aerosud ITC in partnership with Paramount. This aircraft is the first of its kind to originate from South Africa. The aircraft has a twin boom, tandem pilot seating configuration, with a Pratt and Whitney turbine-propeller engine in a pusher configuration. The main structure of the aircraft is a conventional metallic structure, while the fairings and some secondary structures are composite.

This study will focus on the design and development of the composite ventral fin of the first prototype aircraft, the experimental demonstrator model (XDM). It is crucial to ensure that the ventral fin can function safely within the design requirements of the aircraft under the loads which the fin is likely to encounter. Preceding the design process, a critical overview of composite materials used in aircraft applications is provided. This will include the materials, manufacturing methods, analysis and similar work done in this field of study. The literature will be used in the study for decision-making and validation of proven concepts and methodologies.

The first part of this study entailed choosing a suitable composite material and manufacturing method for this specific application. The manufacturing method and materials used had to suit the aircraft prototype application. The limitations of using composite materials were researched as to recognize bad practice and limit design flaws on the ventral fin.

Once the material and manufacturing methods were chosen, ventral fin concepts were evaluated using computer aided finite element analysis (FEA) with mass, stiffness and strength being the main parameters of concern. The load cases used in this evaluation were given by the lead structural engineer and aerodynamicist. The calculations of these loads are not covered in detail in this study. The FEA input material properties used, were determined by material testing by the relevant test methods. The ventral fin concept started as the minimal design with the lowest mass. The deflections, composite failure and fastener failure were then evaluated against the required values. The concept was modified by adding stiffening elements, such as ribs and spars, until satisfactory results were obtained. In this way a minimal mass component is designed and verified that it can adequately perform its designed tasks under the expected load conditions. Each part used in the ventral fin assembly was not individually optimized for mass, but rather the assembly as a whole.

The final concept was modelled using the computer aided design software, CATIA. This model used in combination with a ply book made it possible to manufacture the ventral fin in a repeatable manner. A test ventral fin was manufactured using the selected materials and manufacturing methods to validate the design methodology. In the next step the selected load cases were used in static testing to validate the FEM through comparison.

The result of the study is a composite ventral fin of which the mass, stiffness and strength are suitable to perform its function safely on the first prototype AHRLAC aircraft. The study concludes on the process followed from material selection to FEA and detail design, in order for this same method to be used on other AHRLAC XDM composite parts.

KEYWORDS

Aerospace

Aircraft

CFRTS

Composite

Design

Epoxy

Finite element analysis

Glass fibre

Manufacture

Nastran

Patran

Static testing

ACKNOWLEDGEMENTS

TABLE OF CONTENTS

1   Introduction

2   Aerospace composites overview

Appendices

LIST OF FIGURES

LIST OF TABLES

LIST OF ABBREVIATIONS

ADM	Advanced Demonstrator Model
AHRLAC	Advanced High Performance Reconnaissance Light Aircraft
ASTM	American Society for Testing and Materials
CFD	Computational Fluid Dynamics
CFRTP	Continuous Fibre Reinforced Thermoplastic
CFRTS	Continuous Fibre Reinforced Thermoset
CNC	Computer Numerical Control
CSM	Chop Strand Mat
FEA	Finite Element Analysis
FEM	Finite Element Model
FS	Factor of Safety
GMT	Glass Mat Thermoplastics
HM	High Modulus
HS	High Strength
IM	Intermediate Modulus
MIL-SDT	A United States defence standard
nm	nautical mile
OML	Outside Mould Line
P/T	Pressure/Temperature
RTM	Resin Transfer Moulding
SM	Standard Modulus
SMC	Sheet Moulding Compounds
SRIM	Structural Reaction Injection Moulding
UAV	Unmanned Aerial Vehicle
UD	Unidirectional
XDM	Experimental Demonstrator Model

1 INTRODUCTION

1.1 BACKGROUND

There is a current and actual need for the development of new aircraft worldwide with the application of new technologies, such as lightweight composite structures [1]. The use of these new materials and technologies can minimize weight, increase performance and therefore reduce the carbon footprint of an aircraft. Since the development of the Rooivalk (Figure 1-1) attack helicopter by Denel in the 1980s, the knowledge learnt during this development had a real chance of getting lost with the new generation of South African engineers [2]. While successful aircraft production is characterized by returns from learning [3], the need existed to retain this knowledge.

Figure 1-1: The Denel Rooivalk attack helicopter

Aerosud is an aeronautical engineering company started in 1994 by some of the managing engineers involved in the Rooivalk's development. This company grew from small aircraft modification projects to a large quantity supplier of parts and assemblies to two of the biggest aircraft manufactures; namely Boeing and Airbus. Aerosud saw the need to retain the design engineering capability gained from the Rooivalk project and transfer it to the new generation of South African engineers. They started the research and development company named Aerosud Innovation and Training Centre (ITC) to do exactly this.

Aerosud ITC teamed up with Paramount and identified the need for a low-cost, rugged, two seat aircraft that can be used in Africa's harsh environment for peacetime patrol and pilot training and that can respond to threats in real time. This would be the platform for the transfer of aircraft design capability to the new generation engineers. The growing market for unmanned aerial vehicles (UAV's) has shown the need for a low-cost alternative to high-end military aircraft and helicopters, but the UAV's have high operation and resource cost which a low-cost aircraft would not have.

The aircraft resulting from Aerosud ITC's research and development project was named Advanced High Performance Reconnaissance Light Aircraft (AHRLAC). AHRLAC is a rugged, low-cost and high performance design (Figure 1-2). The aircraft is adapted for rough field landing and low-cost usage in harsh environments with minimal ground support. The AHRLAC was designed to meet the current military and commercial specifications to be able to certify the aircraft with international authorities.

Figure 1-2: AHRLAC concept rendering

AHRLAC's main structure was made mainly from the latest aerospace aluminium alloys to add to its off field repair capability. All double curvature parts and some inessential load bearing parts were made from composite materials in order to reduce weight and due to the increased forming potential of composite manufacturing techniques. See Table 1 for the initial AHRLAC specifications.

Seats	2 in tandem with optional Martin Baker ejection seats
Max take-off weight	3800 kg
Payload with full fuel	800 kg
Take-off distance	550 m with full payload
Powerplant	Pratt and Whitney PT6a-66 950 hp flat rated
Max speed	>503 km/hr
Range	>1100 nm
Wing span	12 m
Length	10.5 m
Height	4 m
Service ceiling	9448 m
Max endurance	7.5 hr

Table 1: AHRLAC specifications

1.2 MOTIVATION FOR THE STUDY

There are three main parameters of concern on any aircraft structure; weight, stiffness and strength. Every aircraft component has a specific requirement with regards to the values of these three attributes. If these attributes are incorrectly proportioned on parts or assemblies, it may have negative effects, like undesired impacts on performance of the aircraft, or, in extreme circumstances, lead to catastrophic failure. Therefore, every part or assembly on the aircraft has to have properly proportioned values of these attributes in order to avoid any negative effects on the required performance. This will ensure that the aircraft is as close as possible to the desired specifications. It is the engineer's responsibility to ensure that these three parameters are adequate; ensuring that the aircraft can function in a safe manner during its intended service life. In addition to these three main parameters, there are others that could be important to the engineer such as cost, aesthetics and other factors that are component function specific.

Since the 1970s, composites started being used in numerous applications on secondary aircraft structures such as doors, rudders, spoilers and fairings [4]. Today on almost all aircraft, composites are used on some secondary structure somewhere on the aircraft. Composite parts and assemblies have in recent years grown in use in military and civilian aircraft construction; this can be seen as the green trend line in Figure 1-3. In the 1980s, the use of composites on aircraft, such as Boeing's 767 and the F-16A, comprised of less than 10 % of their total mass; this grew to in excess of 50 % in 2010 on aircraft like the Airbus A350 and Learjet 85. The complex curvature formability, the ability to tailor material properties, its improved fatigue and improved corrosion resistance are some of the major advantages of using composite materials.
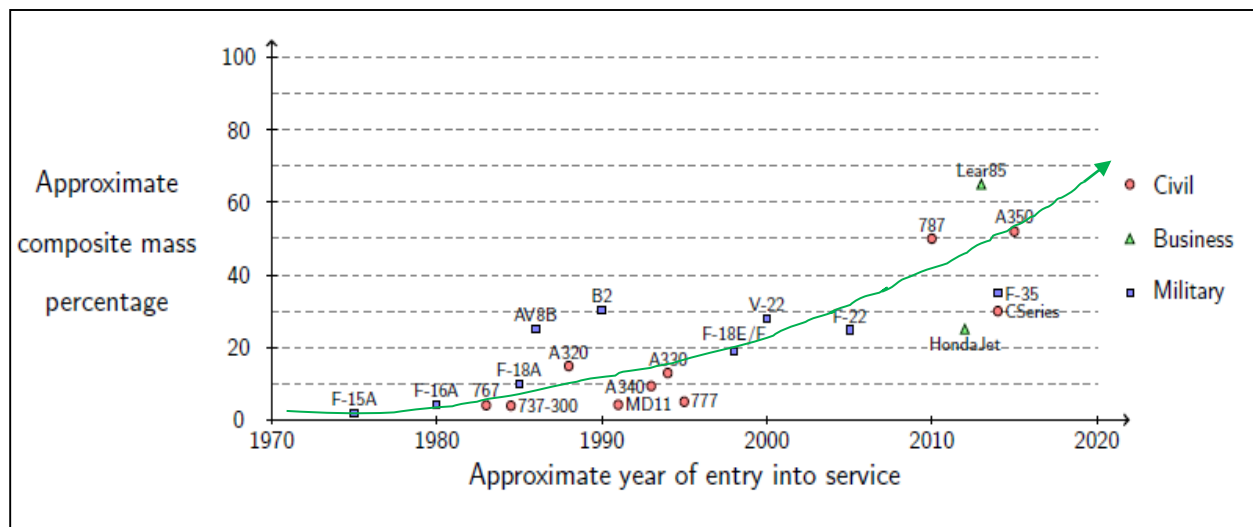
Figure 1-3: Composite material weights of civil, business and military aircraft [5]

Each composite part's stiffness and strength properties can be optimized by varying the number of layers, layer sequencing, fibre direction and materials used in the laminate. This gives the designer much more freedom than conventional metallics and can be very effective in increasing component performance [6]. This optimization requires a thorough understanding of composite materials. The composite design process can be more intensive than their metallic counterparts due to its anisotropic material properties and the large influence the manufacturing process can have on the component properties [4]. In addition, the manufacturing method becomes much more integrated in the development cycle than with metallic structures, as a result of the large influence on part performance. The responsibility of the material properties' definitions has shifted from the material supplier to the manufacturer of parts or assemblies, due to the large influence that the processing, manufacturing methods and ambient conditions have on them [7]. The material supplier can give useful estimate properties, but the final material properties have to be verified by testing as to take full advantage of the composite material's benefits.

There is a need in the development of AHRLAC to design and manufacture composite parts with adequate proportions of mass, stiffness and strength within the resources allocated to the prototype aircraft. This method of design, analysis and testing should be used through AHRLAC's developmental cycle on most other composite structures. Later in the optimization phase of the development, this method can be refined to increase overall performance and efficiency of the composite components. For this study, the ventral fin of AHRLAC's first prototype model (XDM) will be used as the design case.

The vertical stabilizer of an aircraft has two primary functions: the first is to ensure directional stability of the aircraft and the second is the directional control of the aircraft (Figure 1-4). There are two main parameters influencing the directional stability of an aircraft; they are the vertical tail area and vertical tail moment arm. An increase in any of these two parameters will lead to an increase in directional stability of the aircraft. The rudder attaches to and forms part of the vertical stabilizer. The main function of the rudder is the directional control of the aircraft.

Consequently, there exists a combination of vertical stabilizer area and moment arm that would lead to a statically unstable aircraft. The AHRLAC XDM is a conventional linkage controlled aircraft, meaning there are no computerized control feedback systems that keep the aircraft stable, the stability has to be incorporated in the aerodynamic design of the aircraft. The aircraft has to remain statically stable in order to be safe and flyable.

The moment arm of the vertical stabilizer can only be increased up to such a point before it becomes impractical. This is due to the fact that the aircraft has to rotate about its main wheels on takeoff and the rotation has to be enough so that the wing produces sufficient lift to overcome the mass. This angle is limited by the moment arm of the vertical and horizontal stabilizers. On AHRLAC this resulted in the maximum moment arm being defined by the landing gear and wing configuration. To ensure static directional stability, the vertical stabilizer had to have a minimum specified area.
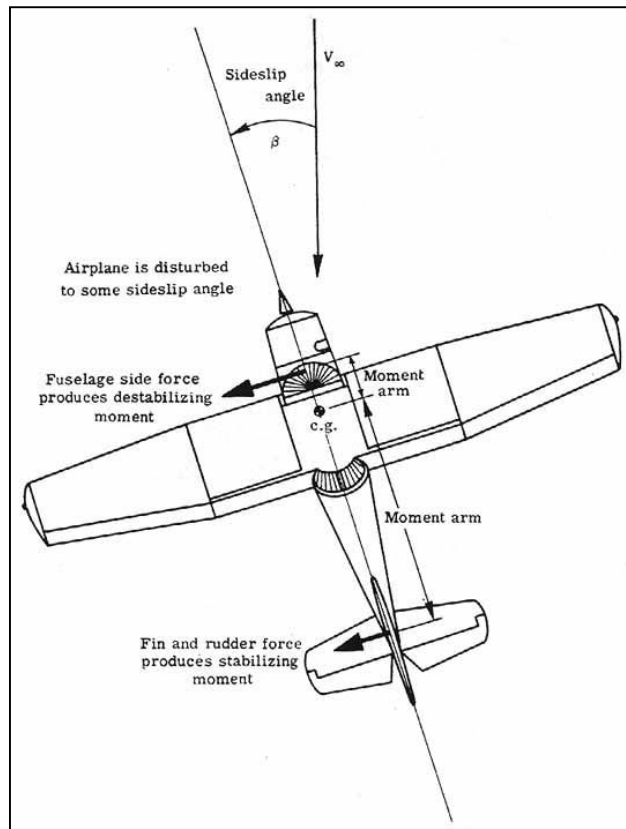
Figure 1-4: Vertical stabilizer and rudder of a conventional aircraft [8]

The ventral fin is a lower extension of the vertical stabilizer and its function is to add area to the vertical stabilizer, without increasing the main stabilizer's cantilever length. In short, the ventral fin increases the area without losing stiffness and strength of the vertical stabilizer. Similar aircraft ventral fins are shown in Figure 1-5.
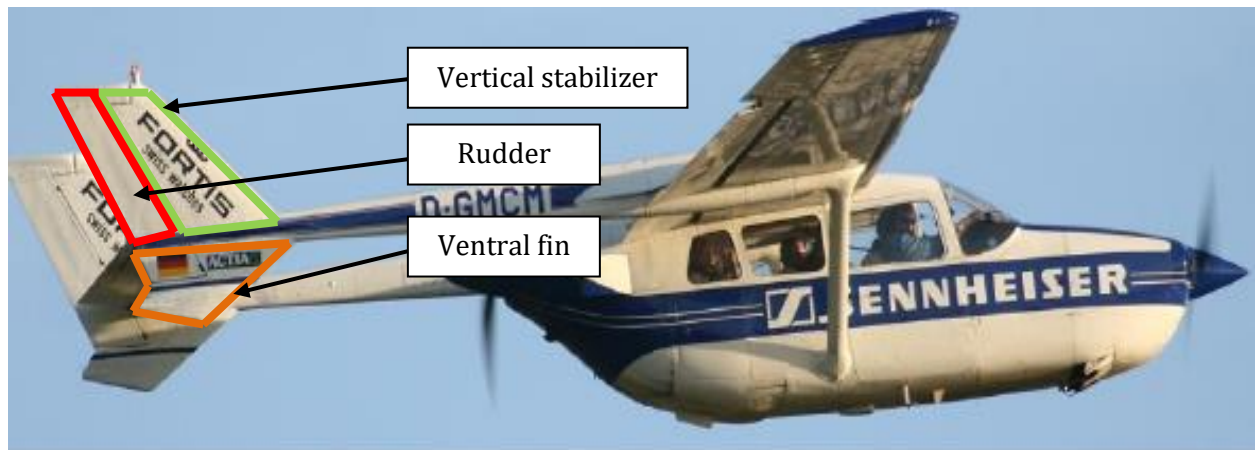
Figure 1-5: Ventral fins on a F337F Super Skymaster

In AHRLAC, the ventral fin was incorporated into the concept and final design for three main reasons. The first reason is the increase of directional stability without increasing the cantilever length of the vertical stabilizers. The second reason is that it acts as a sacrificial component that protects the structure, such as the tail booms and vertical stabilizers, in the event of over rotation during takeoff. Should over rotation occur during takeoff, the ventral fins will scrape the runway and be damaged, but the rudders and the main vertical stabilizes will still function and ensure that the aircraft can continue to fly safely although at lower performance levels. Lastly, they were used on AHRLAC to provide mounting points for the detachable tail cones which can house a variety of sensors.

1.3 OBJECTIVES OF THE STUDY

The study endeavours to design and manufacture a composite ventral fin for AHRLAC XDM which is optimized for mass, stiffness and strength. This will include the selection of materials and manufacturing methods that are in line with the prototyping environment. For optimization of these three parameters, they will have to be analytically determined using finite element software and be tested to validate the methodology followed in their determination.

The background information required for the study is:

- Review literature of aerospace composites on the following topics:
    - Composite materials available
    - Composite manufacturing methods
    - Limitations of composite materials
    - Analysis of composites
    - Similar work done
    - Environmental and safety concerns of composite materials

The goals of the study are:

1. Material selection for use in the composite ventral fin
2. Method selection that will be employed to manufacture the ventral fin
3. Design a composite ventral fin which meets the requirements for weight, stiffness and strength
4. Verify that the design of the ventral fin meets the requirements using finite element software
5. Manufacture the ventral fin and conduct static tests to validate the design methodology followed
6. Conclude the results of the design methodology validation
7. Give recommendations on further studies

1.4 LAYOUT OF THE DISSERTATION

Chapter One introduces the reader to the study; this starts off with the background of the study, followed by the motivation which will be outlined and used to determine the objectives that the study will endeavour to complete.

Chapter Two of the dissertation consists of applicable literature with a current overview of composite usage in aerospace applications. This chapter will introduce the reader to aerospace composite technologies while supporting the methodology of the study, which will include literature on materials, manufacturing methods and limitations of composite materials. The next part of this section will focus on composite analysis and similar work done in this field and finally concludes with health, safety and environmental considerations of composite materials.

Chapter Three pertains to the design of the ventral fin of AHRLAC XDM. The information acquired in Chapter Two will be used in this section. Firstly, the requirements that led to the final design and which were used to aid decision making, will be discussed. The following step was the selection of materials and manufacturing methods that will be used on the ventral fin design. After these were selected, a FEA was used to optimize the mass of the component and verify that the design would be adequate with regards to the design parameters of interest.

Chapter Four contains the validation part of the study; this is where the designed and manufactured component will be tested and compared to the finite element model (FEM), which is done to verify the design methodology used. This will ensure confidence in the assumptions made and methodology followed in the material and manufacturing selection, as well as the analysis of the ventral fin. In this section the composite ventral fin is manufactured in accordance with the FEM and the detail design of the preceding section. Subsequently, the component is subjected to static loads while the deflections are measured and compared to the FEA results.

The study draws its conclusions on the testing and methodology followed in Chapter Five, and also discusses recommendations for further study.

The dissertation ends with the references cited and a list of appendices for additional information.

2 AEROSPACE COMPOSITES OVERVIEW

2.1 INTRODUCTION

For the completion of the design and development of a composite ventral fin, a literature survey will be conducted on the relevant topics that will ultimately lead to the decisions made in the study. This provides the foundation for any study as to familiarize the reader with the technology and methodology of the study. Composite materials and manufacturing methods as well as the limitations of composite materials will be discussed, including the analysis of composites and similar work done. The chapter will conclude with safety and environmental concerns.

2.2 COMPOSITE MATERIALS

Composite materials can be defined as the combination of two or more different materials on macroscale, acting in combination [9]. This definition can be used to describe many materials, for instance leather, wood and continuous fibre reinforced plastics. For the purpose of this study, the use of the word composite will refer to the main materials used in aerospace (Figure 2-1).
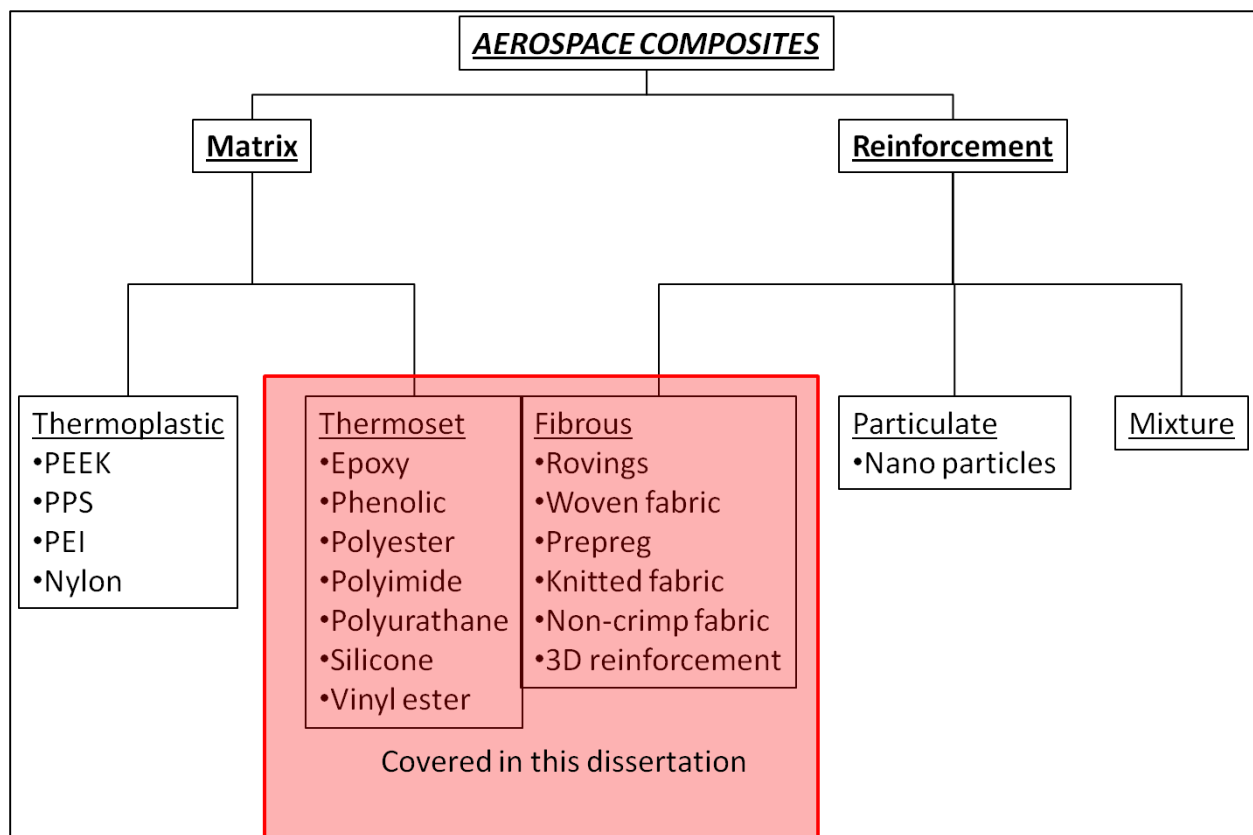
Figure 2-1: Composite material breakdown

Composite materials can be divided into two main parts, namely matrix and reinforcement (Figure 2-1). The reinforcement is the part of the composite that defines the strength and stiffness of the material, while the matrix is the binding agent that supports the reinforcement (Figure 2-2).
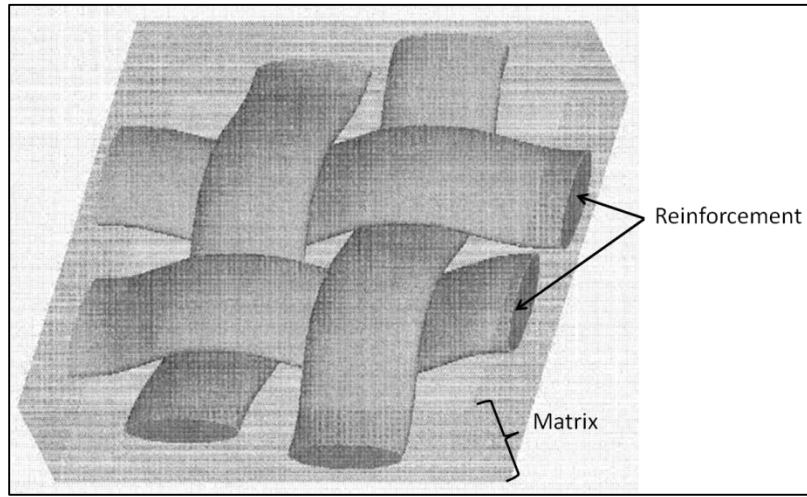
Figure 2-2: Reinforcement and matrix form a composite [10]

2.2.1 REINFORCEMENT MATERIALS

The most commonly used composite materials in the aviation industry are carbon, glass and aramid [11].

Glass fibre

Glass fibre is probably the most widely used composite reinforcement and is commonly regarded as the cheapest. These fibres are produced from raw materials that can be found in almost unlimited supply [12]. Some of the useful bulk and fibre properties are hardness, transparency, resistance to chemical attack, stability, inertness, strength, flexibility and stiffness [13]. Typical fibre diameters range from 3 μm to 20 μm [7] with the most commonly used fibreglass being the "E" type; this is also sometimes referred to as general purpose glass. Other glass types are shown in Table 2 and are referred to as special purpose glass fibres. Glass fibre has a property that is often sought after in aerospace: it is radio transparent, unlike carbon.

Letter designation	Property or characteristic
E, electrical	Low electrical conductivity
S, strength	High strength
C, chemical	High chemical durability
M, modulus	High stiffness
A, alkali	High alkali or soda lime glass
D, dielectric	Low dielectric constant

Table 2: Glass fibre types [14]

Carbon fibre

Carbon fibre has the reputation for having the highest modulus to weight ratio of the composite reinforcements. Carbon fibres can be tailored by the manufacturing method into three main categories regarding stiffness. They are standard modulus (SM), intermediate modulus (IM) and high modulus (HM) carbon [7]. In recent years a fourth category emerged, this is the high strength (HS) carbon fibre. This fibre has a strain to failure of more than 2 % [15]. These properties are influenced by mechanical stretching, heat treatment and amount of spinning in the production process of the fibres. Carbon fibre is also well known for its brittle failure. One of its main advantages is, that unlike aramid or glass fibre, it does not suffer from stress rupture and is fully elastic until failure [16], [17]. This gives carbon a huge advantage in fatigue failure in comparison to other composites.

Aramid fibre

Aramid fibre is the strongest of the composite reinforcements and has the largest strength to weight ratio. Aramid was first introduced in the seventies under the trade name Kevlar by the company E.I. Du Pont de Nemours & Company, Inc [7]. Its light weight and superior strength has been responsible for its main uses in ropes, cables, protective equipment and ballistics.

Properties comparison

Figure 2-3 compares the strength and stiffness of the various composite reinforcements, as well as the unidirectional (UD) fibres and its fabric properties. The difference between fibre and fabric properties is further discussed in Section 2.2.2. This graph is in accordance with all the previously mentioned properties of glass-, aramid- and carbon fibres. It is evident that the strongest reinforcement is aramid (Kevlar 49) with the stiffest being HM carbon. It is also apparent that the properties deteriorate as the fibres are processed into woven fabrics.
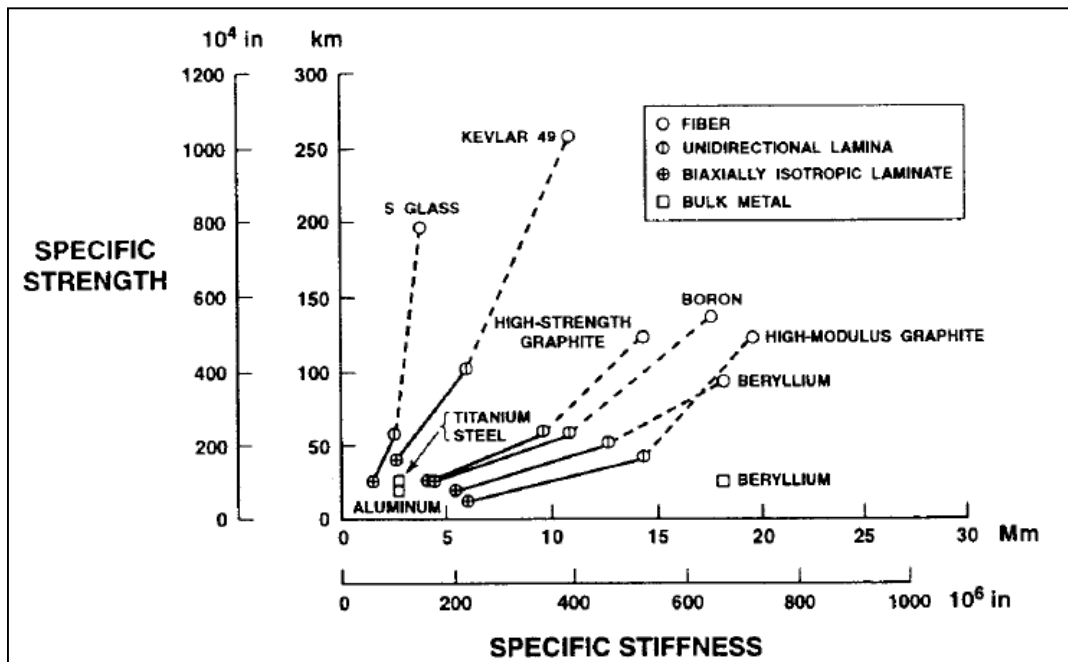
Figure 2-3: Composite properties index [18]

Table 3 and Table 4 are results from a composite reinforcement comparison study [19]. In this research Bader took the most used composite reinforcements in the aerospace industry and did a comparative analysis to equate them with regards to cost, strength and stiffness. All reinforcements were compared using an epoxy matrix, as this is the most used resin system, thus eliminating the effects of the matrix on reinforcement selection. The analysis was done with pre-impregnated laminates in order to reduce the effects of manufacturing methods on the results. Bader used E-glass as his normalized set of properties.

Fibre	Resin	Stiffness critical			Strength critical	
		Tension	Bending	Torsion	Tension	Bending
Performance index >		E/ρ	$E^{1/2}/\rho$	$G^{1/2}/\rho$	σ/ρ	$\sigma^{2/3}/\rho$
E-Glass	Epoxy	1.00	1.00	1.00	1.00	1.00
Aramid	Epoxy	1.88	1.67	1.68	1.51	1.50
HS carbon	Epoxy	3.16	1.99	2.00	2.53	2.02
IM carbon	Epoxy	4.03	2.25	2.22	3.22	2.37

Table 3: Relative performance indices of reinforcements normalized to E-glass [19]

Table 3 shows the relative performance index of the most used composite material in aerospace which confirms the trend shown in Figure 2-3 [19]. It clearly shows carbon reinforcement as having the highest specific stiffness, with aramid second and E-glass the least stiff. The only difference shown between Table 3 and Figure 2-3, is that the strength to density ratio of carbon is slightly higher than that of aramid. All of the previously mentioned literature shows aramid as the reinforcement material with the highest specific strength. This indicates that there is an area of overlap between the tensile properties of aramid and IM carbon.

Fibre	Resin	Stiffness critical			Strength critical	
		Tension	Bending	Torsion	Tension	Bending
Performance index >		$E/\rho C$	$E^{1/2}/\rho C$	$G^{1/2}/\rho C$	$\sigma/\rho C$	$\sigma^{2/3}/\rho C$
E-Glass	Epoxy	1.00	1.00	1.00	1.00	1.00
Aramid	Epoxy	1.12	1.14	1.15	1.03	1.02
HS carbon	Epoxy	1.78	1.30	1.30	1.64	1.30
IM carbon	Epoxy	1.03	0.67	0.66	0.95	0.70

Table 4: Relative cost indices of reinforcements normalized to E-glass [19]

It is well known that glass fibre is the lowest cost reinforcement per meter, compared with aramid and carbon. Table 4 also indicates that IM carbon is relative to density cheaper than E-glass by as much as 44 % in the fields of bending and torsion, though it is the same price in a tension application. HS carbon and aramid are more expensive than E-glass, in all applications, by as much as 78 %. This shows that IM carbon is the best value for money when equated with density, stiffness and strength. E-glass is the second best value for money in most fields. This costing analysis is merely used as a guideline, because the costs of these reinforcements are revised yearly according to the changes in manufacturing technologies.

Skordos et al. designed and analysed a composite dog bone test sample, using different materials; they used E-glass, Kevlar and carbon fibre with various lay-ups [11]. A comparison was done in the deflection and maximum strain energy that can be absorbed by the test sample. The results of their study are shown in Figure 2-4. It validates Bader's research [19] in that carbon results in the least deflection and also shows the overlap region of the various materials.
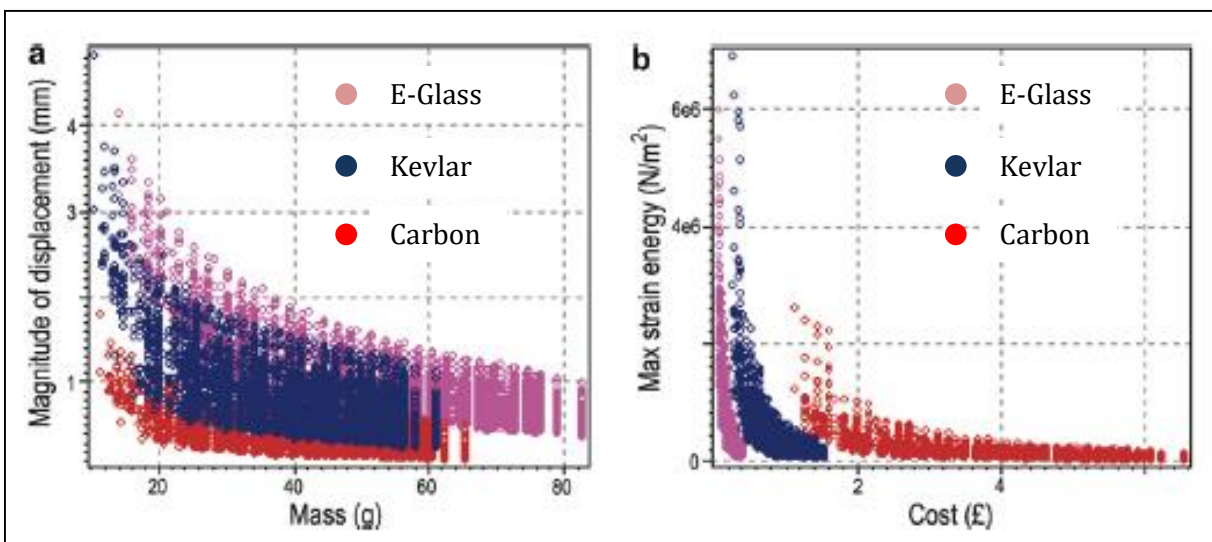
Figure 2-4: Relative performance of reinforcements [11]

2.2.2 REINFORCEMENT TYPES

The reinforcement can be subdivided into three main categories: fibrous, particulate and a mixture of the two (Figure 2-1). This study only covers fibrous reinforcement, which can be found in numerous forms and materials. It can be continuous fibres, such as woven fabric, or short random fibres, such as chop strand mat (CSM), and can also be used in non-woven long fibre form; this is called tape or UD fabric. As stated in the previous section, materials commonly used in aerospace applications are carbon, glass and aramid, which can be used in combination, woven into the same fabric.

The basic form of fibrous reinforcement can be defined as rovings or tows as seen in Figure 2-5 [20]. These are made up from single strands or filaments of fibres, bunched up to from a bundle called a tow. Tows are then bunched up to form a roving. These fibres range from 5 μm to 30 μm and count up from a 1000 to form a roving [19]. These fibres are surface treated to promote adhesion to the matrix; this is done by chemically etching the fibres, leading to an increase in surface roughness and then coating them to aid bonding to the specified matrix [15]. The laminate tensile strength and stiffness are mainly properties of the fibre, while the out-of-plane support is resin dominated. Material suppliers optimize the matrix and reinforcement interface strength, in order to balance these properties. The fracture mechanics and creep properties of composite laminates are functions of these bonding interfaces [15].
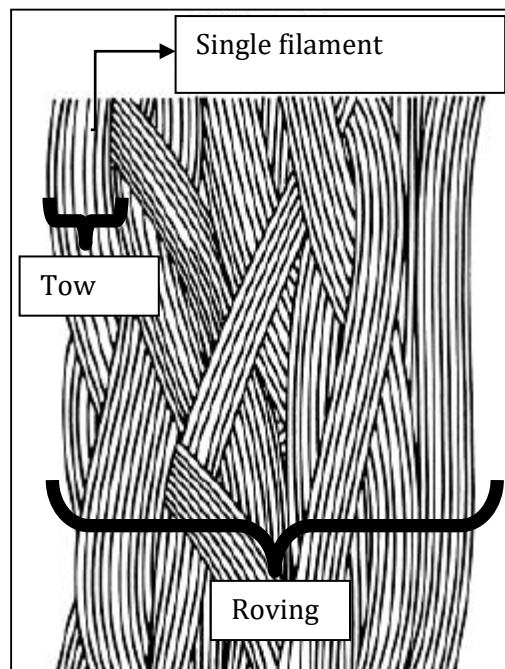
Figure 2-5: Fibrous composite diagram [7]

These rovings or tows can then be supplied and used to produce parts in various forms. The most common forms are: rovings, fabric, prepregs, knitted fabrics, non-crimp fabrics and three-dimensional reinforcements [19].

Rovings

Rovings are the most basic form of reinforcement that is used in aerospace part manufacture and is usually the least expensive. It can be bought as UD reinforcement tape or rolls to reinforce parts in a very specific direction. Rovings are also used extensively in the forming of composite tubes and shafts by using filament winding manufacturing techniques. Material suppliers use rovings to weave and form woven fabrics products.

Woven fabrics

Woven fabrics come in many different weave styles, such as plain waves, twill weaves and various satin weaves [15]. Some of these weave types can be seen in Figure 2-6. These fabrics can be supplied in different filament, tow and roving sizes, which are selected based on the planar weights required. Planar weights range from 100 g/m² to as high as 4500 g/m², with a corresponding thickness of 0.1 mm to 5 mm respectively [19]. Fabrics can be supplied using different types of fibre materials and combinations thereof. They can also have biased fibre volume fractions in two principal directions, which can increase the tailoring capabilities of composite fabrics and, ultimately, structures.

The fabric's ease to conform to complex curvatures is termed drapability; twill and satin weaves are the easier draping fabrics. The heaver the fabric planar mass, the more difficult it becomes to drape on complex shapes. The most used fabrics in aerospace are the satin and twill weaves due to their superior drape and damage tolerant characteristics [19].

Woven fabrics can be supplied pre-impregnated with matrix or as a dry fabric where the manufacturing methods have to introduce the matrix into the reinforcement. Pre-impregnated fabrics have to be stored at a very low temperature to prevent the resin from curing.
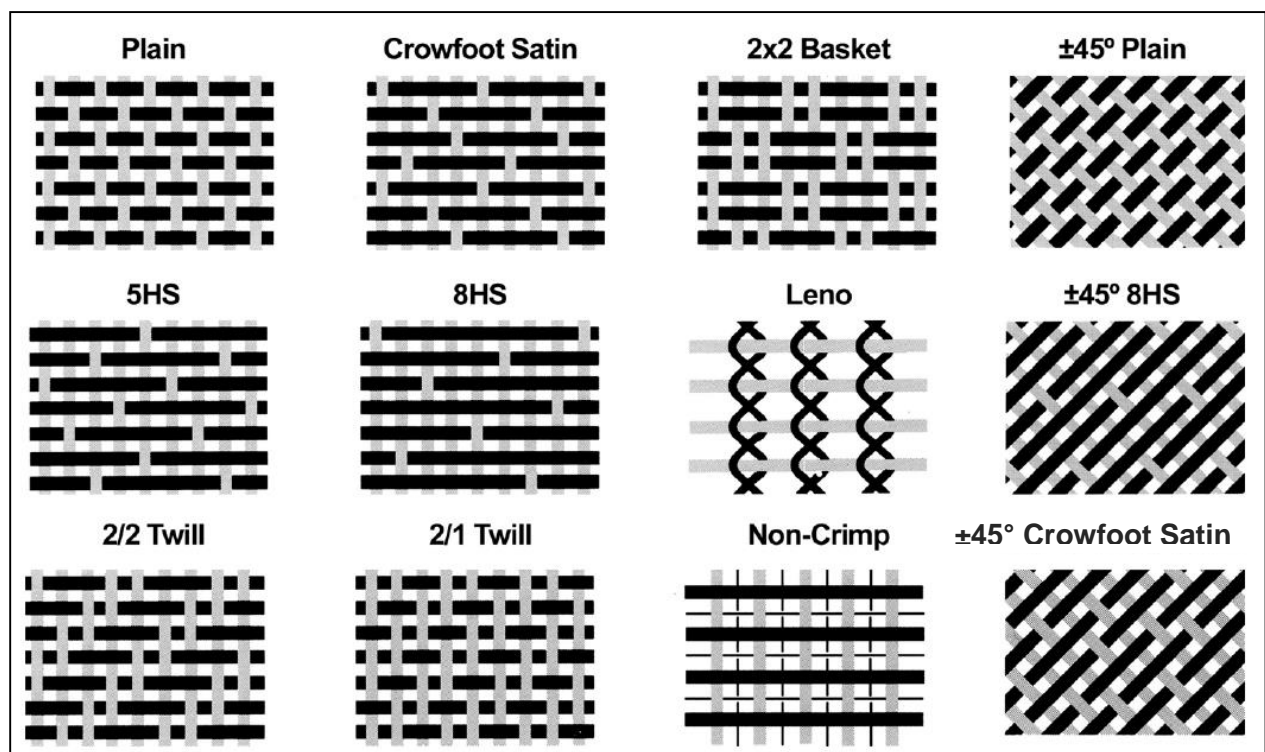
Figure 2-6: Different weave types [21]

Knitted fabrics

Knitted fabrics are woven fabrics that are pre-tailored and delivered as multiple layers of woven fabrics stitched together. It can be preshaped to minimize draping problems and to aid in production time reduction. The knitted fabrics are optimized for production and require large volume orders from the material suppliers [19].

Non-crimp fabrics

Non-crimp fabrics are pre-tailored layers of rovings that are held together by non-load bearing stitching. They are in essence the same as knitted fabrics, but are made up of UD layers (Figure 2-7) instead of woven fabrics. Non-crimp fabrics were developed to minimize the crimping effects of woven fabrics. As with knitted fabrics, non-crimp fabrics are better suited to high production volumes and generally result in a lighter, more optimized structure [19].
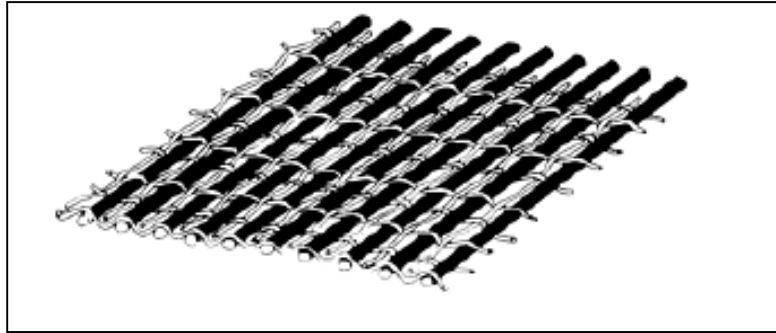
Figure 2-7: One layer of UD non-crimp fabric [7]

Three-dimensional fabrics

Three-dimensional reinforcement is a combination of knitted and non-crimp fabrics that are tailored to a specific shape. It contains a high number of through thickness stitching that is designed to increase out-of-plane strength at the cost of in-plane strength and stiffness. As with knitted and non-crimp fabrics, they are well suited for highly optimized parts and large production volumes [19]. See Figure 2-8 for an illustration.
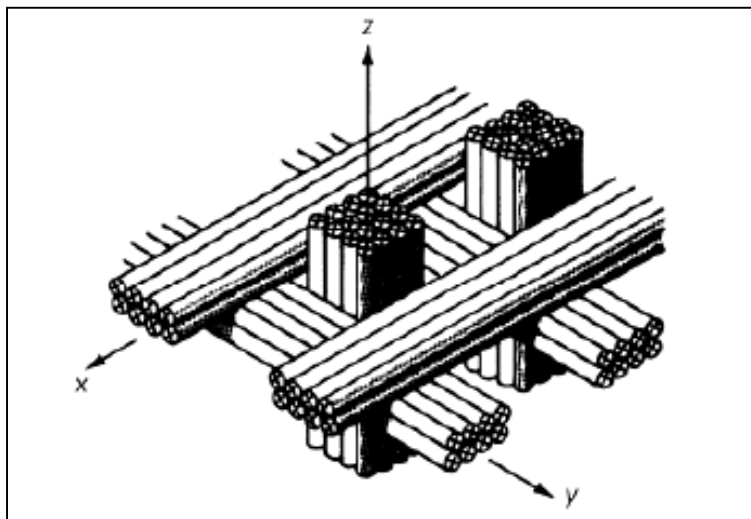
Figure 2-8: Three-dimensional fabric reinforcement [7]

Properties comparison

The reinforcement types have a major influence on the lamina strength and stiffness properties (Figure 2-3 and Figure 2-9). This property variation between fibres and fabrics is a result of the amount of fibres in each direction. The greater the fibre fraction that is in one direction, the greater the properties becomes biased in that direction and vice versa. Figure 2-9 shows the strength of a laminate in one direction versus the fibre fraction in the same direction. It is evident that if the fibre fraction in the loaded direction increases so does the strength and vice versa.
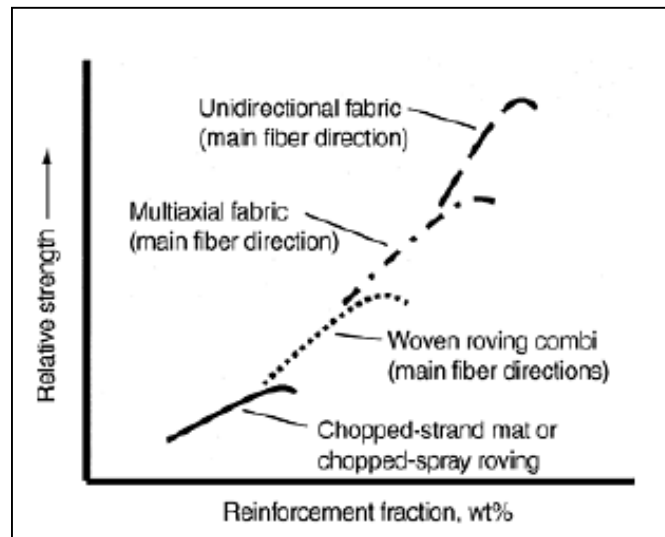
Figure 2-9: The effect of reinforcement type and volume fraction on laminate performance [7]

2.2.3 MATRIX

As discussed in the previous section, the dry fibres are useless unless they are held together somehow. The structural element that keeps the fibres together is known as the matrix; the matrix generally has inferior mechanical qualities when compared to the reinforcement [22]. It has a lower density, stiffness and strength than the reinforcement, but the combination of the two can yield very sought after qualities. The three main responsibilities of the matrix are to:

1. Support embedded fibres
2. Protect fibres from the outside elements
3. Transfer load from one fibre to another

There are many different matrix structures and materials, but only polymer matrices will be considered in this study. Polymer matrices can be subdivided into thermoset, thermoplastic and rubber resins.

Thermoset resins

Thermoset resins require thermal energy to complete cross-linking and to become solid and insoluble. Once the resin is cured it cannot be softened again with the addition of heat, as the curing cycle is a permanent change. Most thermoset resins require the addition of a curing agent or hardener, which initiates the cross-linking of the molecules. Due to the tightly packed molecules, thermoset resins normally have greater temperature resistance, stiffness and strength than thermoplastics.
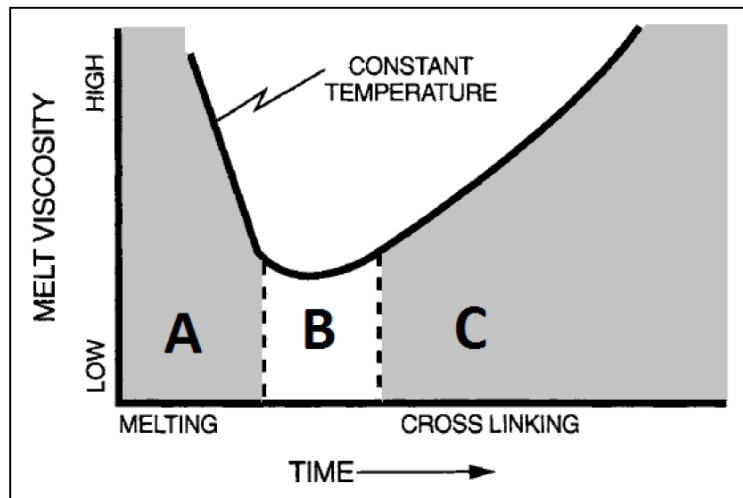
Figure 2-10: Curing stages of thermoset resin [22]

Figure 2-10 shows the curing stages of a typical thermoset resin. At the start of the graph there are almost no cross-links and the resin is considered uncured. As the thermal energy is applied and time passes, the viscosity drops dramatically to its lowest point. This is useful where processing techniques like resin infusion are used, where the viscosity of the resin has to be low in order to flow through the dry laminate. Some resins, such as those used in pre-impregnated laminates, are stopped in this phase by removing the thermal energy. It can then be stored and the process can be continued at a later stage through the addition of heat [22].

As curing continues past the lowest viscosity point, the viscosity increases as the cross-links start to form and continue until they are fully linked and in their final positions [22]. The time lapsed from adding the hardener and mixing all components of the resin, to where it is not feasible to use the resin for impregnation, is called the pot life. This time varies from 20 minutes to 2 hours, depending on the resin. The pot life of the chosen resin has to be considered when deciding on the manufacturing method.

There are a variety of fillers, additives and accelerators available for thermoset resins. They can be used to alter the properties of the final products in the following ways: pot life, electrical properties, dimensional stability, UV resistance and burning characteristics.

From reference [20] the most used thermoset resin in aerospace is epoxy, due to its superior strength. These epoxy type resins normally cure at temperatures ranging from room temperature to as high as 350°C and can be subjected to an additional post cure to gain superior temperature resistance.

Table 5 lists the most commonly used thermoset type resins and their characteristics.

Resin type	Characteristics	Limitations
Epoxy	Excellent composite properties Very good chemical resistance Good thermal properties Very good electrical properties Low shrinkage on curing Can be B-staged (as prepreg)	Long cure cycles Best properties obtained only with cure at elevated temperature Skin sensitizer
Phenolic	Very good thermal properties Very good fire properties (self-extinguishing) Can be B-staged Good electrical properties	Color limitation Alkali resistance Contact with foodstuffs
Polyester	Wide choice of resins - easy use Cure at room temperature and elevated temperature Very good composite properties Good chemical properties Good electrical properties	Emission of styrene Shrinkage on curing Flammability Cannot be B-staged
Polyimide and polyamide-imide	Excellent thermal properties Good composite properties Good electrical properties Good fire properties	Restricted choice of color Arc resistance Acid and alkali resistance
Polyurethane	Good composite properties Very good chemical resistance Very high toughness (impact) Good abrasion resistance	Nature of isocyanine curing agents Color Anhydrous curing Cannot be B-staged
Silicone	Very good thermal properties Excellent chemical resistance Very good electrical properties Resistant to hydrolysis and oxidation Good fire properties (self-extinguishing) Non toxic	Lack of adhesion Long cure cycles Can only be cured at elevated temperatures
Vinyl ester	Good fatigue resistance Excellent composite properties Very good chemical resistance Good toughness	Emission of styrene Shrinkage on curing Flammability No B-stage

Table 5: Thermoset resin characteristics [23]

Thermoplastic and rubber

Thermoplastic type resins are typically materials such as polypropylene, PEEK, PEI and nylon. These engineering plastics have much better impact resistance than their thermoset counterparts [20]. They require much more equipment to manufacture the components and are more suitable for large scale production, because product turnaround times are short and large volume production can recover the expensive equipment cost. These matrix types will not be considered in this study due to the large initial cost and high production volume characteristics.

2.2.4 CORE

In the 1940s, the use of structural cores in aircraft composite structures, greatly increased aircraft performance by maximizing payload and flight time. The main functions of these cores were to replace the conventional skin and stringer design with a composite sandwich skin. The use of this core to form a sandwich structure became a common and accepted structure in the 1950s. Today almost all aircraft have composite sandwich structures somewhere on the aircraft, some load bearing and others aesthetic [24]. A honeycomb core sandwich panel is shown in Figure 2-11.
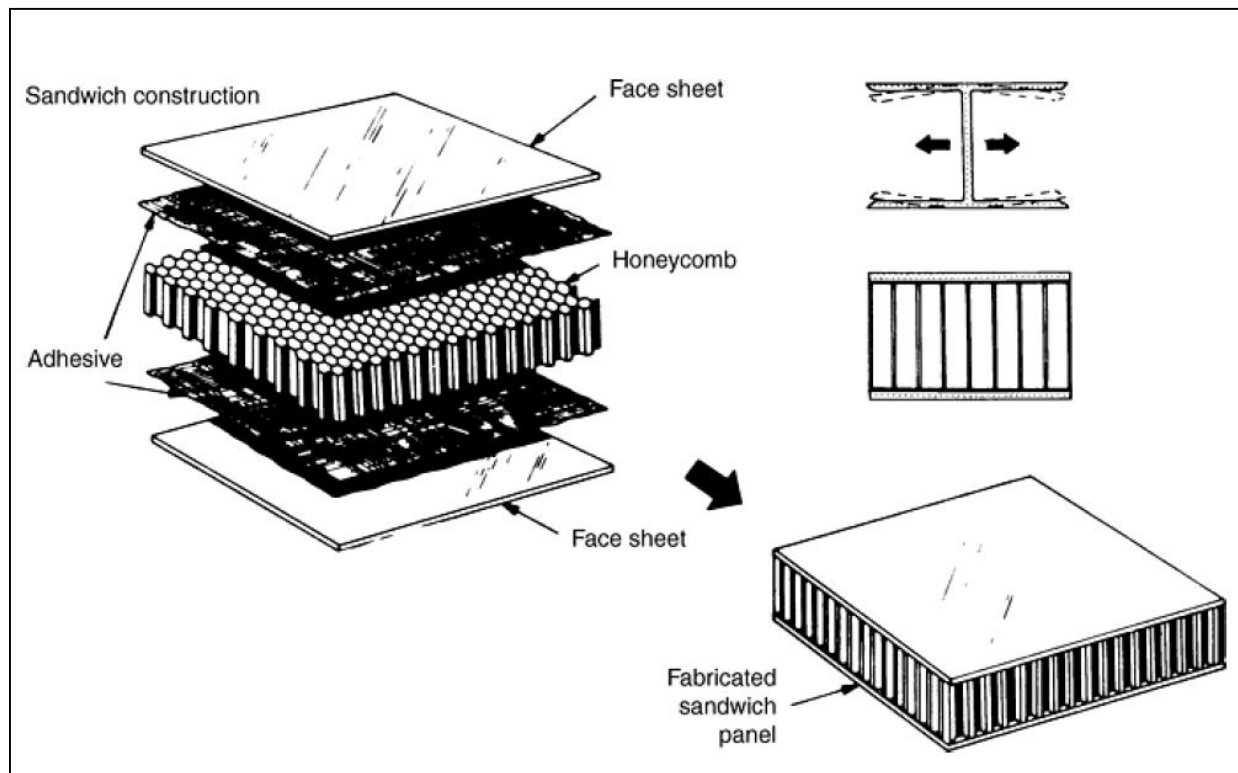
Figure 2-11: Sandwich construction example [7]

The typical sandwich structure consists of two-facing skins that are bonded to a lightweight core (Figure 2-11). The skins are usually made from stiff and strong materials while the core is lightweight and merely used to keep the skins apart. The concept is for the skins to take the bending loads and the core the shear loads, thus the core merely keeps the skins apart in much the same way as an I-beam web keeps the flanges apart. There are three main types of cores used currently in aerospace: honeycomb, foam and balsa cores [24]. The honeycomb and foam categories have many substrate materials that can be used.

Honeycomb

Honeycomb core design is based on nature and as the name suggests, this type of core is similar to the core found in a beehive. These cores' cells can vary in shape, material, manufacturing method and dimensions. In Figure 2-12 some of these cell parameters are shown.
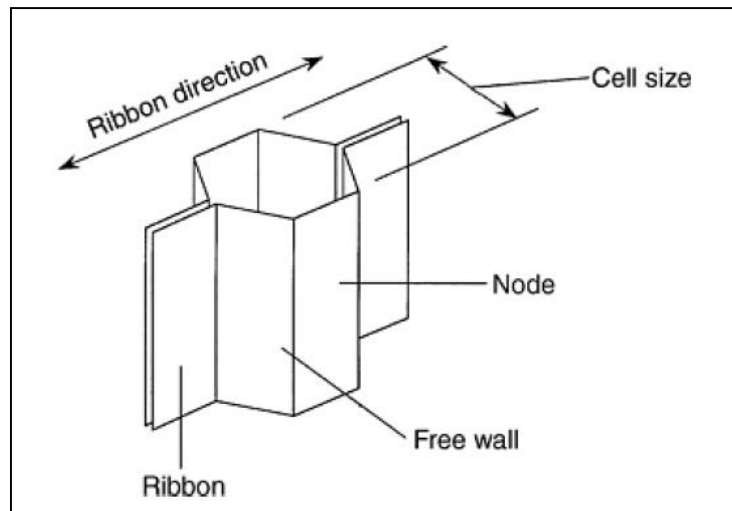
Figure 2-12: Honeycomb terminology and parameters [7]

Commonly used cell shapes are:

- Hexagonal
- Reinforced hexagonal
- Overexpanded (OX)
- Square
- Flex-Core
- Double Flex-Core
- Spirally wrapped (Tube-Core)
- Cross-Core
- Circular Core

Drawings of these shapes are presented in Appendix A.

As with metallic substrate such as aluminium, steel and titanium, honeycomb core can be manufactured from composite materials such as carbon, glass and aramid, using thermoplastic and thermoset resins. They can also be made from combinations of metallic and composite materials.

A short summary of honeycomb materials and their properties [7]:

- *Kraft paper*:
  Lowest cost and strength substrate, but has good insulating properties.

- *Thermoplastics*:
  Relatively low-cost substrate, with good energy absorption properties. Good moisture and chemical resistance and also creates aesthetically pleasing surfaces.

- *Aluminium*:
  Relatively low-cost substrate and has one of the best strength to weight ratios. Good heat transfer and electromagnetic shielding properties. These types of honeycombs are also machinable.

- *Aramid fibre*:
  Very good fire resistance and dielectric properties.

- *Fibreglass*:
  Low dielectric properties with good insulating properties.

- *Carbon*:
  Very expensive with high stiffness and dimensional stability. Has a very low coefficient of thermal expansion and high shear modulus.

- *Ceramic*:
  Very expensive substrate, for use with very high temperature applications. Available in very small cell sizes.

The constitutive material properties of honeycombs are considered anisotropic [7], which means that the material properties differ for the different material directions. The highest stiffness and strength occurs in the T (through thickness) direction, while the other two directions are usually weaker (Figure 2-13). The most important properties of anisotropic honeycomb are [7]:

- Compressive modulus
- Compressive strength
- Crush strength for energy absorption applications
- Shear strength for both W and L directions
- Shear modulus for both W and L directions
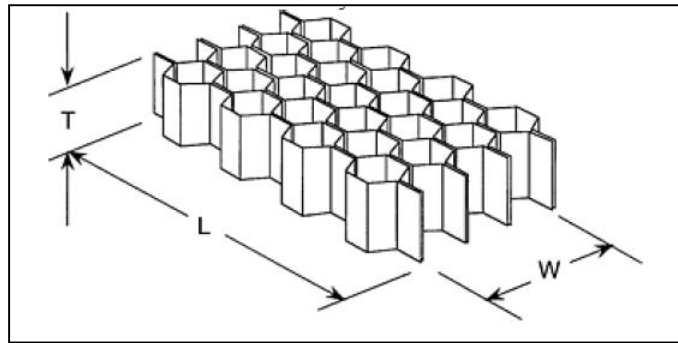
Figure 2-13: Honeycomb principal directions [7]

Balsa

Balsa is a type of natural wood with elongated closed cells. A variety of grades, ranging from aesthetic to structural, are available. Densities vary from 96-288 kg/m^3, which are one half the densities of normal wood products [7]. Balsa is a lot denser than foam and honeycomb and is most often used in hard points of laminates which are subjected to heavy loading.

Foam

Foam has isotropic material properties and can be made from various materials, each having a unique set of characteristics. These foams densities can vary dramatically.

Materials currently used to make foams for sandwich construction composites are [7]:

- *Polymethacrylimide (under trade name Rohacell):*
  Very expensive foam that has superior mechanical properties and is primarily used in aerospace environments.

- *Polyvinyl chloride PVC (under trade names: Divinycell, Klegecell and Airex):*
  Mainly used in structural marine applications and some aerospace applications.

- *Polypropylene:*
  Mainly used in structural automotive applications.

- *Polyurethane:*
  Relatively low-cost and moderate structural properties. Mainly used in automotive applications.

- *Phenolic:*
  Low mechanical properties, but has very good fire-resistant properties. Has very low densities.

- *Polystyrene:*
  Least expensive of the foams and has the lowest mechanical properties. Commonly used for disposable packaging and disposable cores.

Comparison of core materials

Table 6 compares the various cores' characteristics for selection processes [7]. It can be seen that Balsa core is very dense compared to the other cores.

Property or attribute	Honeycomb	Balsa	Foam
Density (typical), kg/m³ (lb/ft³)	Expanded: 32–192 (2–12) Corrugated: 160–880 (10–55)	96–288 (6–18)	32–288 (2–18)
Moisture resistance	Excellent	Fair	Excellent
Chemical resistance	Fair to excellent	Fair to very good	Fair to very good
Flammability resistance	Excellent	Poor	Fair to excellent
High-temperature resistance	Adhesive bonded: to 177 °C (350 °F) Braze welded: to between 370 and 815 °C (700 and 1500 °F) depending on material	To at least 95 °C (200 °F)	Typically to 80 °C (180 °F); varies by type, but mechanical properties decrease significantly at higher temperatures
Strength and stiffness	Excellent	Excellent	Fair
Energy absorption and crush strength	Constant crush strength value	Not used for energy absorption	Increasing stress with increasing strain
Impact resistance	Fair to excellent	Very good	Fair to poor
Fatigue strength	Good to excellent	Very good	Fair to poor
Abrasion resistance	Good integrity	Fair	Friable
Acoustic attenuation	Yes	Yes	Yes
Formability	Various cell configurations for different shapes	Must cut (e.g., scoring), or use joined strips	Requires molds or scoring
Cost	Inexpensive (kraft paper) to very expensive (carbon)	Moderate	Very inexpensive (polystyrene) to expensive (polymethacrylimide)

Table 6: Comparison of composite core variations [7 p. 456]

Figure 2-14 shows the cost comparison of the various core types; honeycomb stretches the entire performance and cost range, depending on the material used. Foams can be tailored from low to average performance and cost, while balsa performs better than the foams, and is better suited for heavy loading applications.
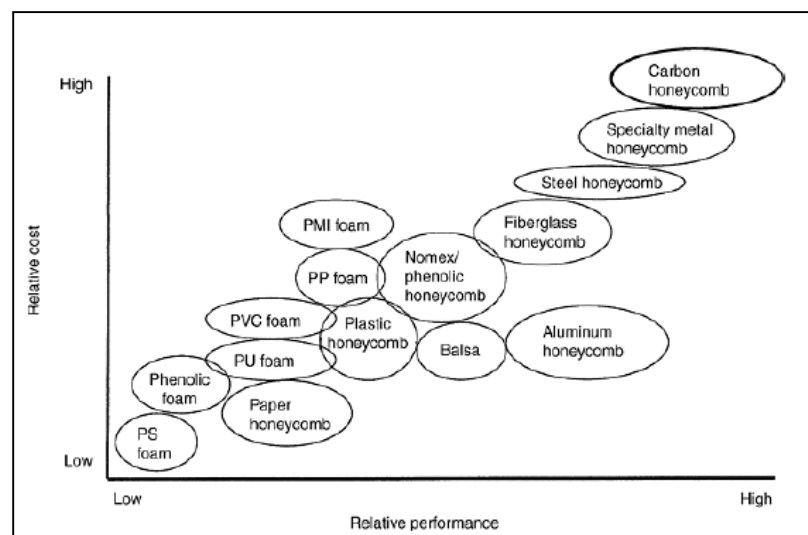
Figure 2-14: Cost comparison of various core types [7]

2.3 MANUFACTURING OF COMPOSITES

There are about as many manufacturing methods in composites as there are different material configurations. There are certain manufacturing methods which are only applicable to specific matrix and reinforcements combinations. Figure 2-15 shows the process diagram with the suitable composite material combinations.
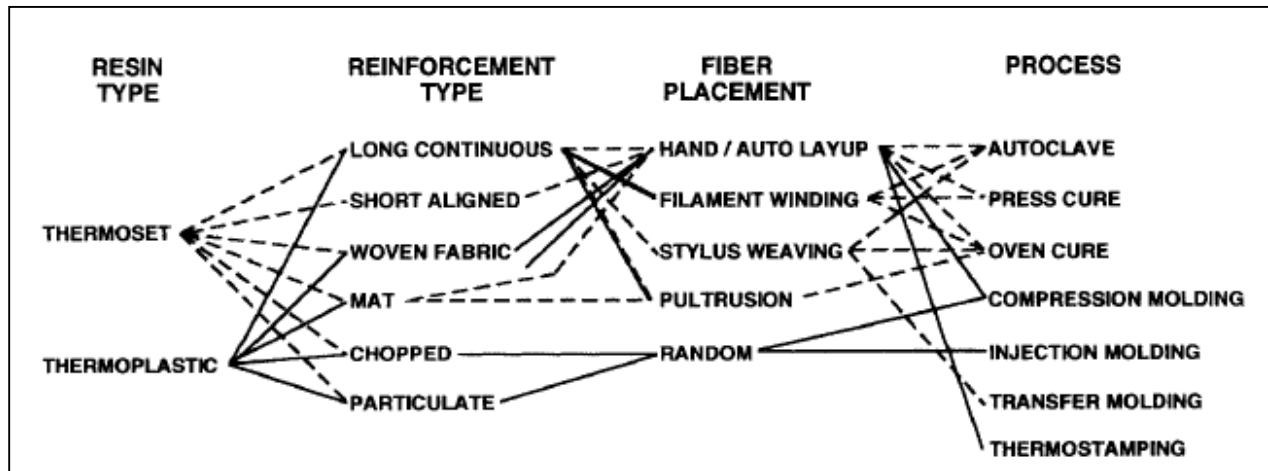
Figure 2-15: Composite manufacturing roadmap [6]

This study will only include the manufacturing methods within Aerosud ITC's capabilities, combined with the material limitations seen in Figure 2-1. The only fibre placement method that will be considered is hand lay-up and the curing processes considered are oven curing and press curing (Figure 2-15). Oven cure refers to an open mould that is placed in an oven for curing, with or without vacuum assistance, while press cure refers to production processes such as resin transfer moulding (RTM).

Figure 2-16 shows the performance versus production volume of the above mentioned manufacturing methods. The spray-up will be excluded from the literature survey, due to it being exclusively applicable to CSM reinforcement. The sheet moulding compounds (SMC) and the glass mat thermoplastics (GMT) will also be excluded, because it is heavily optimized for a thermoplastic matrix, rather than thermoset. What remains is hand lay-up on open moulds, RTM, vacuum infusion and autoclave forming. These processes are applicable to fabrics and UD fibres and are all suited for manual impregnation of the matrix. Prepregs, material supplied already impregnated with the matrix, will be considered as well. The pre-impregnated laminates would have to be suitable for out-of-autoclave processing.
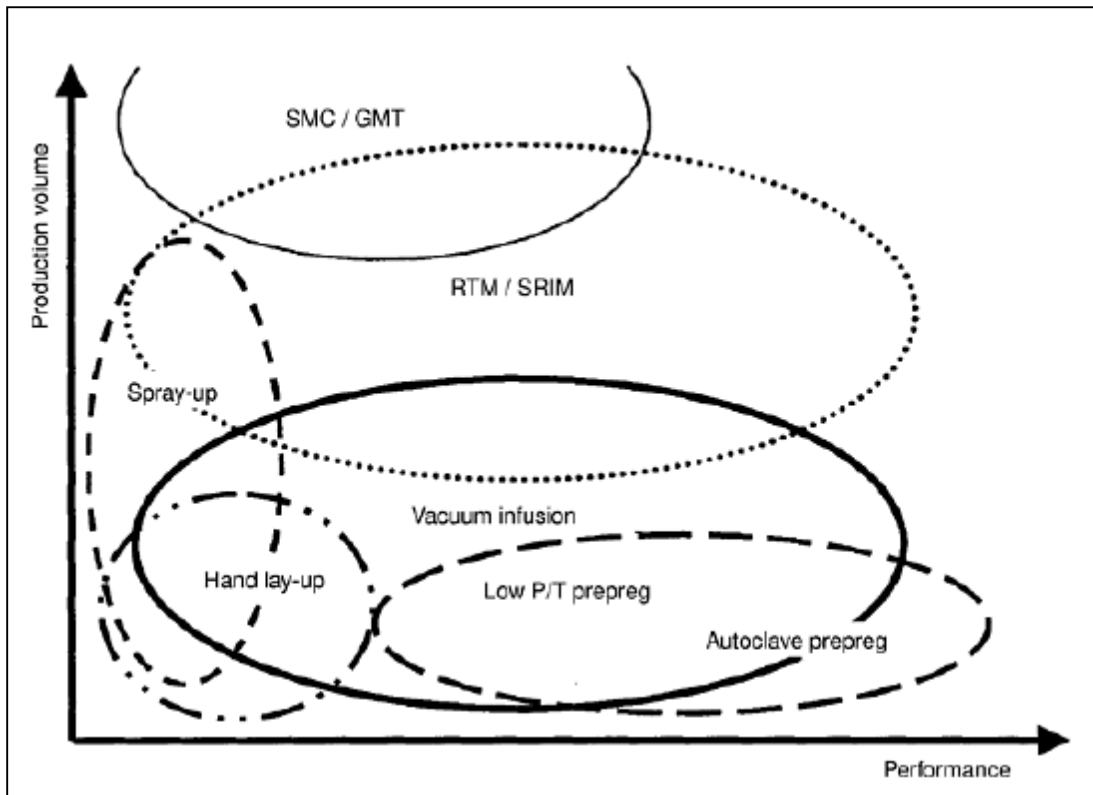
Figure 2-16: Index of composite manufacturing techniques and their performance [7]

Bader investigated the performance and cost of a simple composite component, using different materials and manufacturing processes [19]. The material aspect of his findings was discussed in Section 2.2 and this section will cover the manufacturing segment of his findings. Bader discussed five factors that influence the selection of the most suitable process of composite components' manufacturing and will be discussed in the next section.

2.3.1 MANUFACTURING METHOD SELECTION CRITERIA

Component geometry

Component geometry includes both the size and the shape of the parts. There are two main schools of thought in the composite manufacturing area concerning component geometry. The first is to design the component with as few parts as possible, which leads to very complex parts and tooling. The goal is to produce complete components, such as box sections of a wing, in one moulding. This shifts the cost of manufacturing and assembling from a multitude of small parts, to the manufacturing of a large and complex single component. In many aerospace fields this method is used effectively. The alternative is to lower tool and part complexity as much as possible; this usually results in more, but less complex, tooling. The cost and resources required for each part is lessened, but the consequence is that more resources are used in the assembling of the final components. The path chosen here has a profound effect on the selection of manufacturing methods [7]. The size of the part can limit manufacturing options, such as press or autoclave forming, due to the limitations of the equipment size.

Scale of production

The effect of the production scale can be illustrated by comparing the automotive industry to the aerospace industry. In aerospace, the production rate seldom exceeds 1000 parts per annum, where this could be done in a day in the automotive industry. It is improbable to get more than one part per tool per working day when using autoclaves; this equates to roughly 250 parts per annum. When the component is large and complex, it could take up to a week to set up and manufacture [7]. These components are very high in quality and performance. This process is widely used in aerospace and very seldom in automotive, due to the difference in scale of production between the two fields. RTM can achieve rates of up to 1000 per tool set per annum, while SMC can go up to 10000 per annum. These processes are used in the automotive industry (Figure 2-16).

Tooling

The scale of production will affect the tooling choices. For low volume production, one-sided composite tools are the norm. They are usually made from a master pattern that is machined from tooling boards or similar material. Such tooling can be used up to around 180°C and can manufacture up to 1000 parts depending on the tool quality. One surface of a part made with this type of tooling is in contact with the tool. The surface finish and dimensions can be controlled very well on the one side, while the other is dependent on the skill of the operator. An advantage of using a composite tool is that there is little difference in the thermal coefficient of expansion between the tool and the part; this reduces possible problems when curing at high temperatures. When higher production volumes are sought after, using metal tooling is usually the norm. Matched tooling can be used when much better control of the thickness and surface finish, on both sides, is needed. The design of metal tooling has to take into consideration the thermal mismatch in expansion between the tooling and the part materials. RTM and SMC usually use metal matching tools to achieve high production volumes, while hand lay-up and vacuum infusion are commonly used in combination with one-sided composite tools. Autoclave forming has been used with both metal and composite tooling successfully; the choice is more dependent on the curing temperature than the scale of production.

2.3.2 MANUFACTURING METHODS

Hand lay-up, vacuum assisted and autoclave curing

Hand lay-up is when dry reinforcement is applied to a mould surface and then impregnated manually, usually with the aid of a brush or roller. The moulds used in hand lay-up are normally made from composites. The surface of the mould is usually gel coated and then sanded and polished to give a gloss surface on the finished part. The curing cycles of hand lay-ups are generally below 180°C, because of the limitations of using a composite tool. If a gel coat is needed on the finished part, it can be added before the laminate is laid up on the tool. The gel coat is then brushed on and left to partially cure, after which the laminate is laid up on the partially solidified gel coat.

The tool has to be prepared before the lay-up is done, which consists of cleaning the surface, followed by applying the appropriate release agents. This prevents the thermoset matrix from bonding to the tool surface. An illustration of vacuum assisted hand lay-up can be seen in Figure 2-17. The laminate is laid up on a tool, coated with release agent, and a peel ply layer is added on top of the laminate. This layer will give the bag side of the laminate a rough finish. After the peel ply, a layer of breather cloth is put on top with a layer of release film, so that the breather cloth does not bond to the peel ply. The breather cloth acts as a passage to absorb low pressure air into excess resin.

Hand lay-up can be cured in three ways. Firstly, it can be cured in oven or ambient conditions with no additional assistance. This method is not used on high performance parts as it results in a high void content. The second, more commonly used, method is to add a vacuum bag and cure the laminate under vacuum inside an oven (Figure 2-17). This method minimizes air trapped in the laminate and increases its performance. The third method is to use an autoclave, which is not typically used with composite tools, but rather with metal machined tools. An autoclave applies positive pressure, combined with an additional vacuum and results in the least amount of air in the laminate. The effect of laminate performance, due to air trapped in the laminate, can be seen in Figure 2-9. The more air present in the laminate, the less the reinforcement weight fraction becomes, and so its performance decreases. Autoclaves are generally used in combination with pre-impregnated materials rather than dry fabric resin combinations. Aerosud ITC does not have an autoclave but is in possession of an oven for curing, thus only oven curing will be considered.

Table 7 lists the advantages and disadvantages of open tool hand lay-up (out-of-autoclave).

Advantages	Disadvantages
• Freedom of design • Low mould/tooling cost • Low start-up costs • Low to medium capital costs • Relatively simple process • Tailored properties possible • High strength, large parts possible	• Low to medium parts per annum • Long cycle times • Labour intensive • Exposure of possible volatile compounds • Not the cleanest process • Only one surface has aesthetic appeal • Operator skill dependent • Sharp corners and edges are reduced

Table 7: Advantages and disadvantages of hand lay-up [7]
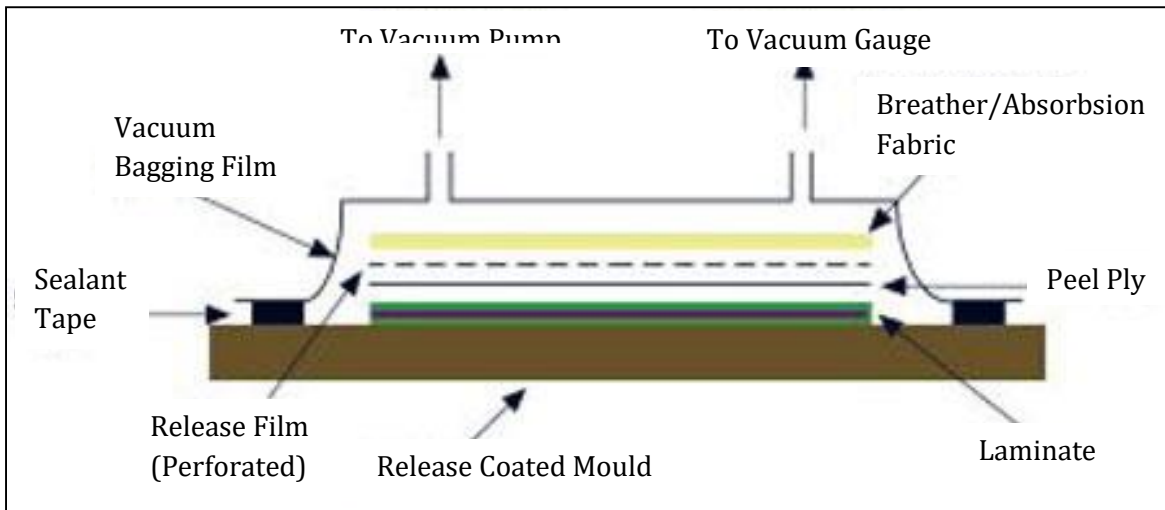
Figure 2-17: Vacuum assisted hand lay-up [25]

Resin transfer moulding and vacuum infusion

RTM and vacuum infusion are both processes where dry reinforcement is placed on the mould and infused with the matrix, with the assistance of a pressure gradient. The difference between resin transfer and vacuum infusion is in the moulds. RTM has matched tooling, while vacuum infusion has a one-sided open tool (Figure 2-18). This gives RTM two aesthetic tool surface sides, but with the disadvantage of higher tool cost. RTM usually yields better part performance than vacuum infusion (Figure 2-16). The curing of these two manufacturing methods are the same as for the hand lay-up method. These two processes are cured under pressure in an oven or at room temperature, depending on the resin requirements.
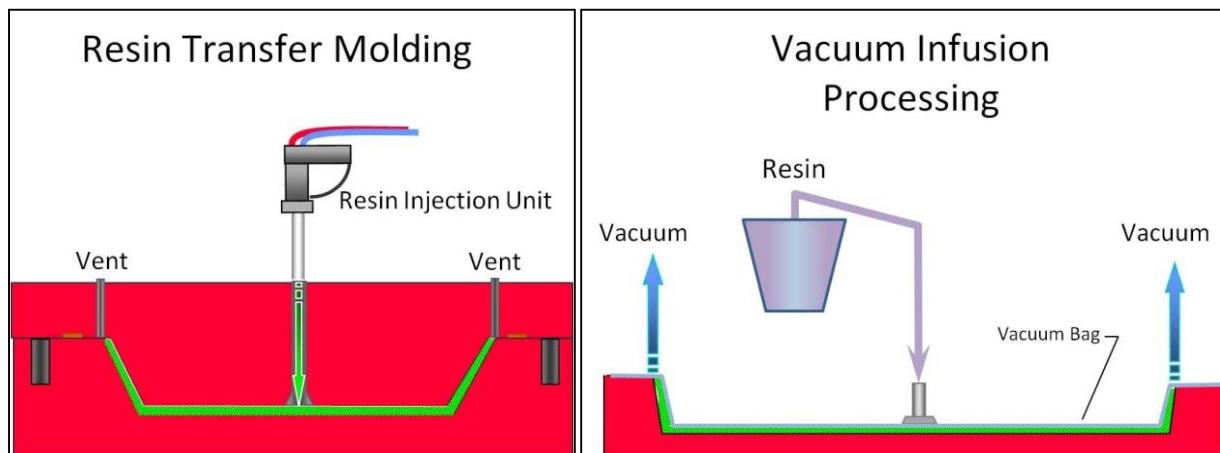
Figure 2-18: RTM and vacuum infusion [26]

2.4   LIMITATIONS OF COMPOSITES

2.4.1   IMPERFECTIONS INTRODUCED IN MANUFACTURING

The imperfections introduced in the manufacturing and processing of components are the main reason for the discrepancy between the ideal data sheet material properties and the actual product properties. Different manufacturing techniques result in a difference in the performance of the final product (Figure 2-16). These differences in performance are caused by the amount and type of imperfections introduced in manufacturing. Imperfections that have the greatest influence on the final part's performance are voids, porosity and shrinkage [27]. There are secondary negative effects, such as placement inaccuracy, bending and breaking of the fibre.

Voids and porosity are air trapped in the matrix of the laminate. The difference between the two is the size of the trapped air pocket - voids are large areas of air, while porosity is clusters of small air bubbles. These two types of imperfections are considered the most critical in composite part manufacturing [28]. These occur when the matrix fails to push out all the air in the dry reinforcement or when gasses, generated from the matrix curing, are trapped in the laminate. Voids are normally found at layer interfaces or in specific plies. Large amounts of porosity and voids can significantly reduce the structural strength of the laminate, while smaller amounts can reduce the interlaminar shear strengths. They can also lead to significant water absorption, degradation and added part thickness [29].

Shrinkage occurs when the thermally induced dimensional change, caused by a thermal curing cycle, leads to volumetric change in the resin. The rearrangement of molecules to a more compact state, during curing of some resins, can lead to shrinkage. Thermal induced shrinkage is when the laminate is cooled down from curing temperatures; this can occur in the mould or the part. Epoxy shrinkage ranges from one to five percent, while vinylester ranges from five to twelve percent [27]. The thermal shrinking can aid in the demoulding of parts if used correctly, but it can also induce negative effects like warping [29].

2.4.2   IMPERFECTIONS INTRODUCED IN PROCESSING

Processing of the composite part is the required actions to finish the manufactured composite part, giving it its final size, shape and finish. This also encompasses joining and assembly of the composite parts.

Machining of composites is the mechanical removal of excess material to acquire a desired dimension or hole. The machining process variables, such as feed rate, speed and cutter shape, are the main variables that govern the damage done to the remaining material [30]. Wear and tear on the cutting tool is one of the main causes of processing damage to composite parts. The cutting of a composite part becomes less efficient if the cutting tool is blunt and results in tearing rather than cutting. Tool wear leads to excess temperature in the composite, because of abrasion; and this could damage the resin system and pull out the fibres. Loss of productivity and dimensional inaccuracy are also coupled with cutting tool wear [31].

The main quality reducing effect of composite machining is delamination, which is the separation of layers or plies of the laminate. Drilling and milling is a possible source of delamination in composite processing [31]. The amount of delamination is directly proportional to the condition of the cutting tool. Sharper tools cut cleanly and thus cause far less delamination than worn tools and can be observed by close inspection of the cutting edge. Protruding fibres on the outer layers of the part is a clear indication of delamination [32]; this is illustrated by Figure 2-19. From this figure it is easy to conclude that if the drill bit is sharp, the force used to push the drill through the laminate is lessened and thus reduces the delamination effects. Delamination severely affects the structural stability and fatigue behaviour of the composite part at the fastener interface. An illustration of delamination is shown in Figure 2-20.
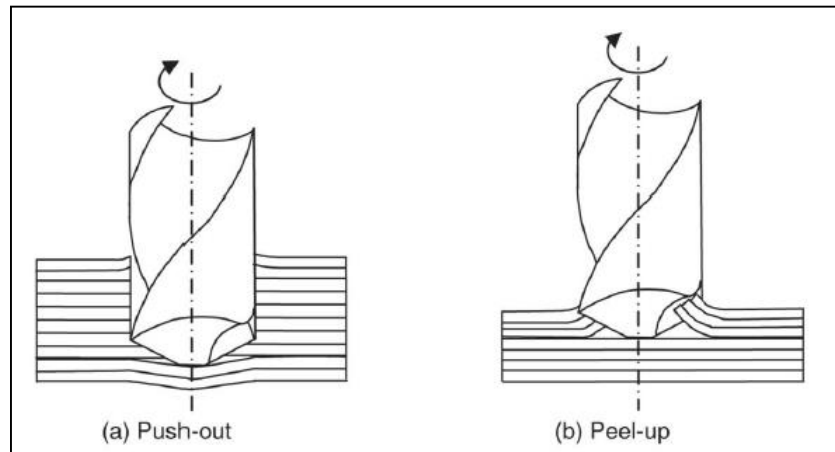
Figure 2-19: Delamination due to drilling of composites [31]
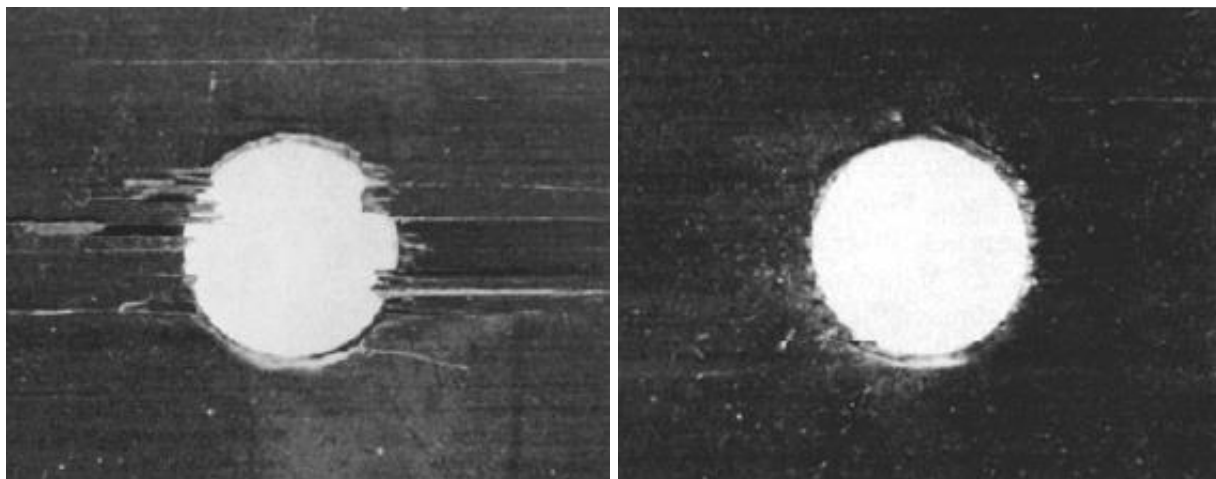
Figure 2-20: Composite carbon drilling specimen showing delamination due to drilling on the left and a clean cut hole on the right [7]

2.4.3 JOINING OF COMPOSITES

The main joining methods for composite parts are mechanical fasteners, adhesive bonding and welding [27]. Welding is specifically used with thermoplastics and will thus not be considered in this study.

Mechanical fasteners

The main variables that define the mechanical fasteners' limitations are joint geometry, laminate lay-up and fastener type [33]. The typical failure modes of mechanical fasteners used in composite structure are net tension, bearing, shear out, cleavage and failure of the fastener itself [34]. Another consideration when using mechanical fasteners in carbon composites is the possibility of galvanic corrosion [35]. Due to carbon's electrical properties and the common use of aluminium in aircraft structure, there have been many instances of a galvanic reaction between the two materials. This is discussed later in the chapter.

Tension failure of composite fasteners is similar to the failure mode in isotropic materials. It is mostly due to an insufficient tensile area, but could also be that the amount of fibres in the main load-carrying direction is too few [28].

Cleavage tension failure is caused by the lack of edge distance, panel thickness and cross plies [18]. Bearing failure is the local compressive failure of the matrix adjacent to the bolt hole and is normally coupled with the buckling of fibres [28]. The influencing factors that affect bearing failure are diameter of the bolt hole, laminate thickness, material type, staking sequence, washer type and clamping force. Bearing failure can be an accepted mode of failure, because it is not a brittle or catastrophic failure [33]. Designing for no bearing yielding can lead to overly heavy parts, but care should be taken not to induce a brittle "crack on the dotted line" failure mode, this is done through good design.
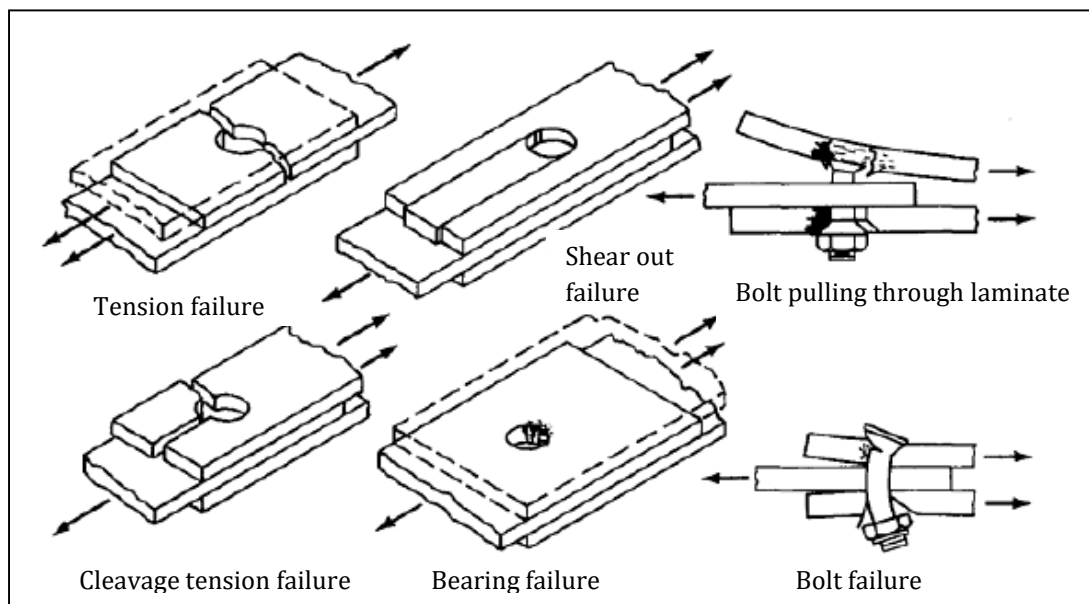
Figure 2-21: Failure modes of fasteners in composite materials [7]

In addition to the failure of the laminate because of a fastener, the fastener itself can fail. Pull-out failure is common when the joint design is inadequate when the wrong selection of fasteners is used [24]. Fasteners should ideally be used in shear rather than tension applications.

Galvanic corrosion

Galvanic corrosion can be defined as the degradation of metallic pats due to an electrochemical reaction within their environment [36]. Between glass, aramid and carbon, carbon is the only reinforcement that is electrically conductive and has galvanic corrosion issues [7]. A galvanic cell forms between carbon (graphite) and the more anodic metals in the presence of an electrolyte such as moisture. This is one of the most common problems with using carbon composites on an aircraft which is mainly aluminium. The potential for galvanic corrosion can be seen in Table 8. The further the two materials are from each other in the table, the more galvanic potential will be produced and thus more corrosion takes place. Carbon has a strong galvanic reaction with aluminium and cadmium; these are two of the most used materials and coating on aircraft fasteners.

The use of titanium, austenitic stainless steel and nickel alloys combined with carbon has become the norm in the aviation industry to reduce the corrosion effects [37]. Graphite is impervious to corrosion itself as it acts as a noble metal, but it will accelerate corrosion in less noble metals [7].

Joining carbon composite to aluminium does present serious corrosion problems but is not prohibited; but it will require special considerations and precautions. Corrosion retardation or prevention can be attained by creating barriers, material changes and isolation from an electrolyte.

ANODIC (Most reative)
Magnesium alloys
Zinc
Alclad 7000 series Al alloys
5000 series Al alloys
7000 series Al alloys
Pure Al and 2000 series alloys
Cadmuim
2000 series Al alloys
Steel and iron
Lead
Chromuim
Brass and bronze alloys
Copper
Stainless and heat resistant steels
Titanuim
Silver
Nickel alloys
Gold
Carbon fiber
CATHODIC (least reactive)

Table 8: Galvanic potential table with seawater as electrolyte [7]

Adhesive bonding

One of the main problems when using adhesively bonded joints on composite assemblies, is the development of through thickness peel stresses [28]. As mentioned earlier, this is the most undesired loading direction for thin composite laminates. In Figure 2-22, the development of this peel stress is shown schematically. It occurs because of the eccentric load path in the joint and can be minimized by proper joint design. It is not limited to a single lap joint and has been seen in double lap joints, even when the laminates are symmetrical about the mid-plane. Some methods to reduce this peel stress in joints, are to taper the thickness of the laminate down on the overlap to limit the amount of peel stress that will be produced. A natural fillet created by excess adhesive that is pushed out of the overlap, also minimizes peel stresses and should not be removed.
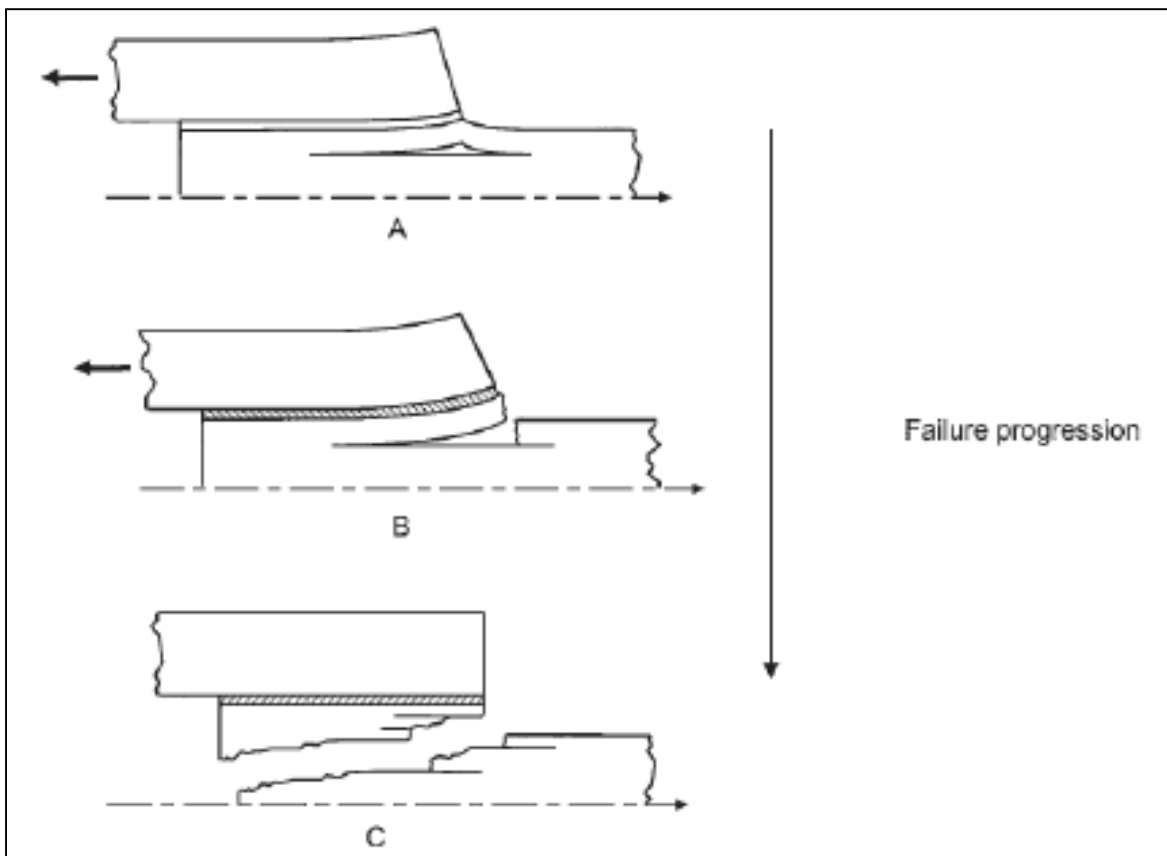
Figure 2-22: Development of peel stress in adhesively bonded composite laminates [28]

2.5 ANALYSIS OF COMPOSITES

Aircraft design has been centred primarily on aluminium since the 1940s, and the use of isotropic analysis has been used successfully for this application. Composites only started being accepted into the aerospace field from the late 1970s [15]. Composites cannot be utilized efficiently through the use of isotropic analysis or design methodologies. They exhibit anisotropic properties and need to be analysed and designed with this in mind. Metallics are well known and have less complicated material properties, which often leads to the exclusion of composites in the selection process.

Figure 2-23 shows the roadmap that is used in the analysis of anisotropic composite materials, which will be discussed in detail in this section.

The direction notation that is used in composite analysis should be noted from Figure 2-23 The principal lamina coordinate system is denoted as 1, 2 and 3 where 1 is the main in-plane fibre direction, 2 is the perpendicular in-plane direction and 3 is the through thickness direction. Thus 1, 2 and 3 are defined by the weave, warp and weft directions and it is these directions that are used in lamina testing. The X, Y and Z directions form part of an arbitrary coordinate system that is used in a laminate lay-up to define the direction of the lay-ups. Thus, if a +45° laminate is specified, it means that the principal direction of the weave should be at an angle of 45° to the zero line defined on the laminate or component.
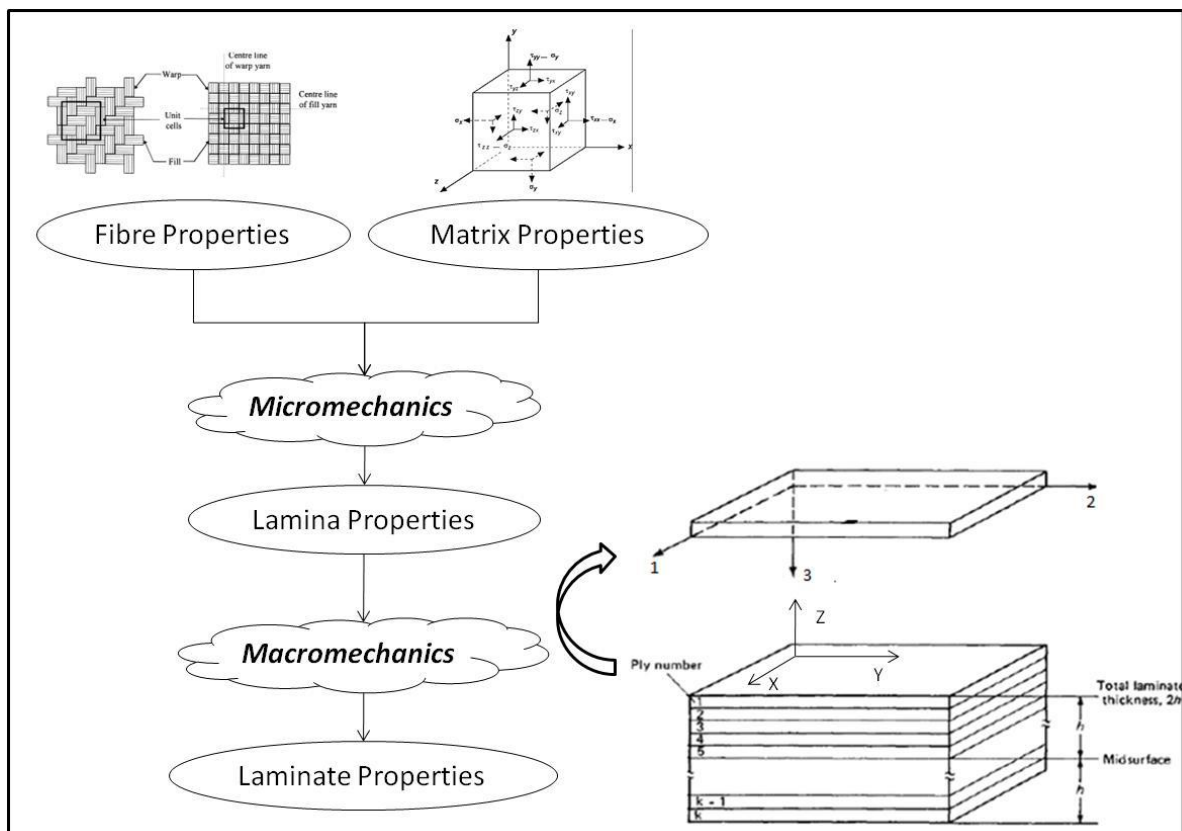
Figure 2-23: The roadmap of composite analysis

The material properties of isotropic metallics do not vary according to the direction of the material, whilst anisotropic or orthotropic composite material properties vary according to the direction in which it is measured. This is due to the non-homogenous nature and the differences between matrix and reinforcement properties. The variation in material properties with respect to direction of a UD composite lamina is illustrated in Figure 2-24. It can be seen that the carbon fibre rovings are very stiff along the fibre direction, but this stiffness reduces as the fibre orientation angle is changed, so that the load is applied at an oblique angle to the fibre direction. The greater the angle, between 0° and 90°, the less the stiffness and strength become. The minimum properties are obtained if the load is applied at a perpendicular angle to the fibres. This can be visualized by saying that the entire load is transferred by the matrix and none by the reinforcement, if the load is perpendicular to the fibre direction. It could almost be said that the properties of the fibres are evident when the loading is directly in the fibres' direction, while the properties of the matrix are evident when the loading is perpendicular to the fibres.
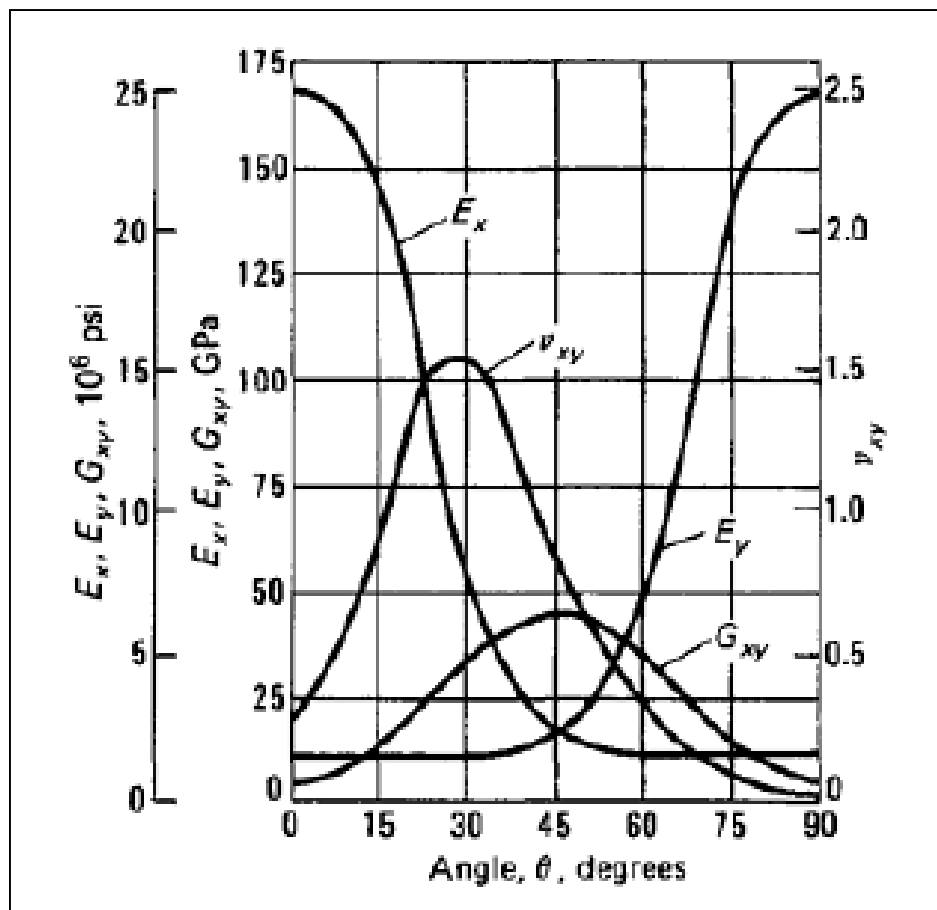
Figure 2-24: Elastic properties of a carbon ±θ lamina [7]

2.5.1 MICROMECHANICS

Partial micromechanics of a thin laminate will be used by the finite element software to determine the lamina properties in various directions, as well as the stress strain relationship of the laminate. In Figure 2-23 it can be seen exactly where micromechanics fits into composite analysis. Micromechanics is the analysis that is used to define the lamina elastic properties in different loading directions under ideal conditions, using the matrix and reinforcement elastic properties as inputs. The analysis is based on the volume fraction rule for composites. In short, the elastic properties of the lamina are defined as the volume fraction of the fibres and resin multiplied by their respective elastic properties. The detail analysis equations are presented in Appendix B.

What macromechanics demonstrates, which is very useful in the design phase, is that the tensile elastic properties of a lamina are dominated by the fibre properties. This is because the fibre tensile elastic properties can be up to a factor 100 higher than the matrix tensile elastic properties, but this is not the case for the compression elastic properties. The compressive elastic properties of a lamina are much more proportionally dependent on the resin than fibre properties. This is due to the fact that the resin compressive properties are very close to that of the fibres, and because the fibres cannot take compression without the support of the resin.

The assumptions used in micromechanics are as follows:

- Laminates are considered thin and are therefore assumed to be in an in-plane stress condition (Out-of-plane shear modulus is zero , $G_{13} = G_{23} = 0$)

Fibres are:
- Homogeneous
- Linearly elastic
- Regularly spaced
- Perfectly aligned

The matrix is:
- Homogeneous
- Linearly elastic
- Isotropic

The lamina is:
- Macroscopically homogeneous
- Linearly elastic
- Macroscopically orthotropic
- Initially stress free

2.5.2 MACROMECHANICS

Macromechanics is used by the finite element software to determine the laminate stiffness properties and the response of the laminate under loading conditions and is also referred to as the classical laminate theory. The input required for this analysis is the lamina properties, which are determined using micromechanics (Figure 2-23). The detail of macromechanics can be found in Appendix B.

One of the main theories that macromechanics demonstrates is that laminates have certain coupling effects under loading. If a laminate has the same number, orientation and materials in a symmetrical distribution about its mid-plane, it is referred to as a symmetrical lay-up. These types of lay-ups are preferred due to the lack of coupling effects that can be analytically seen in macromechanics. This coupling effect is only apparent when a laminate is asymmetrical about the mid-plane. When a pure tensile load is applied to these types of laminates a moment is generated due to the stiffness differential across the mid-plane. This moment generation can cause through thickness stresses, which can lead to failure.

2.5.3 FAILURE CRITERIA

The standard way of determining failure of materials is derived from uniaxial stress states. However, in practice, the materials are usually in a biaxial or triaxial stress state. It would be physically impossible to determine the strength characteristics of laminates in all possible directions, thus there needs to be a method of using the strength data of the principal material directions to evaluate stress fields in any direction.

In composite materials, the well known principal stress and strain methods, such as the Mohr's circle, cannot be used due to the material properties' variation with load direction. Another fact that makes composite strength difficult to determine is that the strength tensor, if one even exists, is much more complicated to transform, unlike the stiffness properties. The strength properties should be of a higher order than the stiffness properties and involve a variety of failure mechanisms that could be influenced by direction change [18]. For this reason the failure envelopes are not derived mathematically from principals, but rather from curve fitting of experimental results. That is why it is called failure criteria rather than theories. Unfortunately with this curve fitting process we lose the ability to determine the mode of failure, but are rather just aware of a convenient stress state at which some sort of failure would occur.

The main failure criteria for composites are used in the biaxial stress state (Figure 2-25). The limitation of these failure criteria is that is does not account for microscopic failure mechanisms that can be induced by manufacturing methods and this compromises the part quality.

This study will only use the Tsai-Hill failure criteria, but below is a list of other criteria.

- Maximum stress failure criteria
- Maximum strain failure criteria
- Tsai-Hill failure criteria
- Tsai-Wu failure criteria
- Hoffman failure criteria
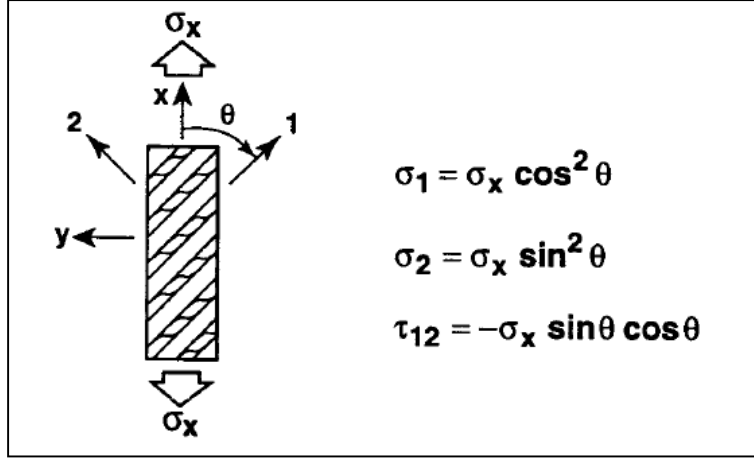
Figure 2-25: Biaxial stress state used in failure criteria [18]

Hill proposed yield criteria for orthotropic materials as follows [38]:

$$(G + H)\sigma_1^2 + (F + H)\sigma_2^2 + (F + G)\sigma_3^2 - 2H\sigma_1\sigma_2 - 2G\sigma_1\sigma_3 - 2F\sigma_2\sigma_3$$

$$+2L\tau_{23}^2 + 2M\tau_{13}^2 + 2N\tau_{12}^2 = 1 \qquad \text{Equation 1}$$

With the stresses and axis system defined in Figure 2-25.

The Hill parameters; G, H, F, L, M and N are considered failure strengths. This criterion is an extension of the Von Misses yield criteria for isotropic materials. Some authors call this the distortion energy criterion. The Hill parameters were related to the usual failure strengths (X, Y and S) by Tsai as follows [39];

If only τ_{12} acts on the body:

$$2N = \frac{1}{S^2} \qquad \text{Equation 2}$$

Similarly, if only σ_1 acts on the body:

$$G + H = \frac{1}{X^2} \qquad \text{Equation 3}$$

And if only σ_2 acts:

$$F + H = -\frac{1}{Y^2} \qquad\qquad \textit{Equation 4}$$

And through thickness stress; σ_3 acts:

$$F + G = \frac{1}{Z^2} \qquad\qquad \textit{Equation 5}$$

On combination of equations 30, 31, 32 and 33 and under the assumption of plane stress ($\sigma_3 = \tau_{13} = \tau_{23} = 0$) with fibres in the 1 direction, the following equation is derived at:

$$\frac{\sigma_1^2}{X^2} - \frac{\sigma_1 \sigma_2}{X^2} + \frac{\sigma_2^2}{Y^2} + \frac{\tau_{12}^2}{S^2} = 1 \qquad\qquad \textit{Equation 6}$$

This equation is usable because the strength terms of the composite are familiar lamina principal strengths X, Y and S. The appropriate compressive and tensile values of the strengths should be used, depending on the signs of σ_1 and σ_2.

The experimental verification of this failure criterion is shown for E-glass-epoxy laminates in the Figure 2-26. There is a good correlation between the failure criterion and experimental results using E-glass – epoxies at various ply angles.
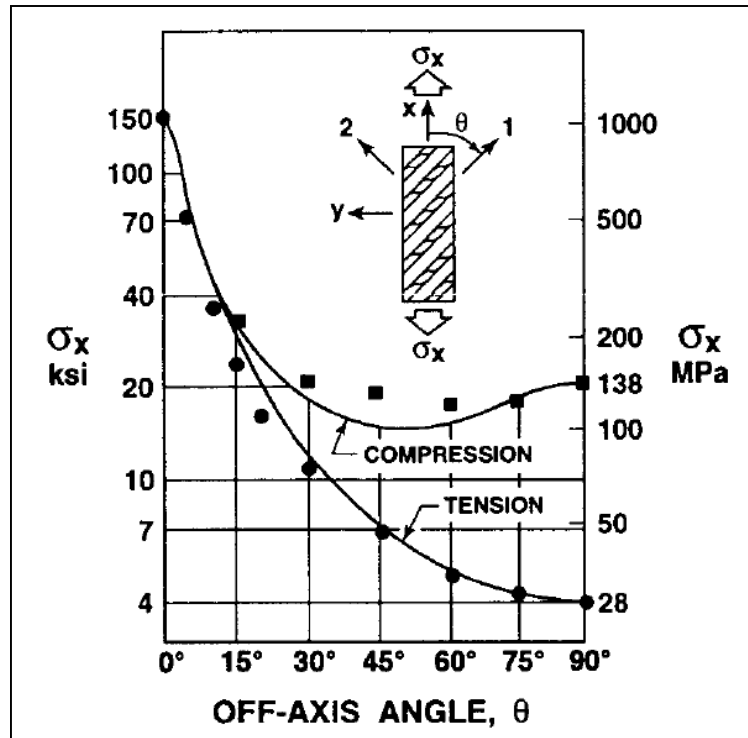
Figure 2-26: Tsai-Hill failure criterion with E-glass-epoxy laminate [39]

The Tsai-Hill criterion seems to be an accurate failure criterion for E-glass-epoxy [18]. This might not be the case for other composite materials, depending on whether the failure mode of the material is brittle or ductile.

2.6 SIMILAR WORK DONE

Vaidya et al. describes the design and manufacture of woven reinforced glass/polypropylene composite for a mass transit floor structure [40]. Although the matrix of this study is limited to thermoset, the analysis and design methodology remains similar to that of thermoplastic. The reason they chose thermoplastic was because of the greater impact resistance combined with high production volumes that was required. The material properties of the glass fibre impregnated with PP were determined using material tests. These material tests were all in accordance with the American Society for Testing and Materials (ASTM) composite testing standards. The material properties were used as inputs in the FEA using ANSYS 7.0 software. The FEM was validated by using a section of the floor, measuring the deflection under static loads and then comparing them to the FEA. This resulted in a weight saving of 40 % compared to the original metal and wood construction.

Two types of mechanical tests were used to determine the material properties of the composite laminate in the design; they were tensile tests and three point bending tests, according to the ASTM D3039M and ASTM D790M standards. The tensile tests were done to determine the ultimate tensile stress and tensile modulus. A tensile testing machine, tabbed specimens and an extensometer were used to determine the modulus. The extensometer was only applied up to 50 % of the breaking strain. The three point bending tests were done on a sandwich panel. This revealed the initial failure mechanism of wrinkling of the compression face and ultimate failure was tensile fracture to the tensile face. These two allowables were used in the FEA.

The detail design was done using CAD software, namely Pro/Engineer, and was used as input into a meshing program (Hypermesh 5.1®). The meshing software was used for pre-processing and mesh generation. SHELL 99 elements were used in the FEA. These elements are two-dimensional elements and have eight nodes, one at each corner and one in between each corner.

The nodes all have six degrees of freedom; these are translations and rotations in each direction. This FEM with boundary conditions can be seen in Figure 2-27.
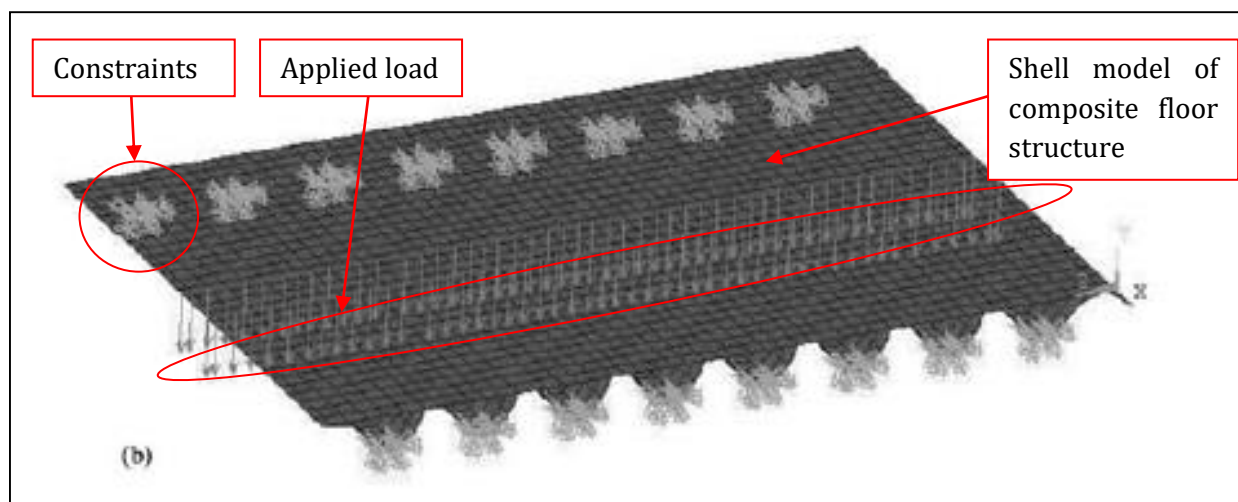
Figure 2-27: FEM of composite floor structure using two-dimensional shell elements [40]

Orthotropic material properties were used in the analysis. The modulus and material limit stress in the principal directions, which were used in the FEA, were the average values from the tensile tests. The shear values of the lamina were calculates by using the micromechanics (volume fraction law) and data sheet values. It was assumed that the lamina consisted of 40 % glass volume fraction. Note that the elastic properties are assumed to have the same values in both principal directions; this is done because the fabric is considered balanced with the amount of fibres in both directions. The fact that the experimental deflections are within 14% of the FEA shows this assumption of no warp and weft interaction is valid. These values are given in Table 9:

Property	Value
E_x	9.91 GPa
E_y	9.91 GPa
E_z	1.03 GPa
ν_{xy}	0.11
ν_{yz}	0.22
ν_{xz}	0.22
G_{xy}	1.8 GPa
G_{yz}	0.75 GPa
G_{xz}	0.75 GPa
E_{fiber}	70 GPa
E_{matrix}	1.03 GPa
G_{fiber}	30 GPa
G_{matrix}	0.75 GPa

Note: Values of E_x, E_y are measured from tensile tests, E_z is considered as the matrix property, The Poisson's ratio values are from literature, shear properties are calculated from rule of mixtures, and the constituent properties are from the manufacturers.

Table 9: Elastic properties of woven glass/polypropylene composite [40]

The static tests conducted to validate the FEA are shown below. LVDT's were used to measure deflection and load cells were used to measure the force that was applied via hydraulic actuators.
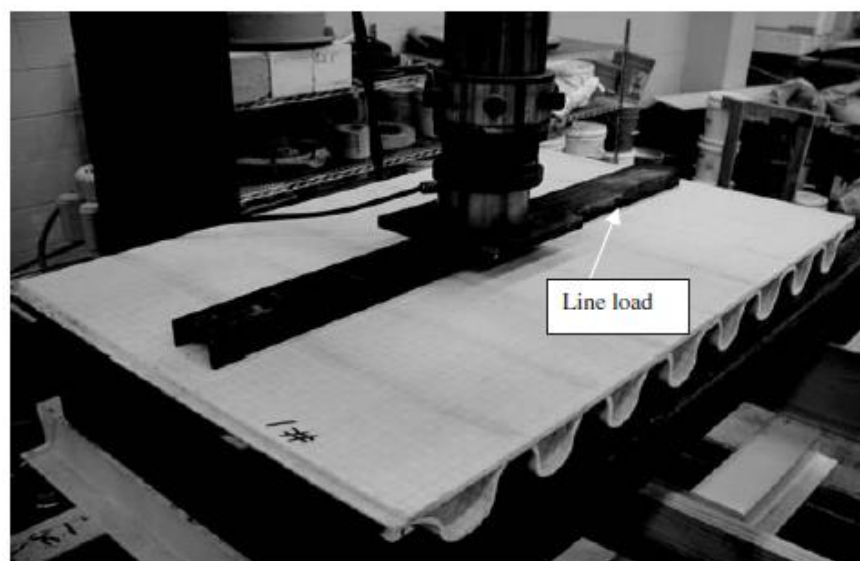
Figure 2-28: Static test of composite floor structure [40]

The comparison of the FEA and static tests are given below:

Case	Boundary Condition	Loading Condition (N)	Maximum Deflection (mm) (Experimental)	Maximum Deflection (mm) (Analysis)	Difference (%)	Maximum Stress (MPa) (Analysis)
1	Simply supported	4448 (concentrated load)	1.3	1.11	14.61	7.92
2	Simply supported	8896 (line load)	1.1	1.24	12.72	8.65

Table 10: FEA validation of composite floor structure [40]

Table 10 shows that the difference in FEA and static testing was around ±13 %. The maximum stress from FEA was 8.65 MPa; this is a very small fraction when compared to the failure stress of glass/PP lamina, which is close to 200 MPa. This means that they only loaded the component to around 4.3 % of the ultimate failure load.

The design of a low mass, dimensionally stable, composite base structure for a spacecraft by Sairaja et al. aims to reduce the weight of the current part by 35 % [41].

The design requirements of the composite spacecraft structure are listed below:

- *Minimum mass*
  Mass should be lower than the aluminium part which is currently being used. This was accomplished by using a commercially available optimizing program named OPTISTRUCT.

- *Dimensionally stable*
  Due to the large temperature difference the spacecraft encounters during service, the thermally induced dimensional changes had to be limited, which was accomplished by using MSC Nastran's thermal analysis and evaluating the displacement results and thermal stresses.

- *Stiffness*
  The stiffness during a launch was critical and the natural frequency was limited. A normal mode analysis using MSC Nastran was used to determine the first mode shape and frequency.

- *Loads*
  The failure criteria used in the linear static analysis was the Tsai-Wu theory under design loads. The buckling factor was checked and limited to 2, using MSC Nastran's buckling analysis.

- *Geometrical constraints*
  Several geometrical constraints were listed. They are interface areas and some interface material definitions.

The material properties of the CFRP, UD and bidirectional reinforcement in the FEA were determined by testing and are listed in the Table 11.

Property	M55J/M18 (UD)	43090/M18 (BD)
Young's modulus, E_{LL} (GPa)	267.0	146.3
Young's modulus, E_{TT} (GPa)	6.3	146.3
In plane shear modulus, G_{LT} (GPa)	3.8	4.1
Poisson's ratio, ν_{LT}	0.26	0.03
Mass density, ρ (kg/m^3)	1600	1660
Ply thickness, t_f (mm)	0.095	0.08
Coefficient of thermal expansion (CTE), α_L (10^{-6}/°C)	−2.7	−1.8
α_T (10^{-6}/°C)	34.8	−1.8
Tensile strength, σ_L^t (GPa)	1.54	0.412
σ_T^t (GPa)	0.021	0.412
Compressive strength, σ_L^C (GPa)	0.375	0.206
σ_T^C (GPa)	0.118	0.206
In plane shear strength, τ_{LT} (GPa)	0.052	0.049

Note: Subscript 'L' represents the fiber direction, subscript 'T' represents direction perpendicular to the fiber, superscript 't' represents the tension and superscript 'C' denotes compression.

Table 11: Material properties of CFRP prepreg [41]

It is clear from the above properties that the thin laminate theory was used in the FEA, as there are no values for the out-of-plane material properties. It is also clear that the properties for the 43090 fabric combined with M18 resin has the same properties in both principal directions. The FEA was done using MSC Nastran with four node layered shell elements. A lumped mass was inserted in the FEM using rigid body elements. The boundary condition at the interface was modelled using multipoint constraints on the edge. This FEM is shown in Figure 2-29 and it demonstrates that a two-dimensional shell element mesh, in combination with a MPC, is used to simulate the mass of the structure.
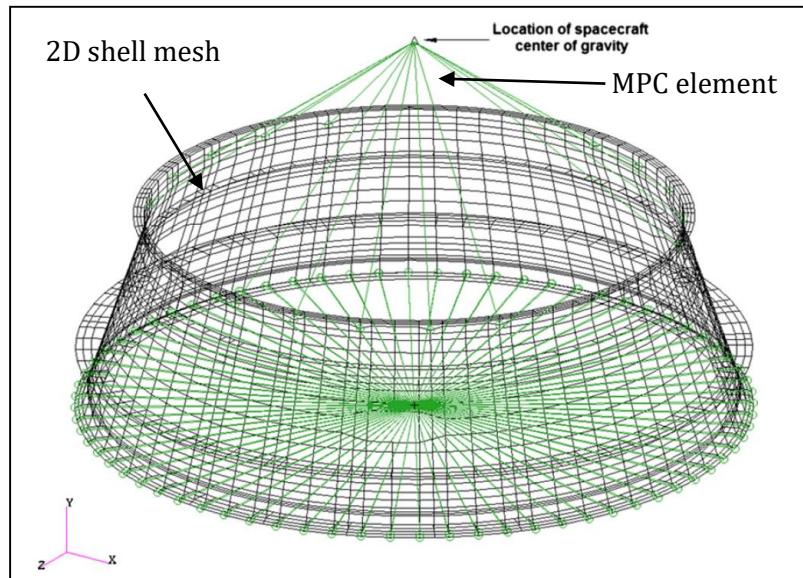
Figure 2-29: FEM of composite spacecraft structure [41]

The manufacturing of the part was done using one-sided female tools; this was used to ensure the dimensional accuracy of the outer surface, which is the interface surface. An autoclave was used in the curing of the laminates. A typical ply detail of the part is shown in Figure 2-30.
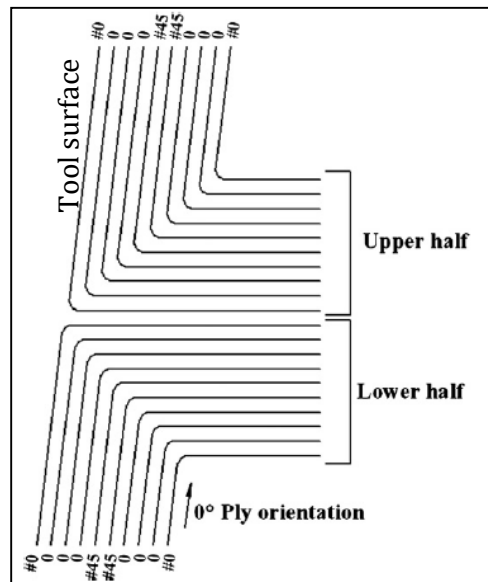
Figure 2-30: Ply detail of composite spacecraft part [41]

Sections of the structure were fabricated separately and bonded together using epoxy adhesive. The bonding assembly is illustrated in Figure 2-31.
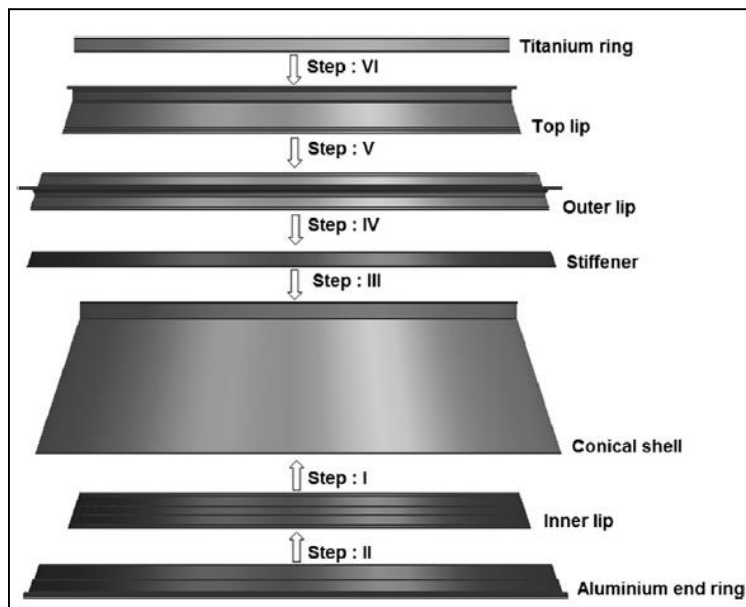
Figure 2-31: Assembly sequence of composite spacecraft ring [41]

Liu et al. describe a multiscale approach to design a carbon composite frame for an electric vehicle [42]. The paper deals with the determination of the elastic properties of the laminate, for use in the FEA of the crash worthiness of the frame. They used a FEM and the homogenizing technique to determine the laminate properties. These properties were validated with biaxial tensile and three point bending tests. This method of composite material characterization showed errors of 4.04 % and 7.79 %, with respect to tensile and three point bending tests. A weight saving of 28 % was achieved compared to the previous glass fibre frame. In the Figure 2-32 the multiscale approach of reference [42] is illustrated.
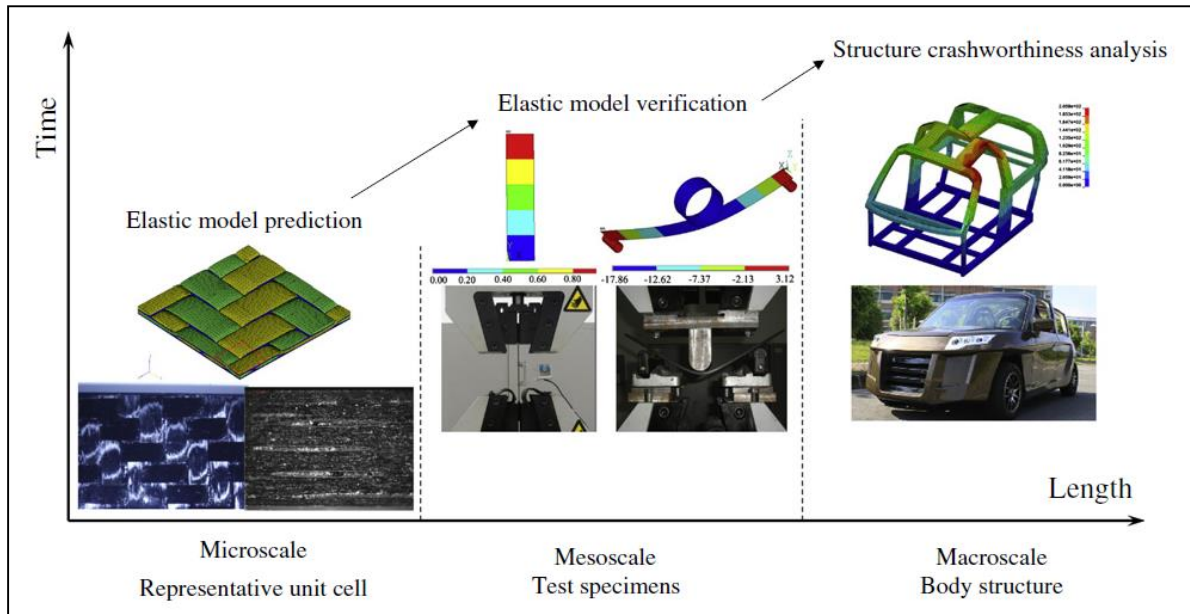
Figure 2-32: Multiscale approach followed in the design of a composite frame [42]

The elastic model prediction of the composite laminate was done using FEA of a unit cell. A volume element, representing the microstructure, was used in this FEA. Various boundary conditions and deflections were used to determine the homogenized properties of the lamina. These constitutive properties were used in the crash worthy analysis of the frame. Below is a summary of the determined material properties compared to tested values:

	E_x (GPa)	E_y (GPa)	E_z (GPa)	G_{xy} (GPa)	G_{yz} (GPa)	G_{xz} (GPa)	v_{xy}	v_{yz}	v_{zx}
This paper	53.81	53.32	7.47	3.34	2.01	2.00	0.13	0.14	0.14
Ref. [21]	55.25	55.05	–	3.55	–	–	0.05	0.06	–

Table 12: Mechanical properties of carbon twill weave laminate [42]

2.7 SAFETY AND ENVIRONMENTAL CONSIDERATIONS

Engineering can be seen as the action that links pure science to society. This creates a social responsibly to the engineer to ensure public safety through the engineering process. This should be placed before all else in the design, development and decision making of the engineer. It is therefore crucial to show that the engineer has shown regard to the public safety and environmental effects of his actions. This is the key to a sustainable future and is often disregarded in the design process.

Persons working with thermoset materials face some risk that the material can affect their health. The persons handling the material have to be educated on the methods that can be used to minimize these risks. The material safety sheet on the chosen materials should list all the possible safety concerns with recommended treatments. Generally there are no health risks with the cured thermosetting resins, but in rare cases it can cause eczema in persons that are already sensitized [27]. Resins and hardeners may cause skin, eyes and respiratory tract allergies in some people. The preferred way to reduce the risk of these allergies is to work in a well ventilated area and to minimize contact with resins by using gloves [27].

Type of composites	Recycling methods	Technology features	Status of the technology
Thermoplastic–matrix composites	Remelting and remoulding	•No separation of matrix from the fibre	More studied for the manufacturing or process scrap.
		•Regrinding – compression or injection moulding/extrusion – compression moulding •Product as pellets or flakes for moulding •Fibre breakage – property degradation	Commercial operation? unknown
	Chemical recycling	•Dissolution of matrix •Fibre breakage – property degradation	Not much studied
	Thermal processing	•Combustion or incineration for energy recovery (option for old scrap)	Not much studied or published
Thermoset–matrix composites	Mechanical recycling	•Comminution – grinding – milling •Products: fibres and fillers •Degradation of fibre properties	Commercial operation ERCOM (Germany) Phoenix Fibreglass (Canada)
	Thermal recycling	•Combustion/incineration with energy recovery •Fluidised-bed thermal process for fibre recovery •Pyrolysis for fibre and matrix recovery	Promising technology
			Hindered by the market for recycled fibres
	Chemical recycling	•Chemical dissolution of matrix •Solvolysis (supercritical organic solvent)/hydrolysis (supercritical water) •Product of high quality fibres, potential recovery of resin •Inflexibility of solvent and potential pollution	Only laboratory studies Promising
Metal–matrix composites	Re-melting – casting	•Dir-cast scrap: direct remelting – casting	MMC is much more expensive than the alloys or reinforcements
		•Foundry scrap: direct remelting with (dry Ar) cleaning •Dirty scrap: remelting – fluxing – degassing cleaning •Very dirty scrap: metal recovery only – remelting and refining to separate reinforcement from Al (alloy)	Aiming at reuse of MMC

Table 13: Current overview of composite recycling technologies [43]

There are more and more directives to ensure that engineers design with the environmental impact as a design requirement. By 2015, the European Union hopes to have all new vehicles designed with an 85 % recyclable strategy at the end of its product life [44]. The aerospace's buy-to-fly ratio is around 1.7 to 1; this means that for every 1.7 kg of material bought, 0.7 kg gets scrapped [21]. At present the most commonly used method for the recycling of aerospace composites is land filling. McDonald Douglas sends on average 49000 lbs (22226 kg) every year for land filling. Table 13 gives a current overview of composite recycling technologies. Currently there are very crude methods for the recycling of composite materials, but the technological growth looks promising for the future and this is when the aircraft components will start to near its end of life stage.

2.8 CONCLUSION

The literature survey introduced the reader to composite materials, their manufacturing methods, its limitations and analysis methods. It also gave insight into the methodology used by others to accomplish similar tasks involving composite component design and development, using FEA and other computer aided software. In short, the following was revealed in the literature survey:

- Only glass, aramid and carbon fabrics will be considered
- Only thermoset resins will be considered
- Only out-of-autoclave, hand fibre placement manufacturing methods will be considered
- Galvanic corrosion will limit the fastening of carbon to aluminium with mechanical fasteners
- All drilling and cutting tools has to be sharpened accordingly to reduce delamination
- Adhesive bonding is to be designed in such a way to reduce peel stresses
- Tsai-Hill failure criterion will be used in the FEA
- Two-dimensional shell elements are the norm in modelling thin laminate components in FEA
- Material input properties will be tested in accordance with ASTM standards
- Validate the FEM with static testing of the component
- Manufacturing should comply with the health and safety data sheet of all materials
- There are sufficient methods for the recycling of composite components

3 DESIGN OF THE VENTRAL FIN

3.1 INTRODUCTION

In this section, the design phase of the ventral fin will be discussed in detail. The design requirements used in the concept generation will be the starting point of this chapter. The process to move from concept to detail design will be an iterative process and is discussed in detail in this chapter. The design will have to take the manufacturing method and the type of materials used into consideration. Composite design is much more integrated with the manufacturing method and the material selection due to the large effect they have on the component properties. The concept to detail design process involves selection and understanding of material combinations, reinforcement types, matrix type manufacturing methods and post-processing effects. The "Trinity" based development cycle (Figure 3-1) will be followed [45]. This design cycle combines classical geometrical design with material selection and manufacturing methods as one integral solution.

This design methodology should be applicable to most other composite parts on AHRLAC XDM and if the same steps are followed, it should result in an adequate composite component. Further, more detailed, optimization can be done to reduce mass, to increase stiffness or to optimize other parameters, but this will not be covered in this study.
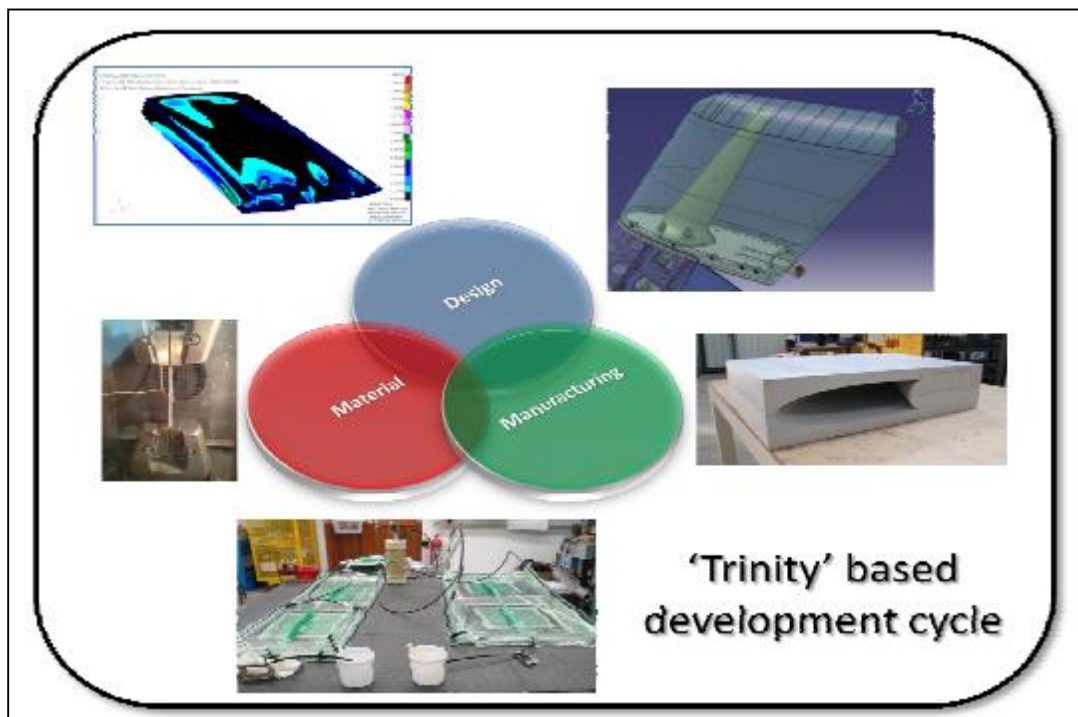
Figure 3-1: Trinity based development cycle [45]

3.2 DESIGN REQUIREMENTS

The design requirements will guide the design phase of the composite ventral fin into an acceptable component concerning all parameters. This is where all the functions of the fin need to be listed combined with the parameters that influence decision making during the development phase. This could well be the most important part of the developmental cycle, because if this is done incorrectly, the chosen concept could be jeopardized and the analysis that follows would be done in vain. The design requirements will be divided into sections centred on the following: geometry, loads and design requirements. A common design method is when the functions that the component had to fulfil are listed, and then designing within these limits [41].

3.2.1 GEOMETRY

In this section the geometric constraints and requirements will be listed and discussed. They are the following:

- Outside mould line   - The outside mould line (OML) of the aircraft as determined by the aerodynamicist.
- Interfaces   - The attachment interfaces of the fin to the rest of the airframe and other parts.

Outside mould line

The OML of the ventral fins, as specified by the aerodynamicist, can be seen in the figures below. This was derived using computational fluid dynamics (CFD) so that the ventral fin can perform its main aerodynamic functions of increasing the effectiveness of the vertical stabilizer. The main function is to stabilize the aircraft in the lateral direction. The outside surface of the fins must have a smooth surface in order to reduce drag as much as possible and is also the aesthetic side of the part. Under aerodynamic loading, the skins of the fin will deflect from the theoretical OML; this deflection has to be limited so that the fin can still serve its aerodynamic function efficiently. This deviation of the airfoil surface under aerodynamic loading is limited by the aerodynamicist to 10 mm locally. The bottom tip surface of the ventral fin is angled so that in the event of over rotation on takeoff, the radius surface would come into contact with the runway completely (Figure 3-5).
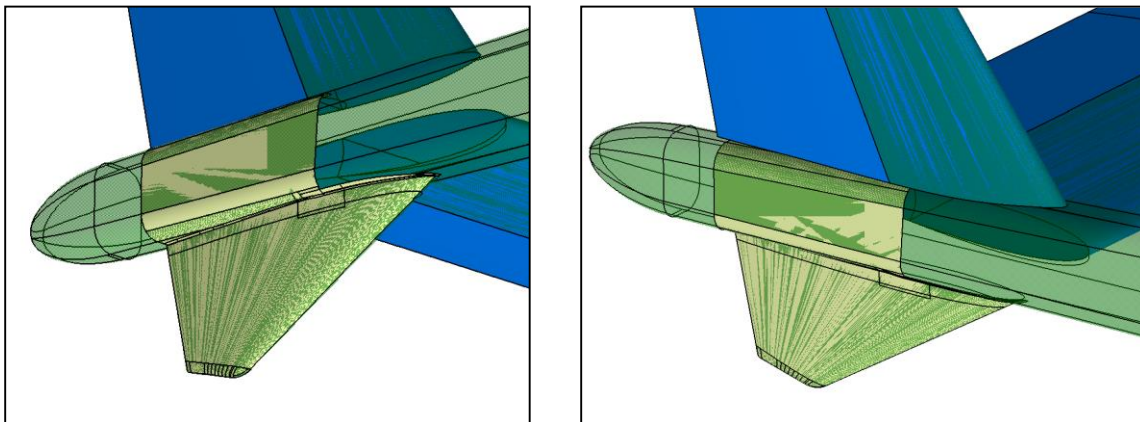
Figure 3-2: Ventral fin OML on AHRLAC XDM

Interface parts

There are three parts that the ventral fin interfaces with. They are the tail boom, tail cone and antenna. The load bearing attachment to the tail boom is the most critical. If this attachment fails the fin will completely detach from the aircraft and the aircraft would lose some of its lateral stability. The other function of the fin is to provide an attachment point for the tail cone. These tail cones are designed separately from the fin as to provide an interchangeable part that can house various electronic sensors. The design weight of the tail cone assembly with sensors is given by the design engineers as 6.1 kg. These are the two main structural attachments and are shown in Figure 3-3 as the green areas and labelled fastener set 1 and 2.

The third part that interfaces with the fin is the antenna. This antenna has to point downward and should be mounted inside the fin to provide protection from the elements. The antenna mounting point can also be seen in Figure 3-3.

All interface flanges of the composite components must have a minimum thickness of 2.5 mm so that the chosen countersink washer can be used without creating a knife edge hole, which would be undesirable from a structural viewpoint.

The last geometrical requirement involves the right hand side fin. This fin has the added task of housing the control linkages to the elevator, however, the linkages do not connect to the fin, they merely pass through it. Under load, the fin should not interfere with the operation of this linkage. The figure below shows the linkage and the proposed cut-out for assembly, in red. This study will only focus on this specific fin. The only difference between the left hand side fins is that there would be no cut-out, as shown in Figure 3-3.
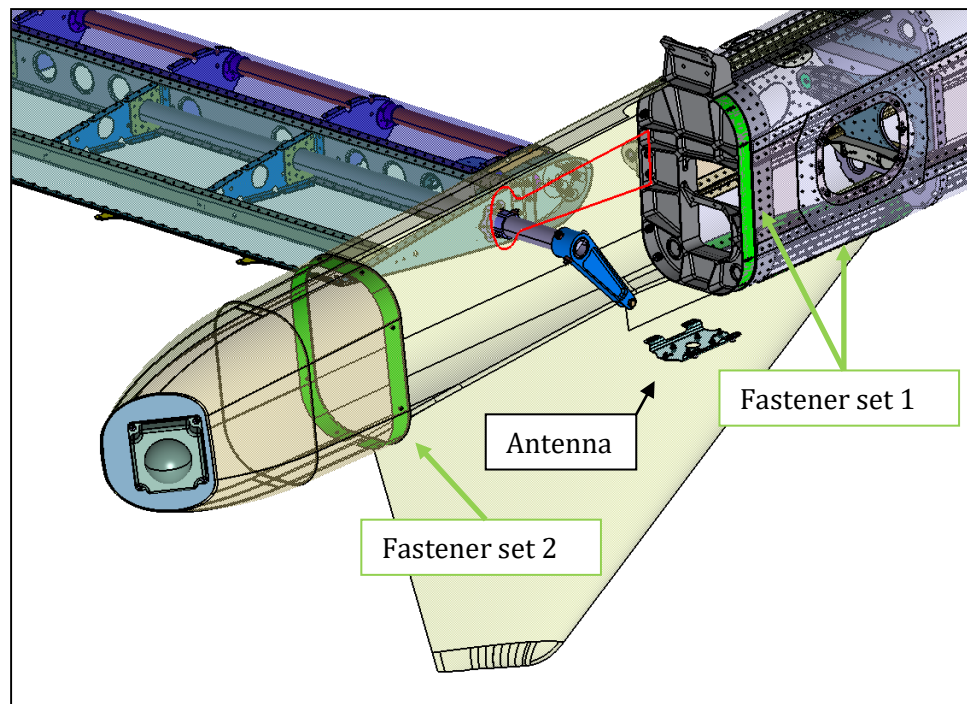
Figure 3-3: Ventral fin with all geometrical constraints and interfaces

3.2.2 LOADS

The loads used in the design of the ventral fin were determined by the lead structural engineer and the aerodynamicist. The derivation of the loads is not discussed in detail in this study. This study's focus is on the development of the composite component with a given set of constraints and load conditions.

Aerodynamic loads

The aerodynamic loads originate from the side slip generated by the aircraft. A side slip angle can be generated, either applied by the pilot through the rudder or because of roll-yaw coupling. When the slide slip angle is present, it is the aerodynamic function of the ventral fin, combined with the vertical fins, which restore the aircraft to zero side slip. The ventral fin works like a wing, but not in the conventional direction of up and down, but rather left to right. Thus, a side slip angle on the fin is similar to an angle of attack on an airfoil and results in a lift force that is directed perpendicular to the airfoil planar surface (Figure 3-4).

Thin airfoil theory and CFD can be used to quantify these aerodynamic loads. The aerodynamicist and lead structural engineer concluded the design load (the total aerodynamic force in Figure 3-4) to be used as 1380 N in the global Y direction (this is the same direction as the angle of attack work line in Figure 3-4) of the ventral fin. This aerodynamic force can be approximated as an equally distributed load on both skins of the airfoil section (Figure 3-16). Deviation from this theoretical OML leads to impaired functionality of the fin and an increase in drag. It is therefore important to limit the deflection of the airfoil section to less than 10 mm under the aerodynamic design loading.
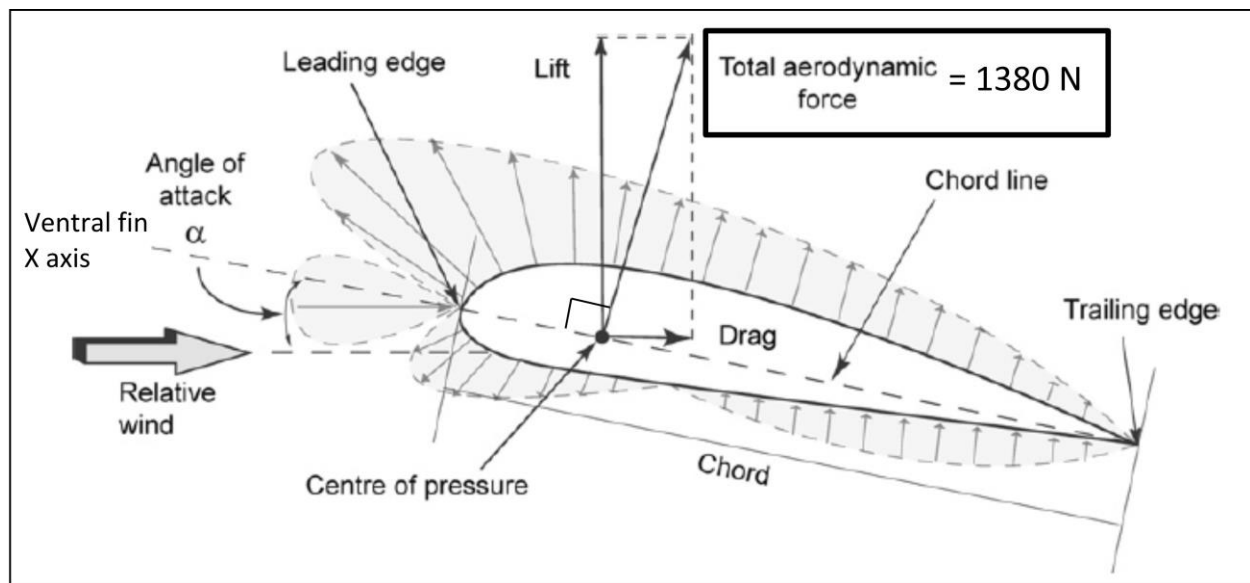
Figure 3-4: Ventral fin aerodynamic forces on the airfoil section, adapted from [46]

Tail strike loads

The tail strike load originates from an over rotation on the takeoff run. This could lead to the ventral fin scraping the tarmac. The load is allowed to damage the fin locally but should not lead to the removal of the fin or limitation in aircraft control. The lead structural engineer concluded that the design load to be used is 1570 N drag load, applied to the bottom of the fin (the surface that would come into contact with the tarmac), and 2000 N vertical force (perpendicular to the surface that would come into contact with the ground) applied to the same area, which is illustrated in Figure 3-5. Note in the figure that the bottom radius surface of the ventral fin would be parallel to the runway in the event of a tail strike. The total magnitude of the force is 2542 N.
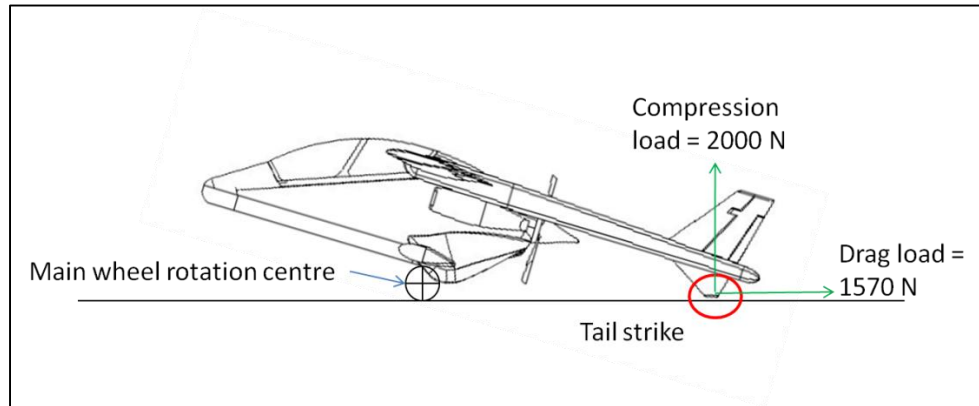
Figure 3-5: Free body diagram of over rotation and tail strike load case

G-force loads

AHRLAC is a high performance aircraft that can be used for fighter training. This means it should be capable of high G manoeuvres. The result being that anything that has mass would become a load on the structure. The G-force factor was given by the lead structural engineer as 8.5 g in the negative Z direction. This would have to be applied to the entire ventral fin assembly and the attaching tail cone with its sensor's weight (Figure 3-19). The mass of the tail cone and sensors is given as 6.1 kg, while the assembly mass of the ventral fin will be determined in the FEA.
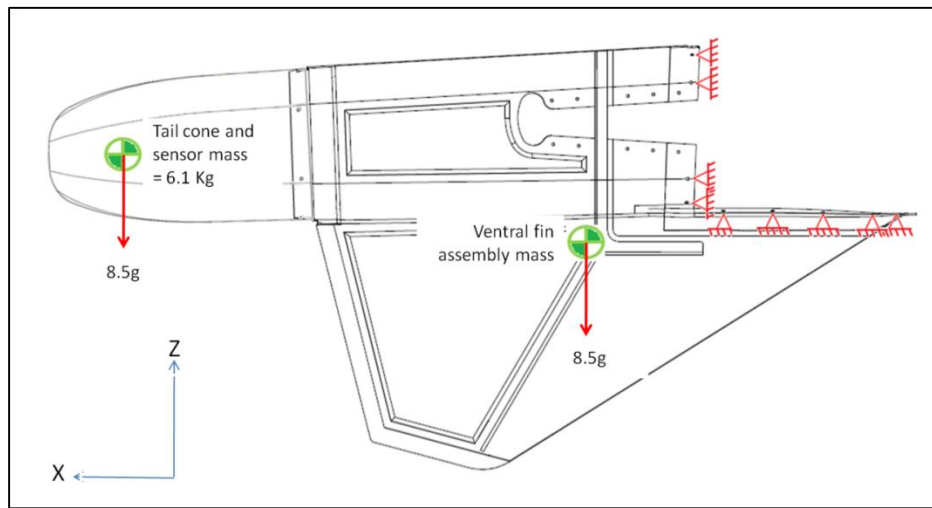
Figure 3-6: Free body diagram of G-force load case

3.2.3 DESIGN REQUIREMENTS

The design requirements are the parameters that would be used to evaluate the concepts and ultimately pass or fail the design. This would define whether the design is considered safe or unsafe.

Mass

In all the previous work done on aircraft structures where the design is evaluated, the mass of the assembly is one of the main criteria of the selection process. This is because the aircraft performance parameters are all negatively affected by the addition of mass. Therefore, the mass of the ventral fin has to be minimized as much as possible, but it must still remain strong and stiff enough to complete its tasks safely under all the expected conditions.

Stiffness

The stiffness of the airfoil skins on the ventral fin is of great concern to the aerodynamic function of the fin. If the fin deflects too much under aerodynamic load, the functionality is reduced and drag is dramatically increased. The deflection is thus only of concern under aerodynamic loading. The aerodynamicist limited the deflection of the airfoil skins to 10 mm under the aerodynamic design load.

Composite failure

The main safety parameter in any structure design is the strength. The failure theories for composite failure are discussed in Section 2.5.3. The Tsai-Hill failure criteria will be used since it is applicable to this type of composite material and lay-up, and is a built-in function in Patran/Nastran, the finite element software. Any composite component should have a minimum factor of safety (FS) under the design load of 2 (except for the tail strike load case, in which local failure of the ventral fin is allowed) but should not detach or limit the functionality of the aircraft. This equates to a limit load of twice the design load within the aerodynamic and G-force load cases.

Fastener failure

The other point of failure in the composite assembly is the failure of the retaining fasteners. This would result in detachment of the fin and the inability to perform its aerodynamic functions. The forces of the fasteners will be determined by using the FEA and be checked against tested values to ensure that the fin remains attached under limit loads. The fasteners have the same limit state as the composites failure. A limit load of twice the design load is required, thus, a minimum FS of 2 is required at the design load.

There are two sets of attachment fasteners on the ventral fin. The first set is the attachment fasteners that connect the ventral fin to the tail boom of the aircraft. The second set is the attachment fasteners of the tail cone and sensors to the ventral fin. The only load case that influences the connection between tail cone and ventral fin is the G-force load case. The other load cases' load paths do not go through this connection set (Figure 3-6).

3.3 MATERIALS SELECTION

In this section the materials considered in the literature review will be evaluated in order to select the most suitable material. The manufacturing methods and functions of the component have to be kept in consideration during the selection process.

The material selected must be capable of withstanding the temperature and environmental effects of the operational theatre where AHRLAC XDM is expected to operate.

The other main factors that will influence the material selection are the local availability and whether the materials are commonly used in aerospace. The fact that this is a prototype aircraft means that changes could be made to the initial geometry of the components. Therefore investing in importing large amount of materials, possibly for only a couple of parts, does not make sense financially.

3.3.1 MATRIX

As discussed in Section 2.2.3, only thermoset resins will be considered. The reason for the exclusion of thermoplastics is because of their large production output and high capital investment. For the current experimental prototype a small number of parts will be required, which fits better with the labour intensive thermoset resins. The resin types considered are:

- Epoxy
- Polyester
- Vinylester

From the above list, epoxy resin was chosen due to its superior mechanical properties and resistance against environmental degradation. It is also the most commonly used thermoset resin in aerospace. The exact type of epoxy will be dependent on the supplier and based on availability. It must have aerospace approval and be readily available within a short lead time. In order to minimize risk of use on a prototype aircraft, it has to be a proven and well known product.

The chosen epoxy resin is AXON's EPOLAM 2022. This is AXON's general aerospace epoxy which is designed to be used in hand laminating and is also suitable for the resin infusion of small parts. The data sheet for this resin is presented in Appendix C.

This resin is a room temperature curing resin, but for optimal mechanical properties and thermal resistance a post cure of up to 100°C would be required. The post cure can be done with the part demoulded from the composite tool, which means that the tool used in manufacture does not have to be subjected to the post curing temperatures.

3.3.2 REINFORCEMENT

Section 2.2.1 discusses the reinforcement material in detail. Table 14 summarizes the advantages and disadvantages of the reinforcement material type, for the application of the ventral fin, and indicates the chosen material. The selection was made to manufacture all parts of the ventral fin from E-Glass fabric. The data sheet can be found in Appendix D.

Carbon was eliminated due to the lack of radio transparency as the fin would house the antenna. This would prevent the antenna in the fin from sending and receiving signals. Aramid was eliminated because of cost and the difficulty to cut and process the material. Due to the difficulty and time intensive methods of modelling damage due to impacts it was decided to monitor the fins during the test flying for signs of damage and if it is discovered that the fins are damaged due to leading edge strikes from foreign objects aramid could be added. This will not form part of this study.

Reinforcement Material	Advantages	Disadvantages	Notes
Carbon	• Highest specific stiffness	• Highest specific cost • Brittle fracture • Not radar transparent	• Due to the antenna mount inside the fin, the use of carbon is not recommended
E-Glass	• Low cost • Radar transparent	• Low strength • Low stiffness	• Good choice
Aramid	• Highest specific strength • High impact strength	• Difficult to cut and process • Expensive	• Can be used to increase the impact strength, but not a good choice for the base material

Table 14: Reinforcement material advantages and disadvantages for the ventral fin manufacture

The different reinforcement types are discussed in Section 2.2.2. They are listed in Table 15, together with their advantages and disadvantages for decision making purposes.

From Table 15, the chosen reinforcement type for the ventral fin manufacture is woven fabrics. UD fibres can be used to locally stiffen the structure, but this will be used as a last resort due to the lack of damage tolerance of UD. The versatility of the woven fabric suits a prototype and its superior impact resistance can be advantageous, because the ventral fin has a leading edge that could be subjected to impacts from foreign objects. The double curvature of the airfoil section and small radii on the OML dictates the use of fabrics which drape easily and reduces the risk of kinking or misalignment of the fibre.

Within woven fabric, the weave must also be selected to best suit the application. The parameters that influence the weave selection are ease of draping, directional properties, surface finish and availability. The chosen weave was a 2x2 twill with low planar mass. This was chosen to increase the drapability and to keep the properties similar in both directions.

Reinforcement type	Advantages	Disadvantages	Notes
UD	• Highest strength and stiffness	• Can only accommodate load in one direction	• Not recommended for base material of ventral fin, but can be used to locally stiffen the part
Woven fabrics	• Very versatile • Can accommodate loads in both principal direction	• Reduction in stiffness and strength in principal directions	• Can be used effectively to create similar properties in both principal directions and good draping properties
Knitted fabrics Non-crimp fabrics Three-dimensional fabrics	• Very optimized in mass and stiffness • Reduces production resources	• Large amount of time needed for optimization • Large volume orders required	• Ideal for large volume production of highly optimized parts, thus not recommended for prototyping.

Table 15: Reinforcement type advantages and disadvantages for the ventral fin manufacture

3.3.3 CORE

Core materials were discussed in Section 2.2.4. In this section the three main core types were discussed: honeycomb, balsa and foam. The honeycomb and foam types can be manufactured in a variety of materials. Firstly, the type of reinforcement must be chosen and only then can the materials be selected for the specified purpose.

Reinforcement Material	Advantages	Disadvantages	Notes
Honeycomb	• Low density • Highly optimizable properties • Large material selection • Good drapability	• Difficult to use with resin infusion and wet lay-up • Requires time to optimize	• Due to the chosen manufacture method of vacuum assisted hand lay-up, honeycomb would not be suitable
Balsa	• Good mechanical properties	• Very high densities	• Balsa would be a good choice in primary structures, but weight is more important in this specific case.
Foam	• Low densities • Large material selection	• Not the best structural properties • Difficult to form on curved surfaces	• Suitable for this application

Table 16: Core material advantages and disadvantages for the ventral fin manufacture

Foam was the selected type of core material to be used in the ventral fin. Honeycomb was eliminated because of its limitations when used with resin infusion. It would have added two manufacture steps, the skins would have to be manufactured separately and then bonded to the honeycomb, whereas with foam, the core could be formed integral to the skin in one step. Balsa was excluded due to its heavy weight and heavy structural application; it would not have seemed excessive to use balsa in a secondary structure with no hard points.

After deciding on foam as the type of core, the material can be chosen that best suits this specific application. The material chosen must have moderate structural properties and be readily available from local suppliers. The most common foam sold by local suppliers for aerospace applications is Airex C71.75. This foam type is regularly used in hand lay-up combined with vacuum curing. The data sheet for this foam can be found in Appendix D. This is a Polyvinyl chloride (PVC) type of foam and has an average density of 80 kg/m^3.

3.4 MANUFACTURING SELECTION

In this section the manufacturing process will be selected. From Section 2.3, the main parameters regarding the selection of the manufacturing process were shown as:

- Component geometry
- Scale of production
- Tooling
- Performance

These parameters with its implications on AHRLAC XDM's ventral fin will now be discussed. The manufacturing methods have to be within Aerosud's current capabilities and thus exclude autoclave forming and mechanized fibre placement methods. What remains are hand lay-up, vacuum infusion and RTM. The ventral fin only has one aesthetic side, the use of matching tooling is therefore unnecessary and are excluded due to the added complexity and cost, thus RTM will not be considered.

The selected manufacturing method was to use hand fibre placement on a one-sided open composite mould. Vacuum assisted curing will be used to decrease thickness variation and increase performance by reducing voids. The manufacturing of the composite moulds was done by computer controlled machining of tooling board to create a pattern. This pattern is sometimes referred to as a splash, plug or master mould. This pattern was then used to create the composite tool using tooling epoxy and glass fibre fabrics. The reason behind this method was; if the tool got damaged during manufacturing, the pattern can be used to create another composite tool. A pattern, tool and part of the ventral fin rib can be seen in Figure 3-7. The decisions why this method was selected will be discussed in detail with reference to the above list.
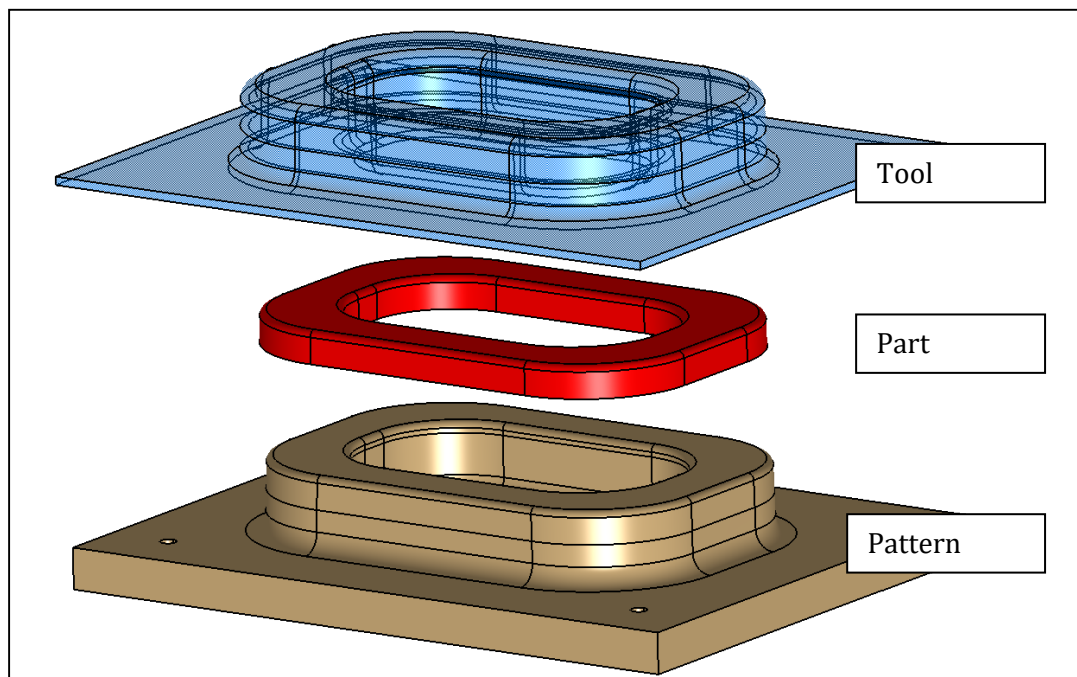
Figure 3-7: The design of a tooling board pattern, composite tool and aft rib

3.4.1 COMPONENT GEOMETRY

The component geometry requires only one surface to be smooth, thus the use of an open mould would suffice. There would be little to no advantage in using matching tooling in the application of the ventral fin. When using open tooling it is necessary to split the skin into two parts, a left and right skin for each fin and then assembling them afterwards. The use of open tooling would ease the placement of fibres and if a vacuum bag is used, reduce the bagging complexity. Careful consideration should be given to the demoulding process. All the draft angles (Figure 3-8) of the tool should ease demoulding and must be greater than 90°. Large radii should be used where possible for the same reason.
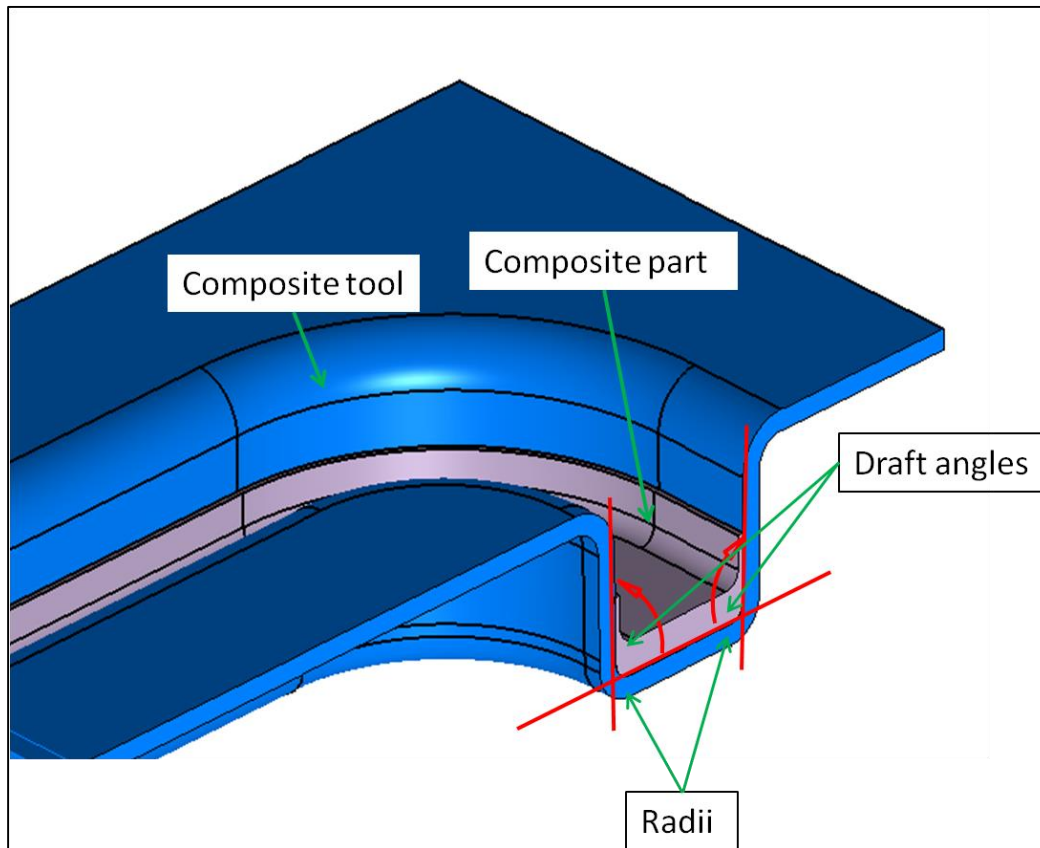
Figure 3-8: Draft angle and radii on aft rib of ventral fin to ease demoulding

3.4.2 SCALE OF PRODUCTION

In the AHRLAC XDM prototype phase, emphasis is placed on getting the prototype to fly in the shortest possible time and using this aircraft as a testing platform to optimize the next version of the aircraft, which is the advanced demonstrator model (ADM). This means that there is an increased risk of composite component change between XDM and ADM. The scale of production for the AHRLAC XDM parts would thus probably be only one or two sets. There will be no need for high cost tooling and large scale manufacturing methods and at this stage, labour intensive, low initial cost methods are acceptable and preferred. The use of skilled workers would be required to ensure the best possible part quality.

3.4.3 TOOLING

As mentioned above, there is little to no value in using high cost, high quality tooling in this stage of AHRLAC's life cycle, due to the high probability of change in the initial prototype stage of the AHRLAC development. The chosen tooling is expected to produce a low number of parts, but must withstand the curing cycle of the resin used in the part. The resin chosen for the part was a room temperature curing resin with a possible post cure of up to 100°C. The epoxy resin used in tooling could be subjected to this temprature without any adverse affects. The pattern will be made from a low-cost tooling board and the composite tool from a tooling fibreglass fabric and epoxy. The skin tool can be seen in Figure 3-9.
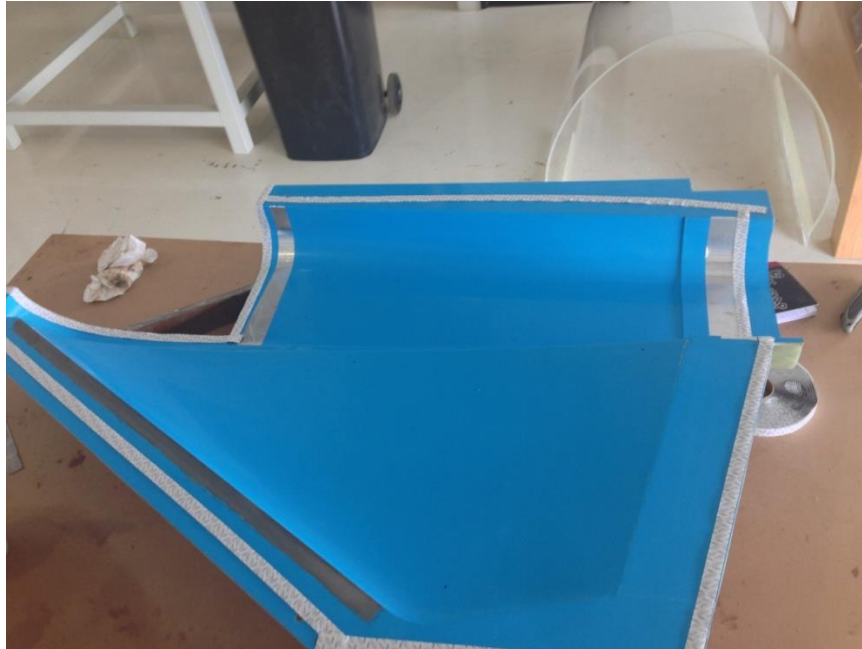
Figure 3-9: Finished and polished composite tool of the ventral fin skin

3.4.4 PERFORMANCE

The manufacturing methods chosen should have low initial cost, this usually relates to low production volumes that require a high skill level and labour recourses. The performance of the parts can be assured through the use of a highly skilled artisan and sufficient quality control. This manufacturing method is used throughout the aviation industry as a fast prototyping method and is considered to produce acceptable component performance if adequate time is spent on ensuring good part quality. To ensure component performance, measures have to be taken to keep the area, and the consumables used, clean and dust free and store the consumables correctly. The use of vacuum assisted curing will also increase part performance.

3.5 FINITE ELEMENT ANALYSIS

3.5.1 BACKGROUND

The FEA program used in his dissertation is MSC Patran/Nastran. It has a variety of different elements that can be used in the analysis to describe the geometry. The main elements types are beam, shell and solid. In this study only shell elements will be considered as these are the norm to model thin composite laminates [46], [41] and [42]. Shell elements are also referred to as two-dimensional or plate elements and are mostly used in thin plate theory, membrane theory or plane stress applications. Typical applications are thin wall pressure vessels, aircraft skins and thin composite skins. There are two main types of shell element used by commercial software; they are tri and quad elements. The quad element is square and has four corner nodes with six degrees of freedom each, while the tri element is triangular with three corner nodes (Figure 3-10).
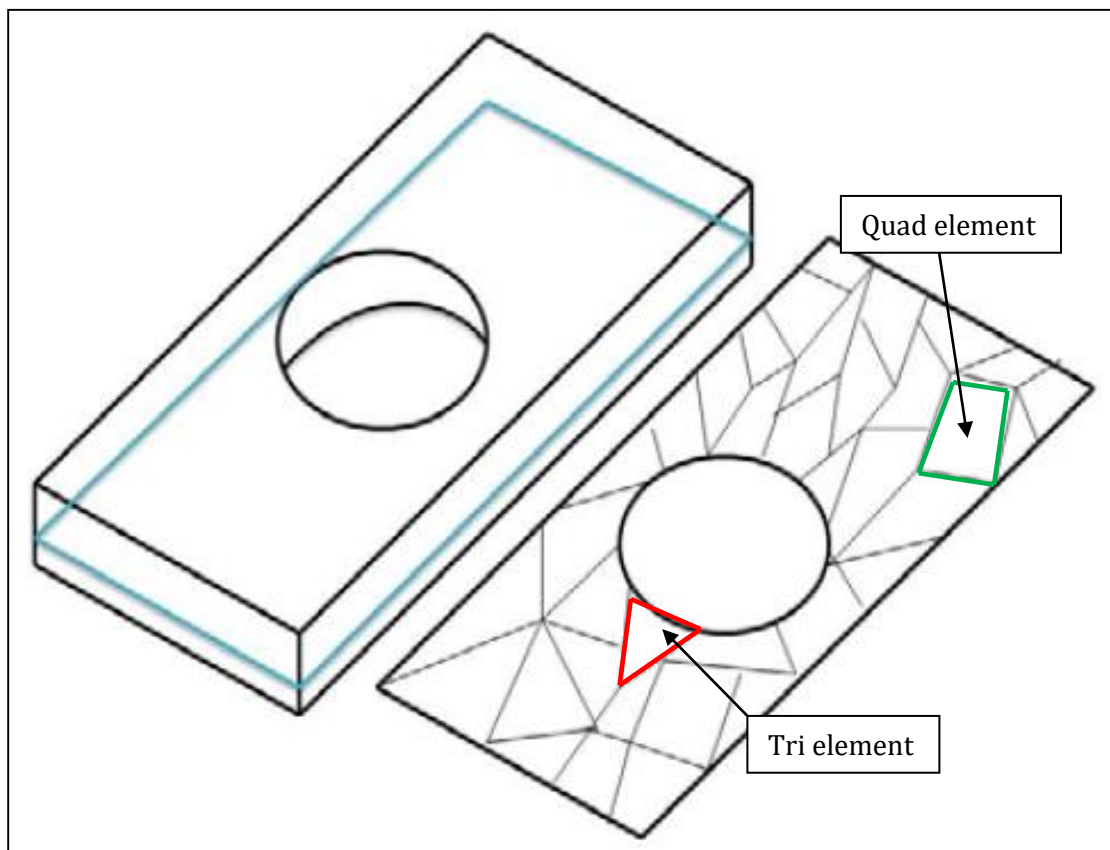
Figure 3-10: Quad and tri two-dimensional shell elements [47]

FEA requires a number of inputs. These inputs depend on the type of analysis done. For example, if a linear static structural analysis is required, the inputs would be the following:

1. Geometry
2. Finite element mesh
3. Material constitutive model and relevant stiffness properties
4. Material limit stresses and failure criteria (only required if failure is to be analysed)
5. Boundary conditions, such as loads and constraints

This list would differ for an aerodynamic analysis and a heat transfer analysis. For this study only linear static structural analysis would be considered.

The use of a linear static analysis is used in both references [40] and [41]. This assumption was tested to be accurate enough if no instability occurs. The assumptions made in the linear static analysis are the following:

- Force versus deflection relationship as well as the stress to strain relationship is linear.
  This assumption can be seen in the material testing results and because the analysis loads are not close to failure of the composite material this assumption should be valid.

- Loads are applied statically and all forces are in equilibrium.
  The loads on the actual aircraft would be dynamic but simplification to a static system is common practice to reduce the analysis time required.

- Geometry behaves linearly; instability effects such as buckling are not taken into consideration.
  Because buckling analysis required much more testing and is often found on slender thin compression members, the decision was made to exclude buckling from the analysis. The static testing would reveal if this assumption was valid.

3.5.2 FINITE ELEMENT ANALYSIS PROCESS

In the next section, the mass, strength and stiffness properties of the ventral fin will be analysed and adapted until the results are deemed satisfactory. This will be accomplished through the analysis of the most basic ventral fin design and adding stiffening elements until the stiffness and strength results are satisfactory. A linear static analysis will be done using MSC Patran/Nastran 2005. A shell model will be constructed with two-dimensional orthotropic laminate properties that are considered linearly elastic. This is the same method that was used in references [40] and [41].
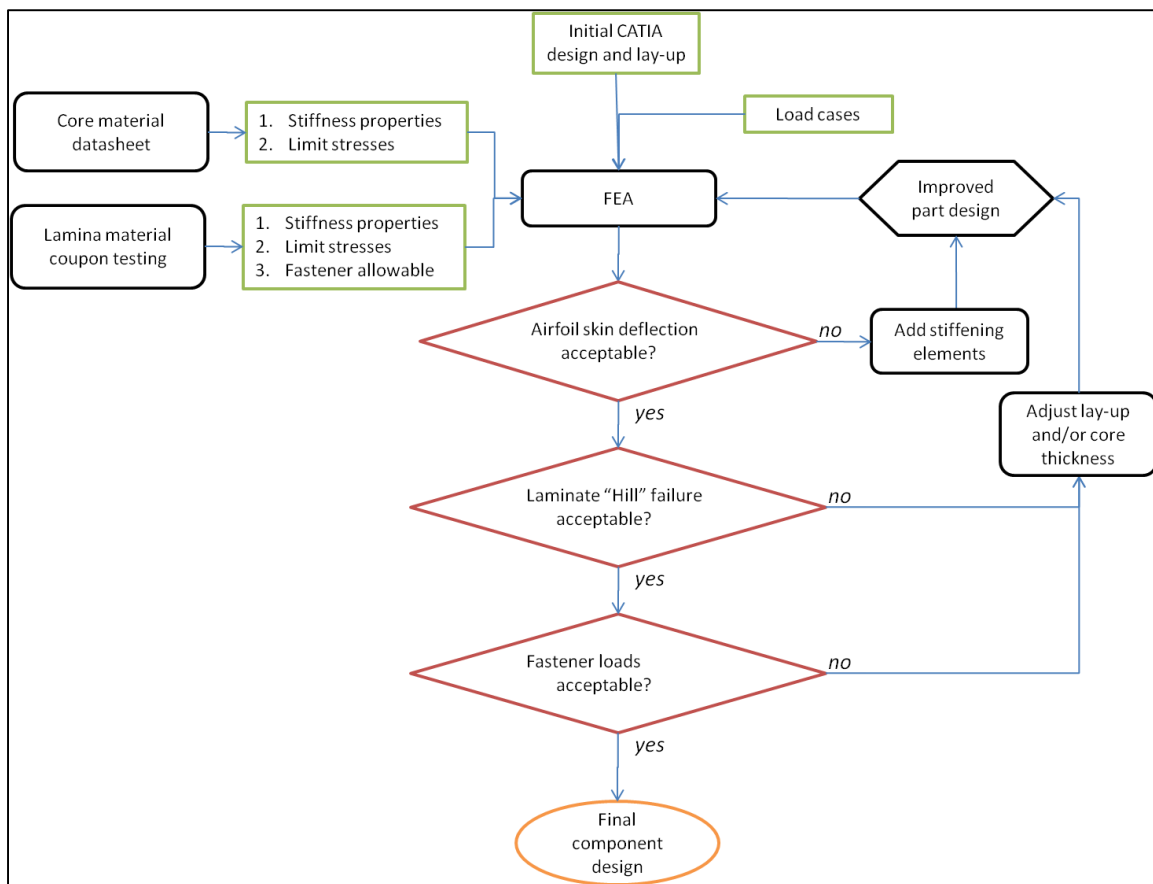
Figure 3-11: Design cycle regarding the FEA of a composite structure derived from reference [45]

Figure 3-11 depicts this design cycle and the use of the FEA of the AHRLAC ventral fin. There are three main inputs required for the FEA. They are shown in the green blocks in the flow chart and are material properties, initial component design and load cases. The material properties will be obtained from the mechanical testing of the lamina and from the material datasheet for the isotropic foam core. The material properties' testing will be in accordance with ASTM test methods, these methods were used in references [41] and [40]. The load cases were given by the structural and aerodynamic engineers working on the project. The last input needed is the initial component design and each part must have an initial lay-up. The initial component design will begin with a minimal design to satisfy the geometrical functions of the ventral fin. The initial part lay-ups were estimated as balanced, symmetrical lay-ups that have similar thickness as other aircraft composite components.

Once all the inputs are obtained, the FEA will be used to determine if the design and lay-ups are acceptable. The three parameters (in the red trapezoids in Figure 3-11) used to determine the inputs are: the aerodynamic deflection of the airfoil skin section of the ventral fin, the composite failure index and the fastener loads. If the aerodynamic deflection is unacceptable, high stiffening elements will be added to the design and if the fastener loads are too high, fasteners can be added or the lay-up adjusted. The lay-up will be optimized if the composite Hill failure index shows local failure.

3.5.3 MATERIAL PROPERTIES

As stated previously, the material properties used in the FEA will be derived from the mechanical testing of the lamina and the isotropic core properties are taken from the data sheet. The assumptions used in the FEA regarding the material properties are:

- **Lamina is considered two-dimensionally orthotropic.**

This is a common assumption in the FEA of composite materials. These assumptions are used by references [40], [41], [42], [45] and [46], and can be seen in Table 9 and Table 11.

- $E_{11} \approx E_{22}$

This implies that Young's modulus is the same for both principal directions. It can be seen by looking at equations 6 and 7 and assuming that a 2x2 twill weave is balanced. The tested values for the 1 and 2 directions are 17 739 and 17 936 MPa, respectively. The 1 % difference supports this assumption.

- $X_t \approx Y_t = T$ and $X_c \approx Y_c = C$

This assumption states that the two principal limit stresses in the lamina are equal. As mentioned in the previous assumption, the fact that the weave is considered balanced, would result in a similar tensile and compressive strength in both principal directions. The compressive limit stresses for a monolith laminate were found to be 160 and 225 MPa in the 1 and 2 directions, respectively. The minimum value of 160 MPa will be used in the FEA, which is done to minimize the risk in placement error of the warp and the weft directions in the laminate. The visual differences in these two directions are very hard to see in a 2x2 twill weave fabric. This method is considered conservative.

- **Maximum lamina shear stress is calculated at 5 % shear strain.**

The shear design strength value was obtained from in-plane shear tests in accordance with the ASTM D3518 and ASTM D3039 standards. These two specifications verify that the 5 % shear strain corresponding stress value to be used as a conservative limit state. A more realistic limit can be determined, but needs special tooling for testing that Aerosud currently does not have. The use of the 5 % shear strain, as a failure stress, is considered very conservative.

- **Operating and testing temperature is set at 55°C.**

This is considered the worst case scenario for the component operating temperature and should yield the lowest limit stresses and stiffness. The performance of the epoxy will degrade as the operating temperature increases. Thus, all material properties used in the FEA will be at this temperature and yields a conservative approach.

- **Core material is isotropic.**

The chosen foam core is of isotropic nature and design values from the data sheet confirm this.

The test plan and relevant testing standards used in this study are given in Figure 3-12. The use of ASTM standards to determine relevant composite properties can be seen in references [40], [41] and [42]. The detail test plan specific to this study is presented in Appendix G and is based on Figure 3-12.

Figure 3-12 shows a flowchart of the macro testing plan and will be used in this study [45]. There are two main sets of properties that are used in the FEA, material stiffness properties and the material limit properties. The material stiffness properties are used in micro- and macromechanics of the composite in the FEA to determine the deflections of the component under a specific load case. The material limit properties are used to determine if the component will fail, either by failure of the composite laminate or failure of the fasteners fixing the component to the structure. Thus, in short, the stiffness properties will define the component's behaviour under load, while the limit properties define the strength of the component.

The stiffness properties obtained from testing are averaged, while the material limit stresses (allowables) will be determined using the B-basis statistical calculations. This B-basis calculation can be found in Appendix H. Figure 3-12 shows two compressions allowable, this is because the addition of a core in a laminate will decrease the compression limit stress due to local deboning from the core and local crippling of the skin. There will therefore be two sets of tests to determine the core and monolith compressive limit state.

The properties of the foam core used in the FEA will be obtained from the data sheet, while the lamina properties will be tested at 55°C as shown in Figure 3-12.
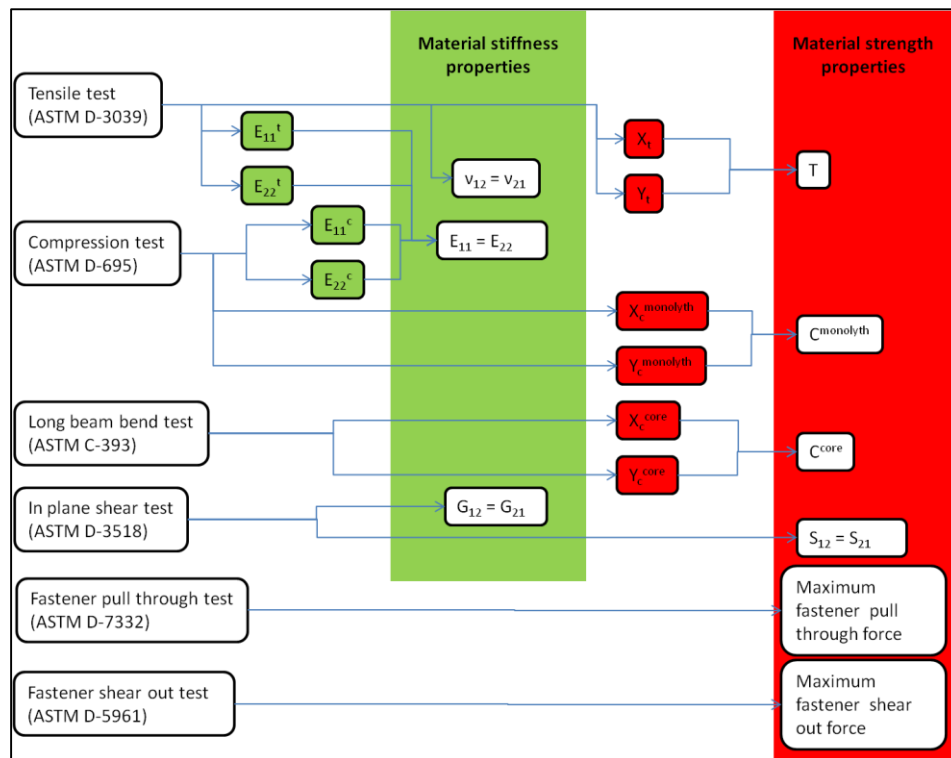
Figure 3-12: Composite material properties testing plan derived from [45]

The results of the material testing plan are as follows:

Matrix: Epolam 2022, epoxy resin
Reinforcement: Interglas 92125, Glass fibre, 2x2 twill, 280 g/m^2
Tested temperature: 55°C

Property	Value	Unit
$E_{11} = E_{22}$ (MPa)	17739	MPa
$\nu_{12} = \nu_{21}$	0.108	-
$G_{12} = G_{21}$ (MPa)	3060	MPa
T	247	MPa
$C_{monolith}$	160	MPa
C_{core}	138	MPa
$S_{12} = S_{21}$	33	MPa

Table 17: Lamina properties

Foam core: Airex C71.75

Property	Value	Unit
E (MPa)	35	MPa
ν	0.3	-
G (MPa)	20	MPa
T (MPa)	1.12	MPa
C (MPa)	1.04	MPa
S (MPa)	0.88	MPa

Table 18: Airex C71.75 core properties

Data obtained from supplier technical data sheet for Airex C71.75 and reduced by the appropriate value to obtain data at 55°C. These data sheets are presented in Appendix E.

For the fasteners within a 9 ply laminate with an edge distance of twice the diameter of the fastener:

Property	Value	Unit
Max shear force	4340	N
Max pull through force	1638	N

3.5.4 FINITE ELEMENT MODEL

Iterative design

The concept design process of the ventral fin was more of an iterative concept growth than a concept selection. The basic concept of only the skins and mounting interface for the antenna was started with, and with this basic model a FEM was created and analysed. Laminate stresses, deflections and fastener loads were checked against the allowable limits and the model was either modified by adding stiffening elements and reanalysed, or accepted and used in the detail design (Figure 3-11). The concept evolved iteratively to the final concept and the final design was completed in four steps (Figure 3-13).

The initial lay-up of each individual part was estimated and only modified very slightly if there was local failure on the part. This means that the individual parts were not heavily optimized with regards to laminate design, but rather the optimization focussed on the assembly as a whole. The axis system used in the FEM is the global aircraft axis system (Figure 3-13 and Figure 3-18). The X direction is in the longitudinal axis of the aircraft, while Y is lateral, and Z is the up and down axis.
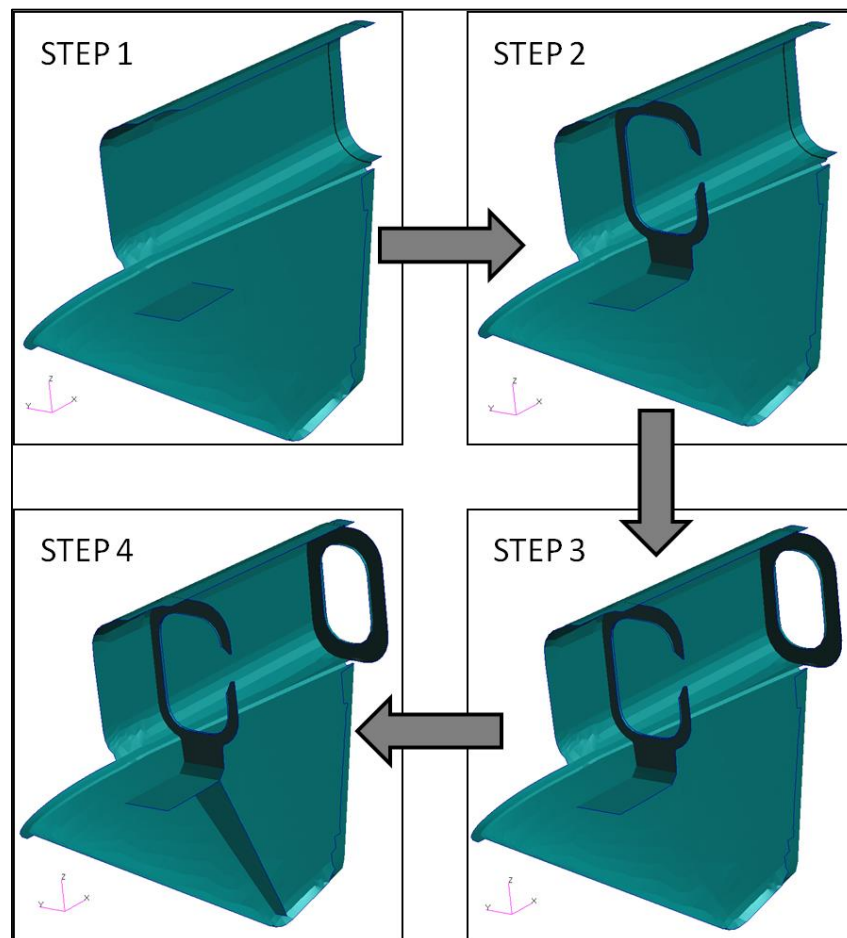
Figure 3-13: Concept development of the ventral fin assembly

Iteration	Pass/ fail with reason
Step 1	Aerodynamic deflection = 20.7 mm > 10 mm
Step 2	Aerodynamic deflection = 11.1 mm > 10 mm and an unacceptable number of elements fail under tail strike loads that implies total failure and possible detachment of the component
Step 3	Aerodynamic deflection = 11.1 mm > 10 mm
Step 4	Acceptable design

Table 19: Finite element results of design cycle iterations

The model description

As previously stated, the FEA was done using MSC Patran/Nastran 2005. The model consisted of two-dimensional shell elements with four nodes and nine degrees of freedom per node. This was the same approach as used in reference [40], [46], [41], [42] and [45]. Two-dimensional orthotropic material properties were allocated to the shell elements and are given in Table 17 and Table 18.

The two skins had a sacrificial layer of glass fibre surface tissue (0.2 mm thickness) on the outer surface. This was done to ensure that when sanding had to be done for painting, the structural layers were not damaged. This layer was not taken into consideration in the FEA.

Figure 3-14, Figure 3-15 and Table 20 show the lay-ups for the final design used in the FEA.
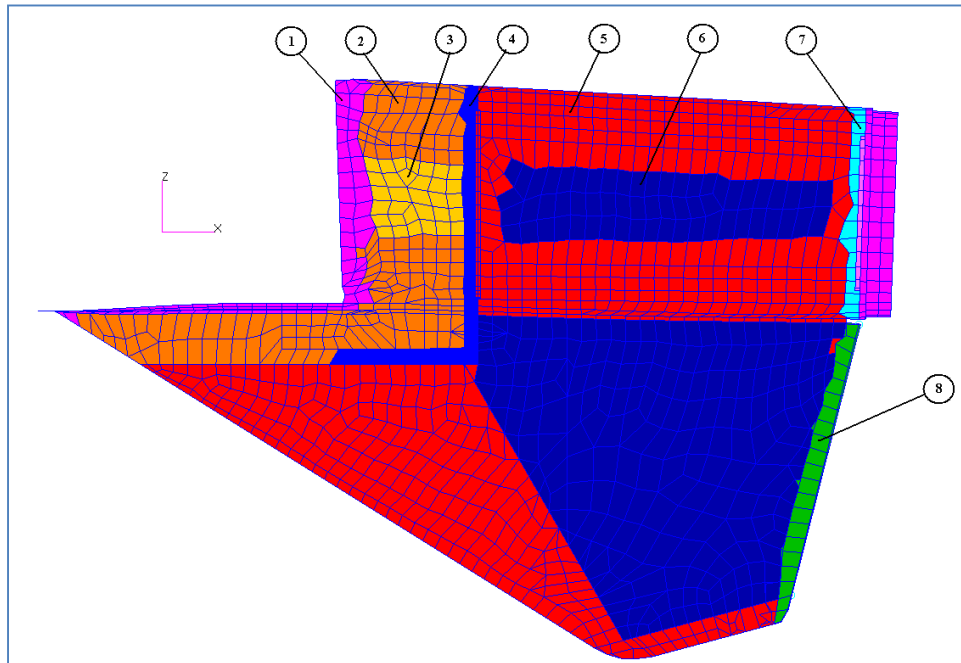
Figure 3-14: FEM of ventral fin skins indicating laminate definitions
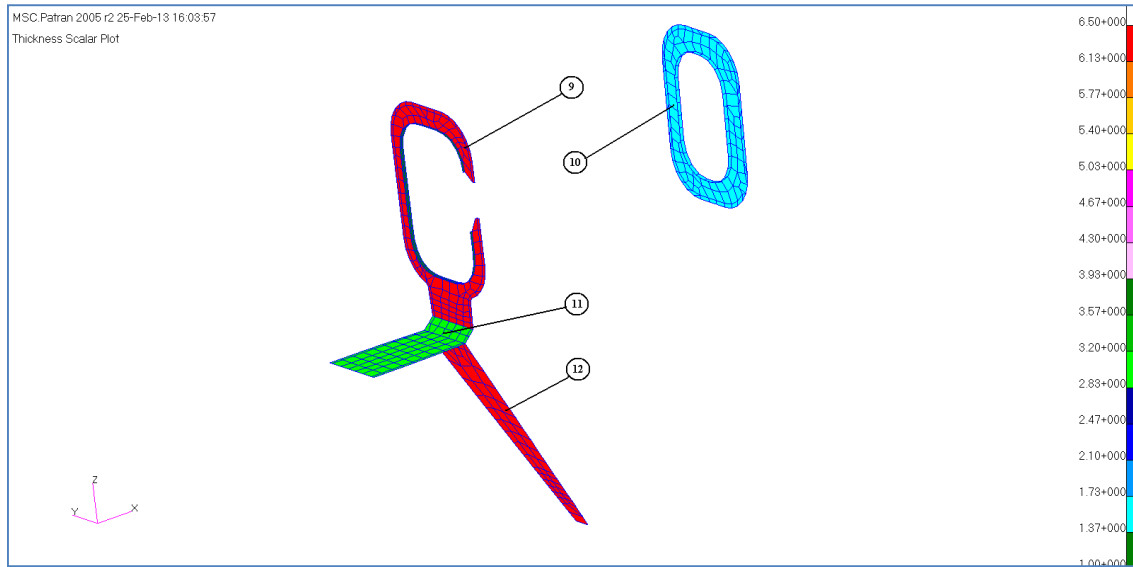
Figure 3-15: FEM of ventral fin ribs and spar indicating laminate definitions

#	Description	Theoretical thickness (mm)	Laminate
1	Edge	2.25	[0/90 ; ±45 ; 0/90 ; ±45 ; ±45 ; ±45 ; 0/90 ; ±45 ; 0/90]
2	Local thickening	1.5	[0/90 ; ±45 ; ±45 ; 0/90 ; ±45 ; 0/90]
3	Local thickening - core	6.5	[0/90 ; ±45 ; ±45 ; 5 mm Airex ; 0/90 ; ±45 ; 0/90]
4	Fore rib flange	3	Fore rib monolith (#11) + Local thickening (#2)
5	Body	1	[0/90 ; ±45]$_s$
6	Body with core	6	[0/90 ; ±45 ; 2.5 mm Airex]$_s$
7	Aft rib flange	3.75	Aft Rib (#10) + Edge (#1)
8	*Trailing edge	5	[0/90 ; ±45]$_{10}$
9, 12	Fore rib - core	6.5	[0/90 ; ±45 ; ±45 ; 5 mm Airex ; ±45 ; ±45 ; 0/90]
10	Aft rib	1.5	[0/90 ; ±45]$_3$
11	Fore rib monolith	1.5	[0/90 ; ±45 ; ±45]$_s$

Table 20: Laminate definitions of FEA of the ventral fin component.

Note: To stiffen the edge artificially to account for foam reinforcement and resin in trailing edge.

Aerodynamic boundary conditions

For the aerodynamic load case, the following was done to simulate the load case. The fasteners were simulated as displacement translation constraints in the X, Y and Z directions. This is similar to most of the literature in section 2.6. The load applied was a complete load of 1380 N in the global Y direction (shown in red in Figure 3-16) and was applied evenly on both airfoil skins. This simplification of the load to the global Y direction split on the two surfaces as opposed o a complex pressure distribution on the skins was done because of the small area of the airfoil section, it would be very difficult to load the actual fin with a complex pressure distribution as shown in Figure 3-4 and the actual pressure distribution would be very difficult to determine due to the effects of the propeller to the airflow. This was given by the lead structural engineer and determined using CFD and classic airfoil theory under certain conditions that the specification requires of AHRLAC. Figure 3-16 shows the area representing the airfoil section where the load was applied to, as well as the fastener locations. A tail cone was not considered in this load case.
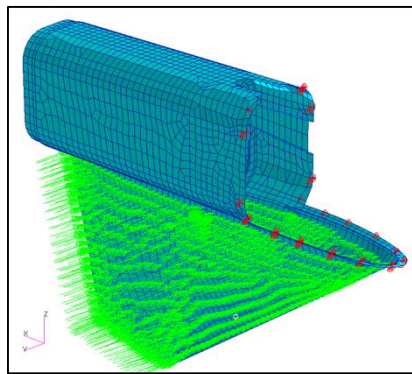
Figure 3-16: FEM showing the aerodynamic load case without rib constraints

Using the above boundary conditions and the deflection results of the analysis, the deflection behaviour of the ventral fin on the tail boom was better represented by constraining the nodes that moved into the space where the tail boom rib would have been. This was only done for the deflection and composite failure results of this specific load case. This modification to the boundary conditions can be seen in Figure 3-17.
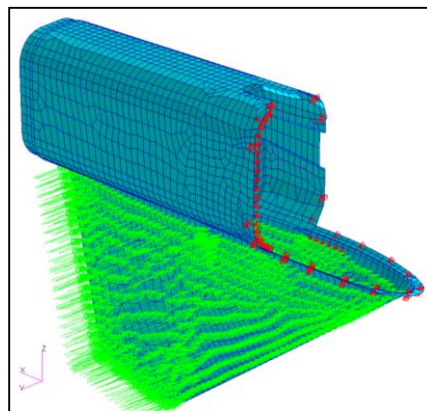
Figure 3-17: FEM showing the aerodynamic load case with rib constraints

Tail strike boundary conditions

The tail strike load case uses the same fastener constraints as the aerodynamic load case. This is translations in X, Y and Z on the fastener location nodes. The tail strike loads were generated by the lead structural engineer, which is a combination of a drag load and compression load on the tip of the airfoil section. The drag load was given as 1570 N in the global X direction, while the compression load was given as 2000 N in the global Z direction. This load was evenly distributed between all the nodes that would effectively touch the ground. The load and the application region can be seen in Figure 3-18.
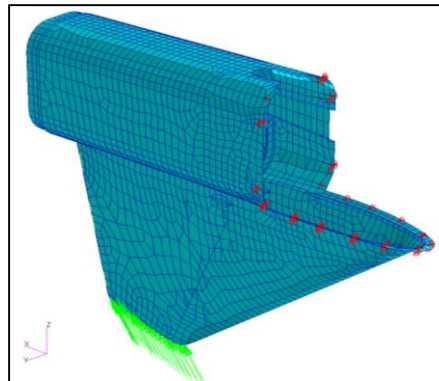
Figure 3-18: FEM showing the tail strike load case

G-force boundary conditions

For the G-force load case the same fastener constraints were used as in the previous load cases. To simulate the sensor in the tail cone, a ridged body element (RBE 3) was used. The independent node represents the CG of the sensor. This was at X = 12733 mm; Y = ±1850 mm (Left and right sensors); Z = 2761 mm. The dependant nodes simulate the tail cone attachment to the fin via the eight fasteners. They are constrained in the three translation directions and were only used in the G-force load case. In Figure 3-19, the RBE simulation of the tail cone and sensors are shown. The force of the estimated weight of the ventral fin assembly (4,850 g) was multiplied by the G-force factor of 8.5 and applied throughout whole model. This was done to specify a maximum allowable assembly mass. The mass of the tail cone with its sensors was 6.1 kg and this was also multiplied with the G-force factor and applied to the independent node of the RBE 3 element. This can be seen in Figure 3-19.
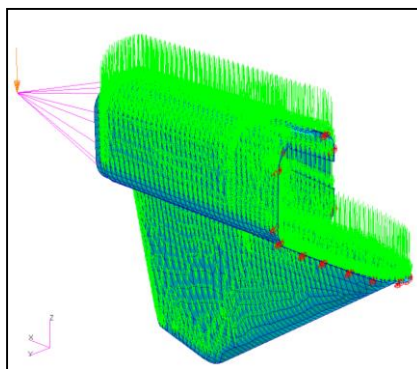
Figure 3-19: FEM showing the G-force load case

3.5.5 RESULTS

The results of the FEM will be discussed in the following three sections: fasteners, composite failure and deflections. These were the three results that were used to evaluate the concepts and decide on a final version. Only the last step of the concept growth will be discussed in this section, but the same procedure was followed for each step. Only the worst case load case in each result will be discussed. This section would verify that the final design for the ventral fin satisfies all the design requirements as set out in Section 3.2. Table 21 summarizes the results from the FEA.

Load Case (Design load):	Aerodynamic	Tail Strike	G-force
Fastener set 1 FS	2.9	2.1	2.2
Fastener set 2 FS	NA	NA	6.4
Composite FS (Tsai-hill)	2.1	1.6	2.4
Deflection (mm)	9.39	27.9	18.6

Table 21: FEA of final design ventral fin results summary table

From Table 21 it can be seen that the fastener sets perform adequately under all load cases. They have a FS of greater than 2 for all the load cases, which exceed the fasteners' minimum requirement. The fastener set 2 is only part of the load path in the G-force load case and therefore only has a FS listed under that load case. This shows that under all expected load cases at the maximum component operating temperature of 55°C, the ventral fin should not detach and an adequate margin remains for gusting and larger load magnitudes.

Regarding the composite failure, it can be concluded that the minimum FS is greater than the required FS of 2 for the aerodynamic and G-force load cases (Table 21). In the tail strike load case, the composite FS drops to 1.6, but this is still acceptable as local damage to the fin is allowed, but complete failure is not. This verifies that the final design and laminate definitions are more than adequate for safe operation in the expected load cases.

The only deflection requirement was that the fin airfoil skins do not deflect more than 10 m under the aerodynamic design load. The expected deflection is 9.39 mm which passes this requirement (Table 21).

These results will be discussed in detail in the next part of this section.

Fasteners

To simulate fasteners and their respective holes with detailed FEA would have dramatically increased analysis and set-up time, thus fastener failure was rather determined by comparing the tested fastener allowable to the constraint forces determined by the FEA. The FEM does not contain the detailed fastener holes, thus all elements that fall within the fasteners' hole area will be analysed as follows: In Figure 3-20, the constraint node is in the centre of the yellow circle, this yellow circle represents the countersunk hole (diameter of 10 mm) for the fastener. All elements containing nodes within the circle are discarded from the composite failure analysis and passed by the comparison to the fastener testing.
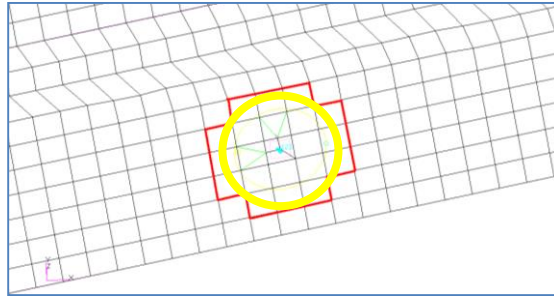
Figure 3-20: FEM of fastener hole

The maximum allowed shear force for a nine layer glass fibre laminate was determined through the testing as 4.3 kN. The fastener loads generated by the tail strike load case can be seen in Figure 3-21. It clearly shows the compression side on top of the fin, with the fasteners trying to push the fin away from the tail boom. The lower section of the fin is in tension with the fasteners, trying to prevent the fin from tearing away from the boom. The maximum fastener shear load under the design load is 2 kN, which is 47.6% of the maximum load allowed.
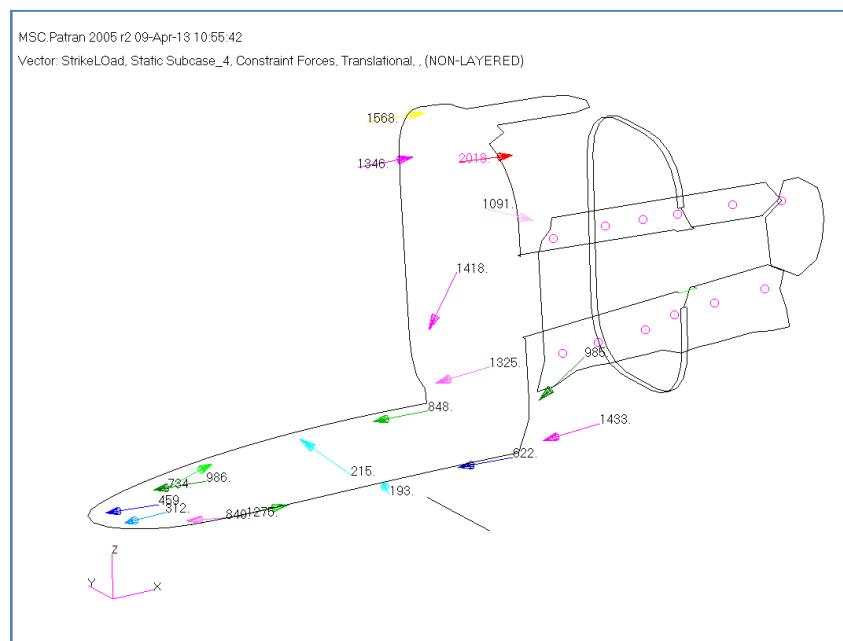
Figure 3-21: Fastener forces from the FEA of the tail strike load case

Composite Hill failure

The worst case load case for the composite failure was seen to be the tail strike load case. This section will only look at this load case. Figure 3-22 displays the Tsai-Hill failure factor for the tail strike load case. The elements shown have a FS of less than 2 (Hill failure factor > 0.25), while red elements indicate failure (Hill failure factor > 1).
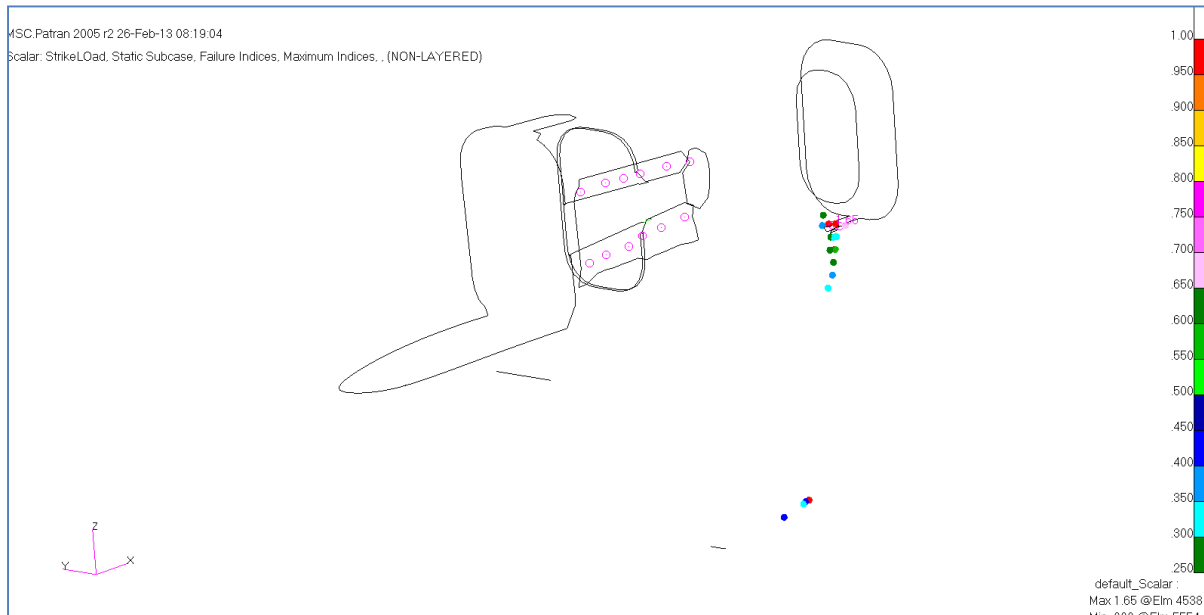
Figure 3-22: Composite Hill factor plot of the tail strike load case

There are two areas of concern. The area where the load is introduced will be discarded, because it is considered acceptable if this area is damaged during a tail strike. This area is also not a critical load path and it would not affect the functionality of the ventral fin if it is damaged.

The trailing edge area is shown in Figure 3-23. These trailing edge elements were modelled as a 20 layer monolith, while the actual part will be filled with resin and a foam wedge as this is the bond between the two skins. This was done to simulate the stiffness created by the resin and cotton flocks. The element at the top that fails is a tri element at a 90° bend and thus not considered accurate. The maximum Hill factor of 0.361 will be recorded for this case, which equates to a FS of 1.66.
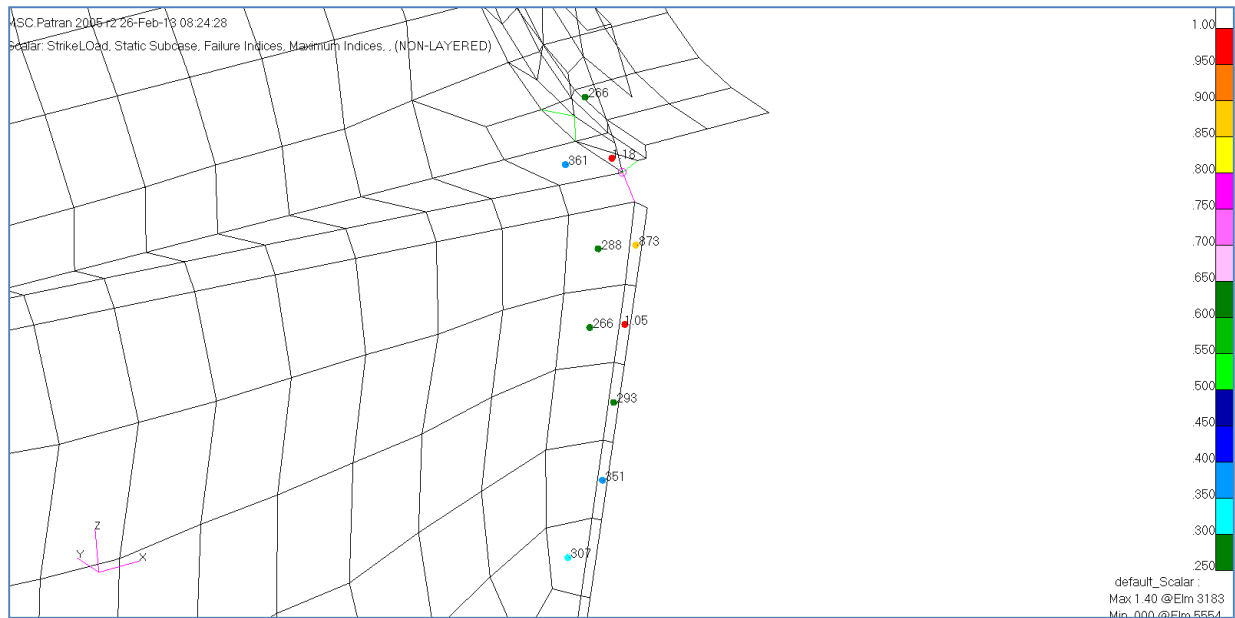
Figure 3-23: Detail view of the composite Hill factor plot of the tail strike load case

Deflections

As mentioned at the start of this section, the only deflections that could limit the functionality of the ventral fin are those under aerodynamic loading. This deflection is plotted in Figure 3-24. The plot shows the fin torque around the tail boom axis as expected. The deflections are larger in the flat airfoil skin areas that have reduced through thickness stiffness.
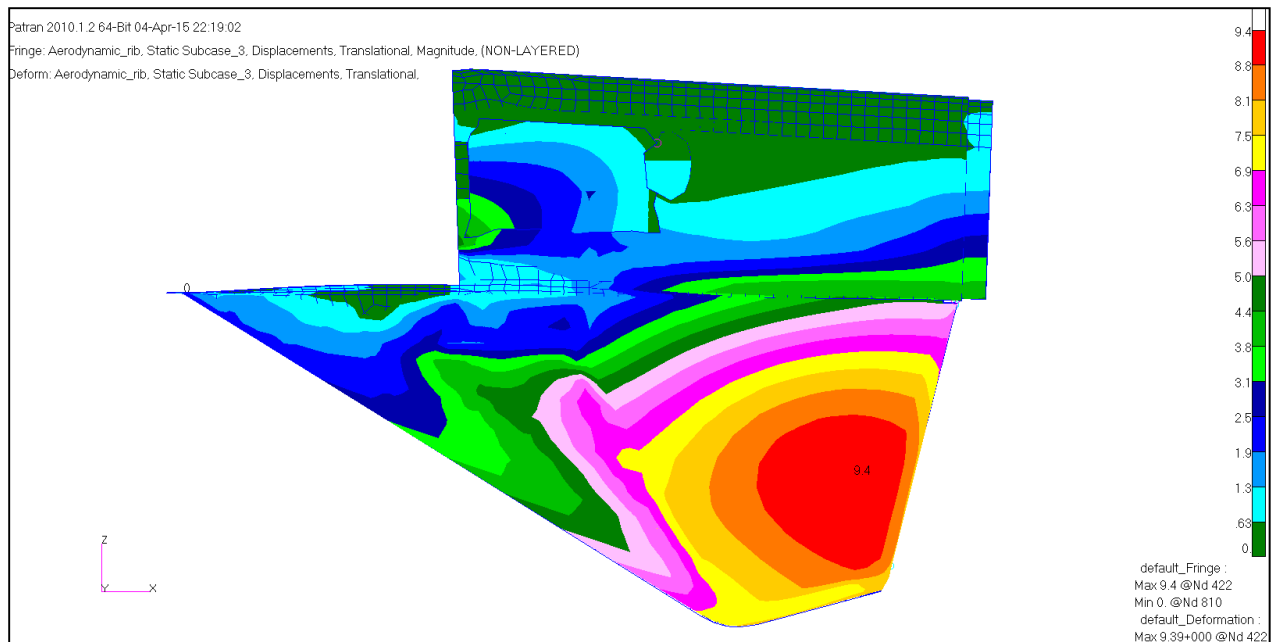
Figure 3-24: Deflection plot of ventral fin under aerodynamic loading

3.6 DETAILS OF THE CHOSEN DESIGN

In this section the detail design of the ventral fin will be discussed and motivations given for the decisions made. The results of the FEA were used here to generate a detail design with ply books for manufacturing. The detail CAD model was generated by the designer. The ply book and assembly instructions can be found in Appendix F. Both the ply book and CAD model will be used in the manufacturing of the ventral fin.

3.6.1 ASSEMBLY

The assembly of the ventral fin with the attached tail cone can be seen in Figure 3-25. This is the right hand assembly, with the cut-out for the control linkages for the elevator and shows one of the possible antennas.
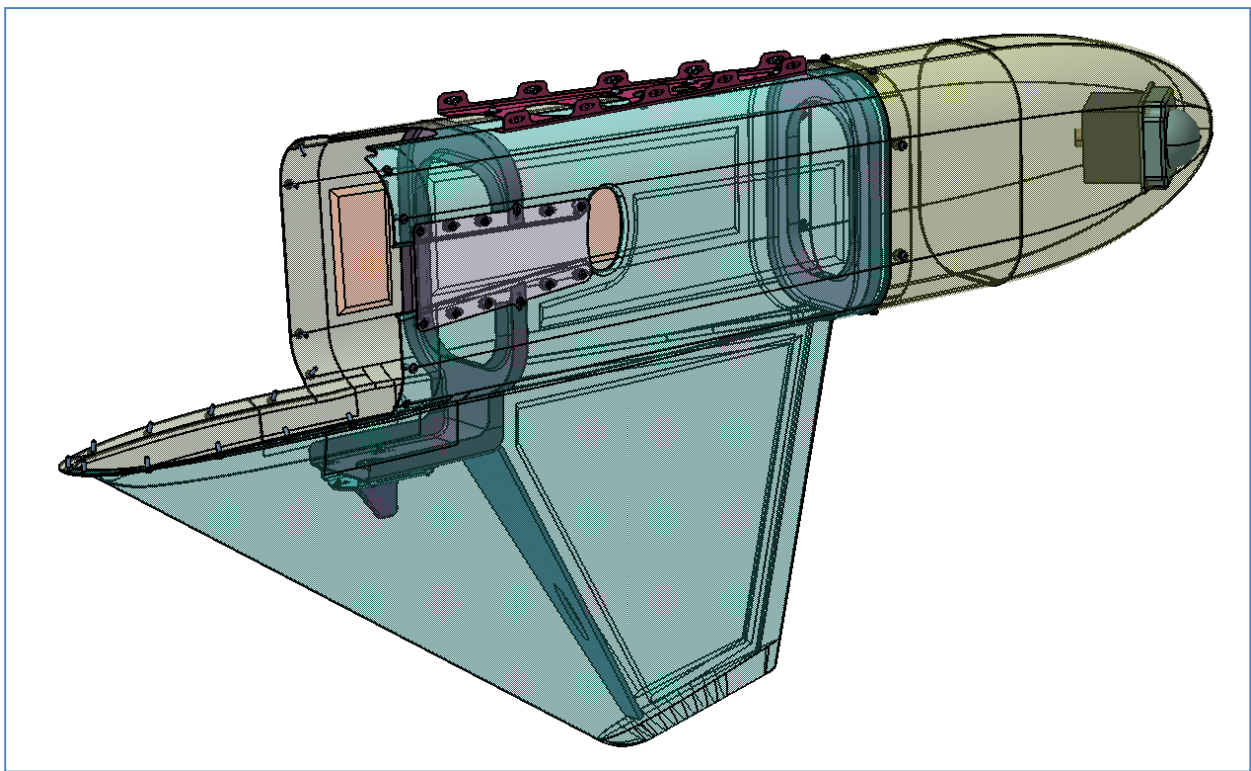
Figure 3-25 : Ventral fin assembly with tail cone and sensor

3.6.2 SKINS

The skins were made in two pieces that would be bonded together and form the complete fin skin. This was to done to stay within the selected manufacturing method of one-sided tooling using vacuum assisted hand lay-up. The bonding of these two parts is done with a scarf joint using joining glass fibre layers and epoxy resin (see Appendix F for details).

The use of foam sandwich laminates on the flat, thin skins were preferred to minimize the through thickness deflection caused by aerodynamic side loads. The foam sandwich structure could not be used in the radii due to the foam's lack of formability. The radii themselves add geometrical stiffness and were thus not a problem. On all areas where ribs would be bonded, the design was to be made monolithic to reduce the peel stresses. If a sandwich laminate was used here, the peel stress developed would likely have peeled the thin skin from the foam.

All edges which would have fasteners were designed with a minimum thickness of 2.5 mm and a quasi isotropic lay-up. This is to avoid knife edges when using countersink fasteners and eases the design of interface steps.

The mould for the skins would have the tool surface on the outside of the OML. This means that the outside surface of the skin will have a smooth, tool finish for aesthetic and aerodynamic purposes. However, the inside surface will have a rough finish which is not ideal as this is the surface that the ribs will interface with. A large tolerance will therefore be required between the interface surfaces of the rib and the skin. A mould for the skin can be seen in Figure 3-9.

A sacrificial outside layer of glass fibre with low planar weight will be placed on the outer layer of the laminate. This layer will not be taken into consideration in the FEA, because it is not seen as load bearing but rather to provide a sacrificial layer for sanding and other preparatory functions for painting.
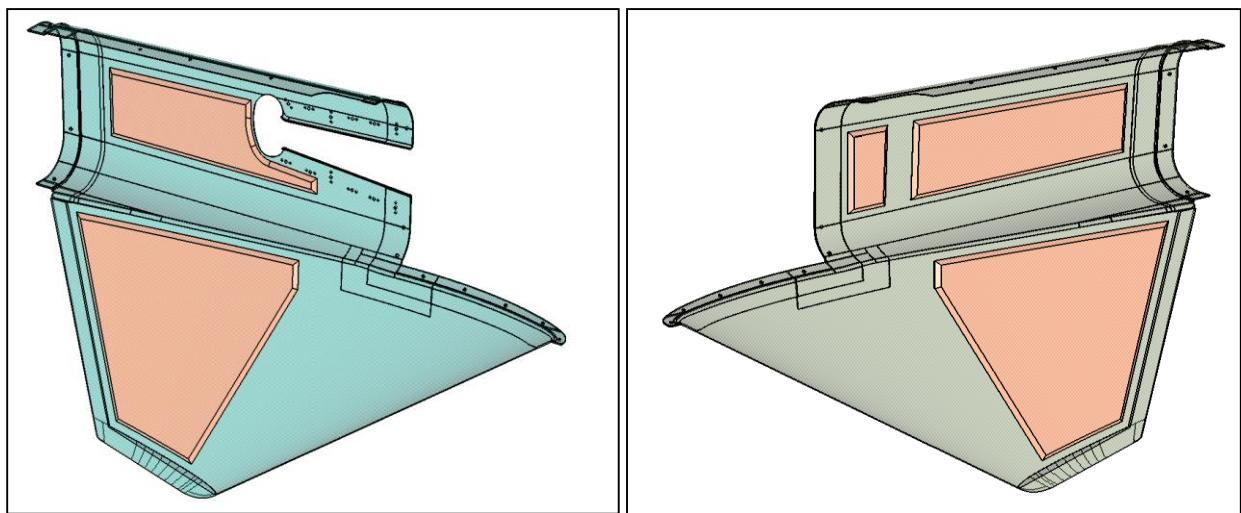
Figure 3-26: Ventral fin skin design RH and LH, respectively

3.6.3 RIBS

The ribs were designed to prevent the skins from collapsing and to stiffen the whole assembly near the attachment points. The front rib provides the mounting point for the antenna. These ribs have an outer flange for bonding and an inner lip to stabilize the web out-of-plane. To ensure that the web of the ribs remain free of local crippling, they will be designed with a foam sandwich construction.

The tooling for both ribs has the same philosophy as the skins. The outside surface of the rib is the surface that will be bonded to the inside surface of the skins. To avoid tolerance build-up the outside surface of the ribs will be the tool surface; this will also ensure a good and even bonding surface. Figure 3-27 shows the patterns, moulds and parts for both ribs. It can be seen from this figure that the pattern's (brown) outer surface is the same as the tool's (blue) inner surface and the part's (red) outer surface. This is the interface surface to the skin and must have controlled tolerance for the correct fitment.
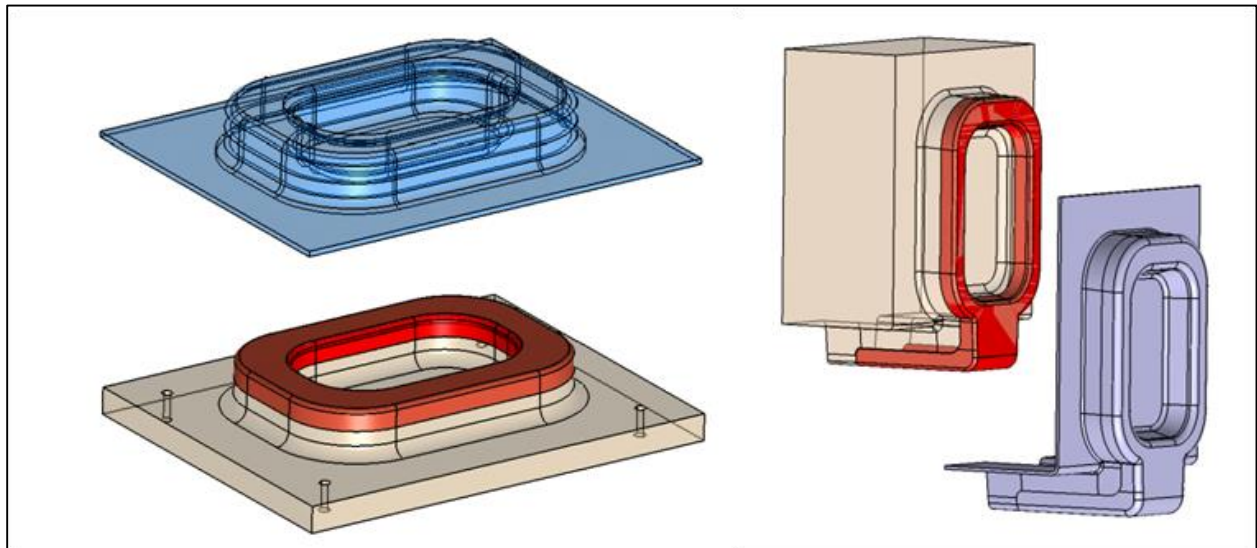
Figure 3-27: Pattern, tool and ribs

The bonding of the ribs to the skins would require a suitable adhesive that has good gap-filling properties, because of the fact that a tool surface would be bonded to a bag surface. To reduce the number of required materials, the same epoxy resin used to manufacture the parts will be used for the bonding application. The epoxy will be mixed with cotton flocks to increase the viscosity and aid in gap-filling.

3.6.4 SPAR

The main function of the spar is to stabilize and stiffen the skins under the aerodynamic loading. It provides a load path from the skins through the spar to the rib and finally into the tail boom attachment. The secondary function is to provide additional stiffness in the event of a tail strike, the angle of the spar is designed that the compression force generated by a tail strike is in the same work line as the spar.

To reduce the tooling, this spar will be manufactured on a flat surface and then routed to shape. It will be a foam sandwich construction to minimize the risk of buckling. This spar will be bonded in the same manner as the ribs. A hole will be cut into this spar for the antenna to pass through.
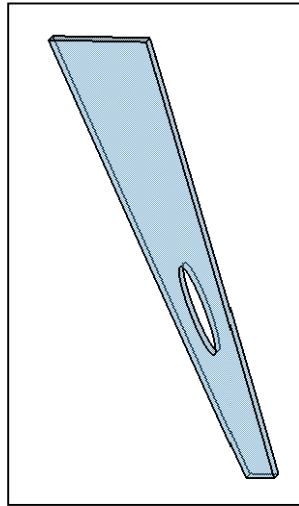
Figure 3-28: Spar of the ventral fin

3.6.5 ACCESS PLATE

The aluminium access plate is designed to cover the gaping hole where the control linkages for the elevator have to fit through. This plate is not designed to take up load and therefore will be omitted from the FEA. Special floating fasteners are used to ensure that no load is transferred to this plate.
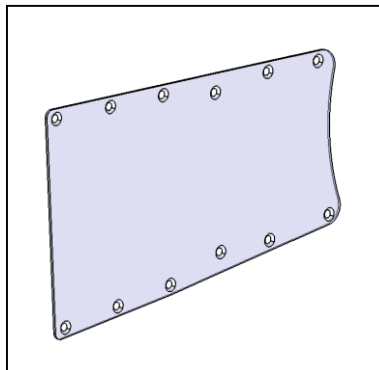
Figure 3-29: Access plate of ventral fin

3.7 Conclusion

A detail design of a ventral fin that is theoretically sufficient with regards to the three parameters of concern (mass, stiffness and strength) is now available. The detail design was verified by FEA to meet the strength and stiffness requirements under the expected loading of the ventral fin. They are the deflection of the airfoil under aerodynamic loading, the composite failure index and the fastener failure loads. There is an adequate CAD model and ply book on how to manufacture the fin and assemble the final product, which can be used to manufacture multiple assemblies of the same quality and performance. This section of the study could be applied to most of the composite components on AHRLAC to obtain a first-order detail design. This method of design will be verified using static testing and by comparing it to the FEA.

The FEA did not take into consideration the stability effects, such as buckling. Also no detail on the adhesive bonding between parts was modelled or analysed. The FEM was simplified in these areas to reduce model complexity and analysis time. The static test would indicate if there is a need to include these in further analysis.

This design is a first-order design and can be optimized further for each of these parameters to reduce the mass, if necessary, later in the project's life cycle. The further optimization process is not part of this study.

The detail design is divided into two sections: The first being the detail CAD model, which is modelled on CATIA, and the second, which is the ply book, that defines the lay-up and directions of the fibres. These two should be used together to manufacture the parts and assemblies. The ply book can be found in Appendix F.

4 MANUFACTURE AND TESTING

4.1 INTRODUCTION

The goal of this section is to validate the design methodology followed in Chapter Three by the manufacturing and static testing of the ventral fin (Figure 4-1). The validation process will determine if the FEM represents the actual part behaviour as it would occur on the aircraft. The validation process would thus only be applied to the ventral fin assembly, but if it is proved that the design methodology can be used reliably, it could be used on all composite components of AHRLAC XDM.

The first part of the validation of the design methodology is focused on the manufacturing of the ventral fin. The manufacturing methodology of a composite component is an integral part of the design procedure and the successful manufacturing of the ventral fin, which will be used for testing, will be the first part of the validation of the design process.

The second part of the validation process is focussed on the FEA of the ventral fin. This would validate the mathematical model used in the FEA, the material testing done to determine the input properties and the quality of the manufacturing method. The behaviour of the ventral fin under static load would be compared to the FEA of the same loading conditions. The loading conditions used in testing would be an approximation of the loads used in the FEA and therefore have the possibility to occur on the aircraft. Three static tests were done: the aerodynamic test, the tail strike test and the G-force load test. In the following paragraphs these tests will be discussed in detail.
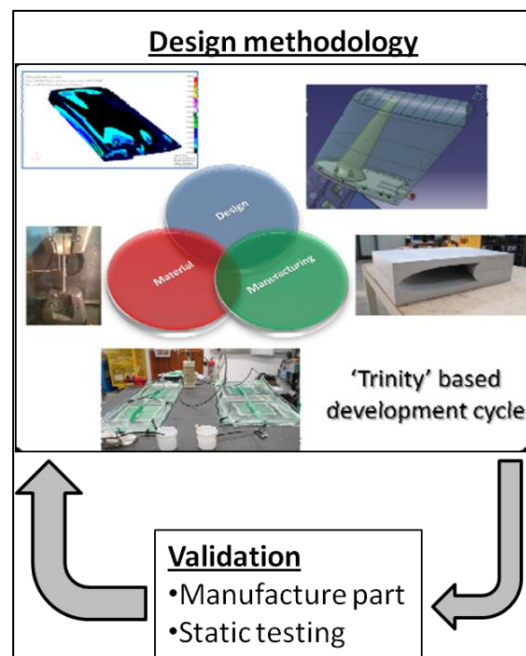
Figure 4-1: Validation of the design methodology

4.2 MANUFACTURING OF THE VENTRAL FIN

The output of the design methodology was a detail design of the ventral fin complete with a ply book and detailed CAD model, this design was verified by FEA to be sufficient in terms of mass, stiffness and strength. The ply book can be seen in Appendix E and the CAD model in Figure 3-25. These two items were used to manufacture the ventral fin assembly. The manufacturing was done by qualified aircraft composite artisans to ensure high component quality. The result of the detail design shows that the ventral fin will comprise of the following parts:

- Ventral fin assembly
  - Left/right skin
  - Fore rib
  - Aft rib
  - Spar

4.2.1 TOOL MANUFACTURING

The first part of the chosen manufacturing method was the Computer Numerical Control (CNC) routing of the patterns. These patterns will be used to manufacture the composite tool that will be used in the lay-up of the actual composite parts that will be used in the ventral fin assembly. The patterns were cut from bonded stacks of tooling board using a CNC router. They were then finished by sanding and applying a coat of primer then polishing the surface to a smooth tool surface. The composite tool will be laid up against the patterns; therefore the outer surface of the pattern will define the tool's outer surface and ultimately the part's outer surface (Figure 4-2).

This method is used so that the patterns can be kept in safe storage. If the tool is damaged during manufacturing there will still be a pattern to create another tool from. An illustration of this method can be seen in Figure 4-2. This method was used on all the parts of the assembly except for the rib, which was laid up on a glass table and cut to final size.
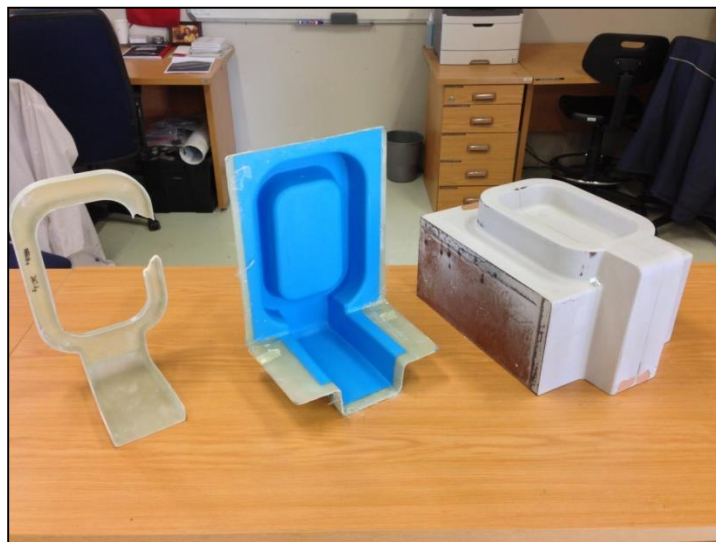
Figure 4-2: From left to right: final trimmed part, tool and pattern for the fore rib of the ventral fin

The tools were made from a heavy weave, commercial, fibreglass fabric which is impregnated with commercial grade epoxy. The preparations of the lay-up of the tools start with applying a release agent to the pattern surface. When the release agent is dry, a layer of gel coat is applied and left to partially cure until tacky. At this stage, multiple layers of heavy weave fibreglass and epoxy are applied with the hand lay-up method and then left at room temperature for two days to cure. After curing, the tool is demoulded from the pattern and trimmed to its final dimensions. The pattern, tool and final part for the fore rib can be seen in the centre of Figure 4-2.

This method of tool manufacturing results in a tool with large void content and thickness variations. This is acceptable as the tool performance is only influenced by its dimensional stability and surface condition. Reducing the overall cost is the main motivator for using the low performance manufacturing method of the composite tools. The tool would be acceptable as long as enough glass fabric is used to ensure dimensional stability and the gel coat is adequately polished for a good surface finish. The epoxy used in the composite tool should be able to withstand the curing temperatures of the epoxy used in the part.

4.2.2 PART MANUFACTURING

The same manufacturing method was used for each part (skins, fore rib, aft rib and spar). The manufacturing method details were discussed in Section 3.4, where hand lay-up with vacuum assisted curing was chosen. This method entails impregnating the dry fabric with epoxy by using a laminating brush, then covering the component in a vacuum bag and placing it under vacuum to cure at room temperature for 24 hours, after which the part is demoulded and trimmed to its final dimensions. This manufacturing method is illustrated in Figure 4-3 and the layer used in the vacuum bagging can be seen in Figure 2-17. Refer to Appendix F for the detailed ply book.
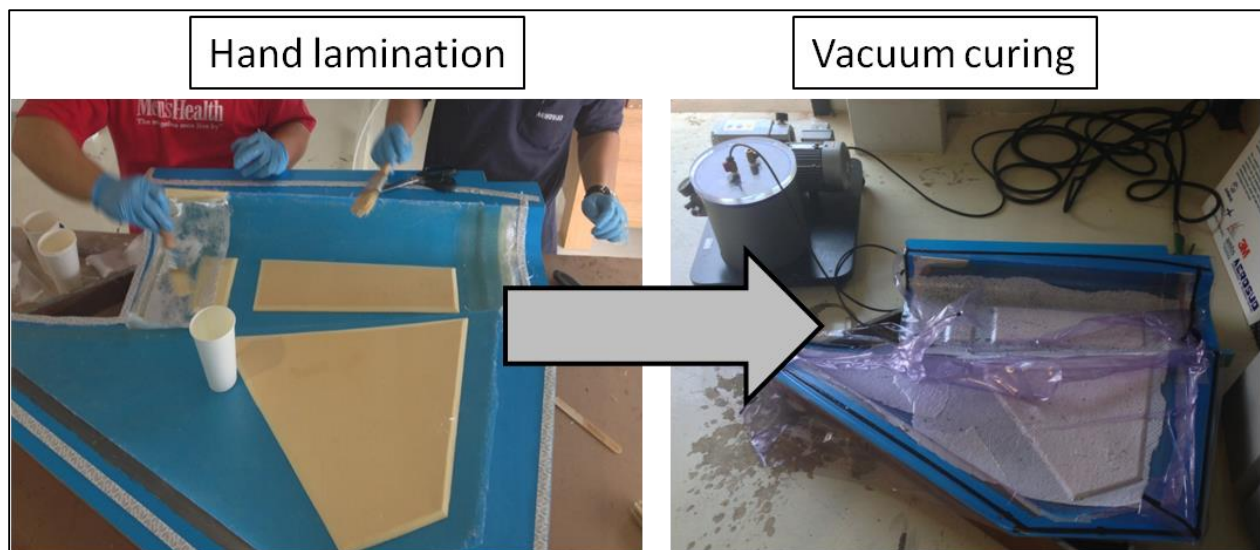
Figure 4-3: Hand lamination and vacuum curing of the ventral fin skin

4.2.3 ASSEMBLY MANUFACTURING

Once all the parts were cured, demoulded and trimmed accordingly, the final assembly of the ventral fin could take place. The selected assembly method was to bond the left and right skins together, with all the ribs and spars in place. This was done by using the same epoxy and glass fabric used in the parts. The epoxy was mixed with cotton flocks to give it gap-filling capabilities to account for thickness variation between interface parts, such as the ribs and skins. The detail on the joining can be seen in the ply book in Appendix F.

Trimming of the assembly was done with an air grinder and special composite cutting disks; the holes for the fasteners were cut with an sharp drill bit. The parts were visually inspected for signs of damage, delamination or large voids after processing, due to manufacturing defects, as discussed in Section 2.4.
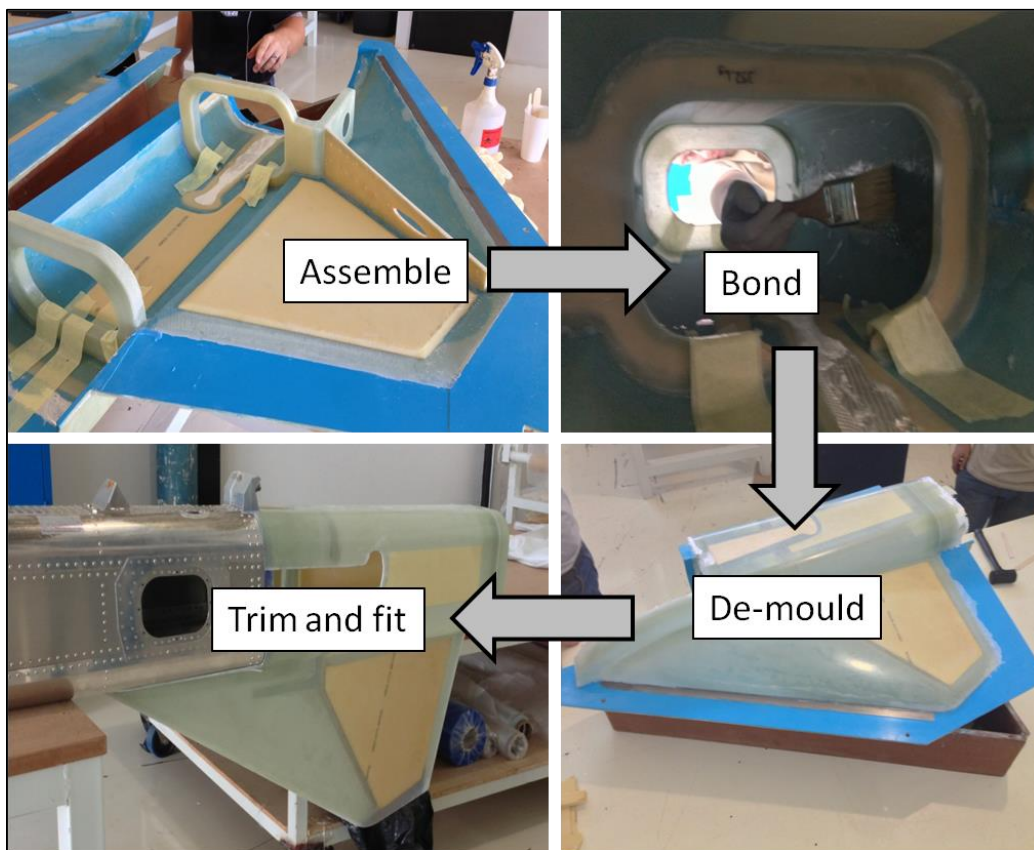
Figure 4-4: Assembly of the ventral fin

4.3 TESTING OF THE VENTRAL FIN

In this section the test set-up used for each of the three, non-destructive, static tests will be discussed in detail (Table 22). The purpose of these tests is to serve as the second validation stage of the design methodology, with the first stage being the manufacturing of the test ventral fin.

The static testing of the ventral fin assembly is necessary to obtain confidence in the methodology used in the design phase, which will include the material testing and FEA. The assumptions made in these two sections of the study will be tested by comparing the results of the FEA with the static tests. These tests do not include the testing of failure criteria as this was previously proved [38]. Thus, the test will not increase the load to a point where the ventral fin fails, but rather only to the ultimate loads. At these loads failure should not occur accept for the tail strike load case in which local failure is allowed. For this specific load case the load will only be increased to the design load.

Test description	Loading conditions	Parameters of concern
Aerodynamic test	Ultimate load of the aerodynamic case. Total of 2760 N as four point loads on each skin.	• Ventral fin deflection behaviour • Failure of composite • Failure of tail boom attachment fasteners
Tail strike test	Ultimate load of the G-force load case of the combined mass of the tail cone and sensor unit Total of 2542 N as one point load.	• Ventral fin deflection behaviour
G-force test	Ultimate load of the G-force load case of the combined mass of the tail cone and sensor unit Total of 1018 N as one point load.	• Ventral fin deflection behaviour • Failure of tail cone attachment fasteners

Table 22: Summary of the ventral fin static test conditions

In all the testing, the loading would be done by incrementally adding weights to a loading saddle and then taking measurements between loadings. The test area should be quiet as to listen intently for audible indications of cracking. After the required test load is reached, the structure would be unloaded and inspected for signs of visual damage, including mounting holes and visual delamination.

In all testing load cases, as part of the set-up, a small load (typically 10 % of the design load) will be applied to the structure and then removed. This is done to settle the structure and eliminate the free play before the actual test commences.

4.3.1 MEASURING EQUIPMENT USED

The main parameters that had to be measured in each test are load and deflection. In all three tests, the load versus deflection graph will be compared to the FEA results.

The deflections expected from the FEA for each test case are in the region of 1 mm to 10 mm. The measuring of these deflections will be done using Mitutoyo dial gauges mounted on magnetic bases (Figure 4-5). These dial gauges have a measuring resolution of 1/100 mm. They have more than enough resolution to obtain a meaningful deflection result. The only negative aspect of using these manual gauges is that the deflection has to be recorded manually after each loading increment.

The load will be applied by using steel weights which are added to a loading saddle and the saddle's weight will also be taken into consideration. The mass of each loading block and loading saddle is measured using a digital scale that has a maximum load of 120 kg and a resolution of 1/100 kg. It is more than sufficient for meaningful mass measurements of the loading block, which weighs between 5 and 25 kg. Again, the only disadvantage of using this manual measuring method is that each block will have to be recorded manually and added to the loading saddle. The loading method also lacks the addition of small loads which would be problematic when the deflection is expected to be non-linear and curve fitting is required, but the load deflection curve is expected to be a linear curve and the curve fitting would be acceptable using this relatively large load increments.

Figure 4-5: From left to right: Dial gauge, magnetic base and digital scale used in static testing

4.3.2 AERODYNAMIC LOAD CASE

The aerodynamic side load was calculated by the aerodynamicist at maximum side slip and speed, at sea level. This yielded a design side load of 1380 N on the airfoil surface area of a fin. The load in the FEA was applied on the whole airfoil surface as a distributed load. The worst case direction of the load was the direction that would lead to the side cut-out closing. This direction was used in the FEM and testing.

Under aerodynamic load, the fin had to withstand the ultimate load of twice the design load (1380 N x 2 = 2760 N). The fin also had the added requirement of not deflecting more that 10 mm under the design load of the airfoil section. Under the ultimate load in this load case, the laminate and the fasteners should not fail.

The conventional way to apply a distributed load on an airfoil section, such as a wing, is to load the lower surface of the wing with bags of sand or lead shot. This becomes impractical when the surface area is small compared to the number of bags that is needed to simulate the load, which was the case with the ventral fin. The more practical way of introducing a distributed load would be to use a wiffle tree. The wiffle tree is a component that distributes a single load evenly into multiple connecting points. For the aerodynamic load case, a wiffle tree with four mounting points will be used on each skin. These four mounting points should have a centre of force point that is co-linear to the centre of pressure of the airfoil section, in order to accurately simulate a perfectly distributed load (Figure 4-6).
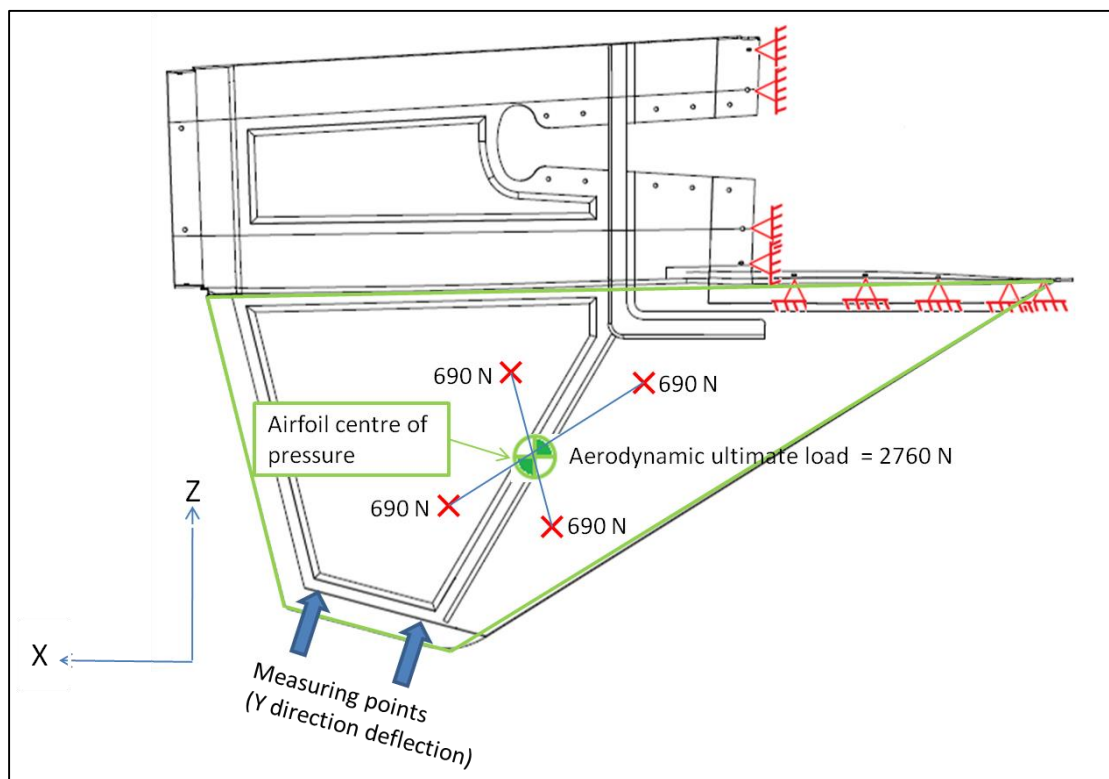
Figure 4-6: Diagram of test set-up of the aerodynamic load case

Figure 4-7: Aerodynamic test set-up showing tail boom connection and measuring points

To simulate this distributed aerodynamic load in testing, four hooked rods that passed through both skins (red axis in Figure 4-8) combined with large washers and foam squares were used to introduce the load into the two skins. These four rods were hooked to a wiffle tree that was used to distribute the load to the rods evenly, despite of the deflection of the part. A saddle hooked onto the wiffle tree and this point was co-linear with the centre of area of the airfoil section (green axis in Figure 4-8). Steel weights were then weighed and placed on the saddle to simulate the force magnitude of the aerodynamic loading.
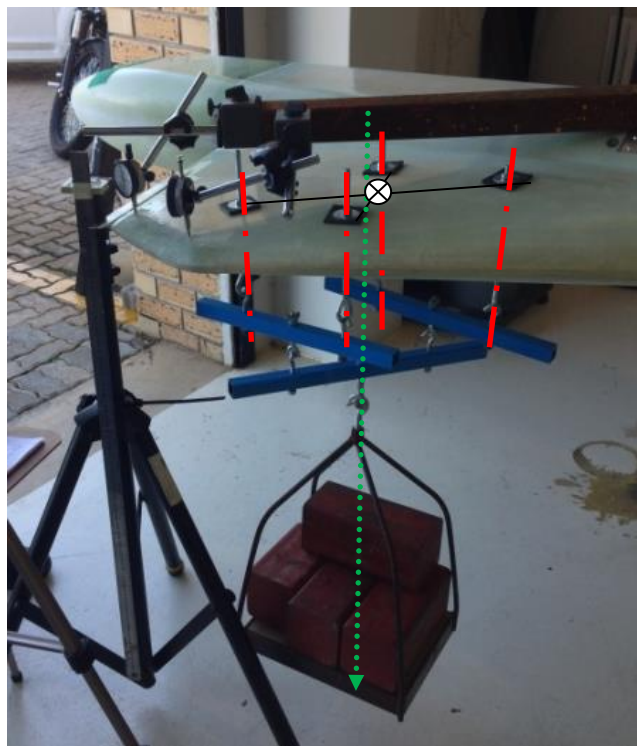
Figure 4-8: Aerodynamic load case static test set-up

This does not simulate a distributed load perfectly but it is accurate enough for this test, as the local deflection will not be taken into consideration, but rather a more global deflection. Deflections were measured by using two dial gauges that were mounted on the aft end of the tail boom. This was done to ensure that the tail boom's deflection was not taken into consideration. Measuring points were on the lower two corners of the airfoil section. This is far enough away from the load introduction points in order to limit the local load simulation deflection errors. The average of these two dial gauges will be compared to the FEA. Care was taken to ensure that the dial gauges were in the global Y aircraft direction; this is the pure lateral deflection of the airfoil section.

4.3.3   TAIL STRIKE

The tail strike load case consisted of two combined loads (Figure 4-9). The first being the reaction load introduced by slamming the fin into the ground: this force is 2000 N in magnitude. The second is the load as a result of friction between the ground and fin; this force is 1570 N in magnitude. The directions of these forces are illustrated in Figure 4-9, which is the design load for the tail strike case. At this load, the laminate has a FS of 1.6 and the fasteners 2.3. Therefore, no failure is expected at the design load.

For this test the loading will cease at the design load. The deflection will be used as a measure of the accuracy of the FEA.

The test set-up was angled by adjusting the tail boom angle so that the strap used in the load introduction, was at the correct angle with respect to the bottom edge of the ventral fin.
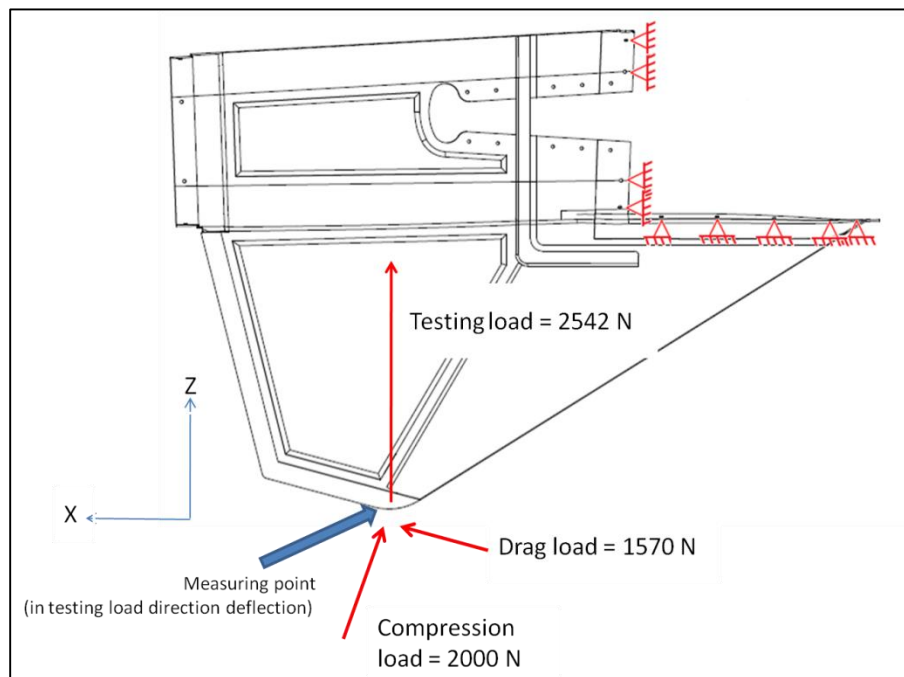
Figure 4-9: Tail strike design load case free body diagram

4-9

Figure 4-10: Tail strike load case test set-up and load introduction

4.3.4 TAIL CONE G-LOAD

For this load case, the design load comprised of the mass of the tail cone with sensors (6.1 kg) and was multiplied by the G-force load factor of 8.5 and applied in a co-linear line to the centre of gravity of the assembly. At this design load the laminate should have a minimum FS of 2 and thus an ultimate load of 1016 N. This is the maximum load that would be applied in the static test.
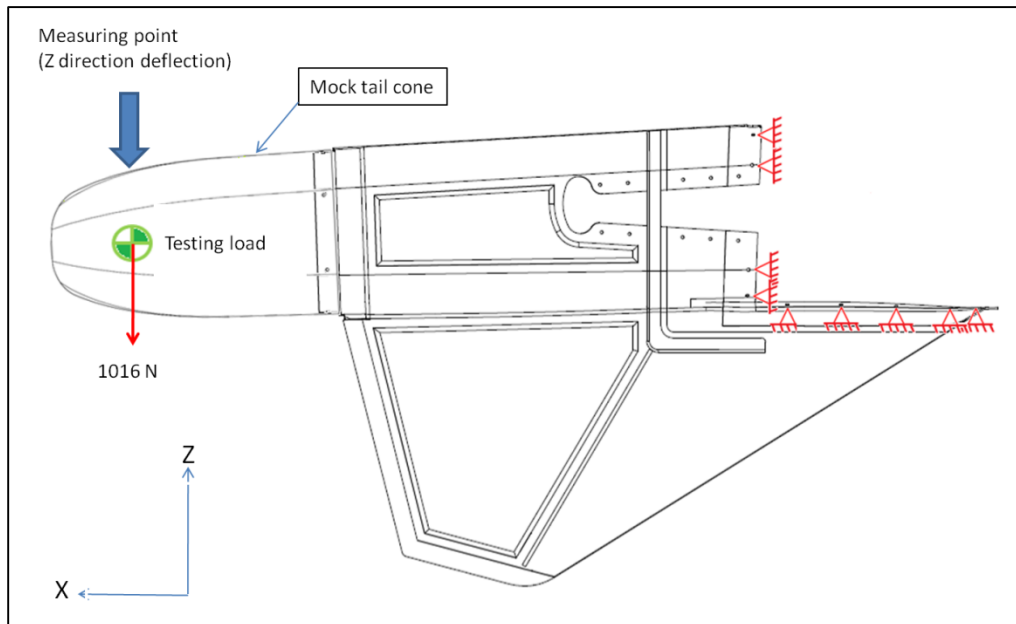
Figure 4-11: G-force load case test set-up

For this test a mock tail cone was manufactured from the same glass fibre and epoxy as the ventral fin. This representative tail cone was added to a separate FEA so that the measurements could be taken from the tail cone. All the same material properties and assumptions were used on this tail cone as the ventral fin. The set-up can be seen in Figure 4-12.

Figure 4-12: G-force load case test set-up and load introduction

In this test two results will be examined to validate the design methodology. This validation process would involve comparing the displacement of the tail cone to the FEA and during this test the fasteners are not expected to fail at the ultimate load. The displacement will be used to gain confidence in the FEM and the assumptions used in the material testing.

4.4 RESULTS AND CONCLUSION

In this section the manufacturing of the ventral fin, as well as the results of the three static tests will be given and discussed. This will include a deflection graph compared to the FEA, and a short report on any damage found after each test.

The ventral fin assembly includes the tail cone attachment on the fin, but does not include the tail cone itself. A mock tail cone was added to the FEA in the case of the G-force load, but all the same assumptions were made on the tail cone as with the ventral fin.

4.4.1 MANUFACTURING OF THE VENTRAL FIN

The composite materials selected for use in the ventral fin was a glass fibre 2x2 twill weave fabric which was impregnated with an aerospace grade, room temperature curing, epoxy. The core material that was selected was low density structural foam. These materials fulfilled the requirements of radar transparency, structural strength and stiffness. It was also an easy material to use for the selected manufacturing methods.

The manufacturing of the ventral fin was done using a detailed ply book and the final dimensions of the CATIA models.

The selected manufacturing method of the ventral fin was in line with the low initial cost and high skill requirement of the prototyping environment. The selected manufacturing method was to cut a pattern from tooling board using a CNC router. This pattern was painted with a suitable primer, polished and then used to create an open, one-sided, composite tool. This tool was made from glass fibre fabric and epoxy. By using this method, the tooling cost was kept to a minimum while still ensuring geometrical quality of the tools to be used in the manufacturing. Care had to be taken to create the tools with enough run-out to allow for final trimming and vacuum bagging; a 100 mm run-out was more than sufficient. The tools had to be airtight so that it could be used in combination with vacuum bagging. This was not found to be a problem with the one-sided composite tools. Both the pattern and tool surfaces were highly polished to a gloss finish, which resulted in a very good part finish and aided in demoulding. Parts were designed with these tools and the demoulding process in mind, to minimize problems with demoulding all parts had a draft angle that made it possible to demould to one side. The use of small radii on the parts was avoided to aid in demoulding.

These one-sided, open tools were used to create the individual parts. The parts were made by hand placement of the dry fibres and manually impregnating it with resin. The part was then bagged and placed under vacuum to cure. These parts were demoulded after a full cure and manually trimmed and processed to the required dimensions, after which they were assembled using the same epoxy. This was a very time consuming manufacturing method, but was in line with the low initial cost of prototyping. The part quality was insured by using highly skilled artisans to carry out the laminating work.

The ventral fin's stiffness and strength properties were very dependent on how accurate the artisans could lay the fibres in the correct directions. The hand lay-up is not a very accurate method of placing fibres, but was found to be sufficient for this purpose.

The resin to fibre ratio also has a large influence on the material properties and is not very well controlled in the manual impregnation of fabric with resin. The vacuum added after lamination aids in removing excess resin, but if the laminating process takes too long and the resin starts to get tacky before the vacuum is applied, the resin to fibre ratio will be compromised. All parts were manufactured in temperature controlled environments to reduce the curing reaction and great care was taken to ensure the parts were placed under vacuum within the pot life of the epoxy.

The assembly of the ventral fin was done by bonding the individual parts together, using epoxy mixed with cotton flocks. This is common practice to give the epoxy gap-filling properties. All parts were made on one-sided tools, therefore one side of the part had a tool finish and was very accurate according to the CATIA geometry, while the other side was the bag side of the laminate and varied largely from the CATIA geometry. This was the reason for designing with loose tolerance fits between the bonded parts in the assembly. These bonding methods performed satisfactory during testing.

The final assembly was visually inspected and found to be of high quality for this specific manufacturing process. The complete manufacturing method was deemed satisfactory for the prototype aircraft.

4.4.2 STATIC TESTING

Aerodynamic load case

After the test was concluded, the ventral fin was inspected for any signs of damage and none were found. Thus, the ventral fin assembly has passed the test without any failure. The deflection of the static test compared to the FEA is given in Figure 4-13.

The FEA is 42 % less stiff than the test model under ultimate load; there are three possible reasons for this discrepancy. The first reason could be that the FEA used material properties that were tested at 55°C, while static testing will be conducted at a room temperature of 23°C. The literature review revealed that the material properties of epoxy composite deteriorate as the temperature increases. The FEA was done at an elevated temperature to ensure safe operation of the fin in all expected conditions of the AHRLAC XDM operations. By using the compressive test results, the knockdown factor between these two temperatures were found to be 13.8 %. This would decrease the difference from 42 % to 16.8 %.
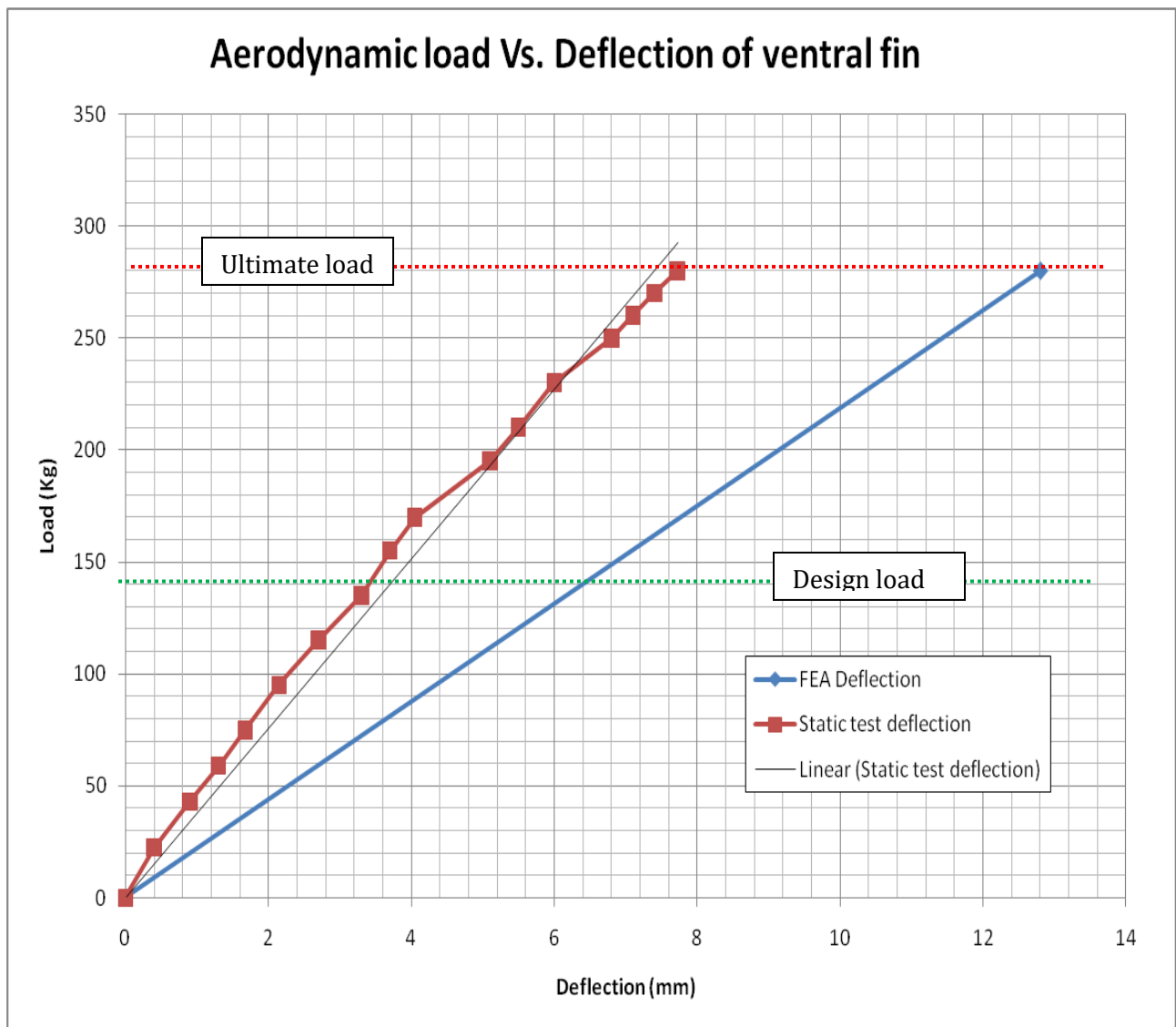
Figure 4-13: Results of static test compared to FEA: Aerodynamic load case

The second reason for the difference between the FEA and static test results is termed the membrane effect and illustrated in Figure 4-14. This effect is not taken into consideration by the finite element software, but could be one of the reasons for the discrepancy between the static test and the analysis results. The load in this load case in the FEA is modelled as being distributed perpendicular to the thin surface of the airfoil section on the skin of the ventral fin. The plane stress theory used in the FEA does not allow the skins to carry bending load and results in a relatively large deflection of the skin in the through thickness direction ("small" deflections in Figure 4-14). In the static test it could be that the large deflection of the skins in the through thickness direction was not achieved due to the membrane effect ("large" deflections in Figure 4-14). This is where the skin's deflection is large enough so that it starts working in tension as a membrane and therefore becoming stiffer. This is quite common in thin composite structures with through thickness loads.
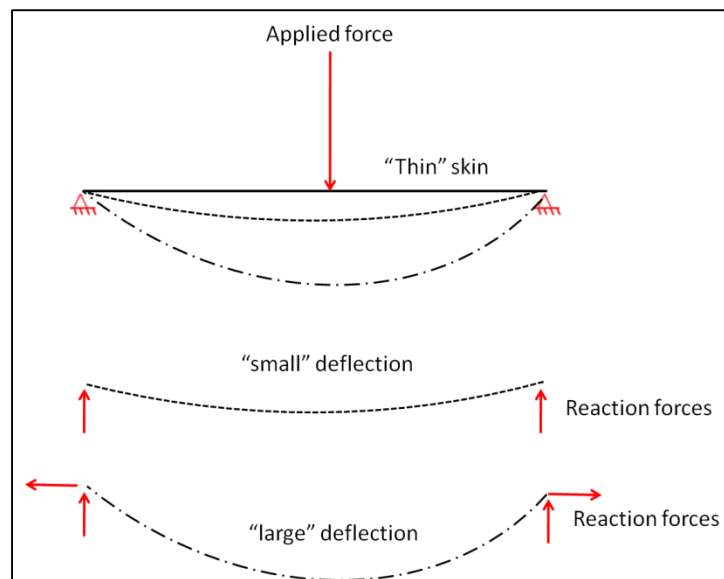
Figure 4-14: Diagram illustrating membrane effect

The third reason for the discrepancy in the results could be due to the measuring direction by the dial gauges during the static test. The FEA deflection results are measured in the global Y direction, thus any deviation of this angle caused by human error in the placement of dial gauges would lead to less accurate results.

A fourth reason could be because the FEA loads both skins with perfectly distributed load while the testing was done with four point loads on each skin. This difference in load introduction could lead to local deflection differences.

Tail strike load case

After the conclusion of this test, the ventral fin was inspected for any signs of damage. None was found. Also no audible signs of damage were heard during testing. Thus the ventral fin assembly has passed the test without any failure.

With respect to Figure 4-15, the FEA is 14 % less stiff than the test model under the design load, which is much more accurate than the 42 % stiffness difference seen in the aerodynamic load case. This is another indicator that the membrane effect could influence the aerodynamic load case test results, because no load was introduced in the tail strike test perpendicular to a relatively thin surface.

As with the aerodynamic load case, the material properties used in the FEA were determined at 55°C, whilst the test was done at room temperature. This should account for up to 13.8 % of the stiffness difference. This shows a very close correlation with the FEM and all assumptions made in the material testing.
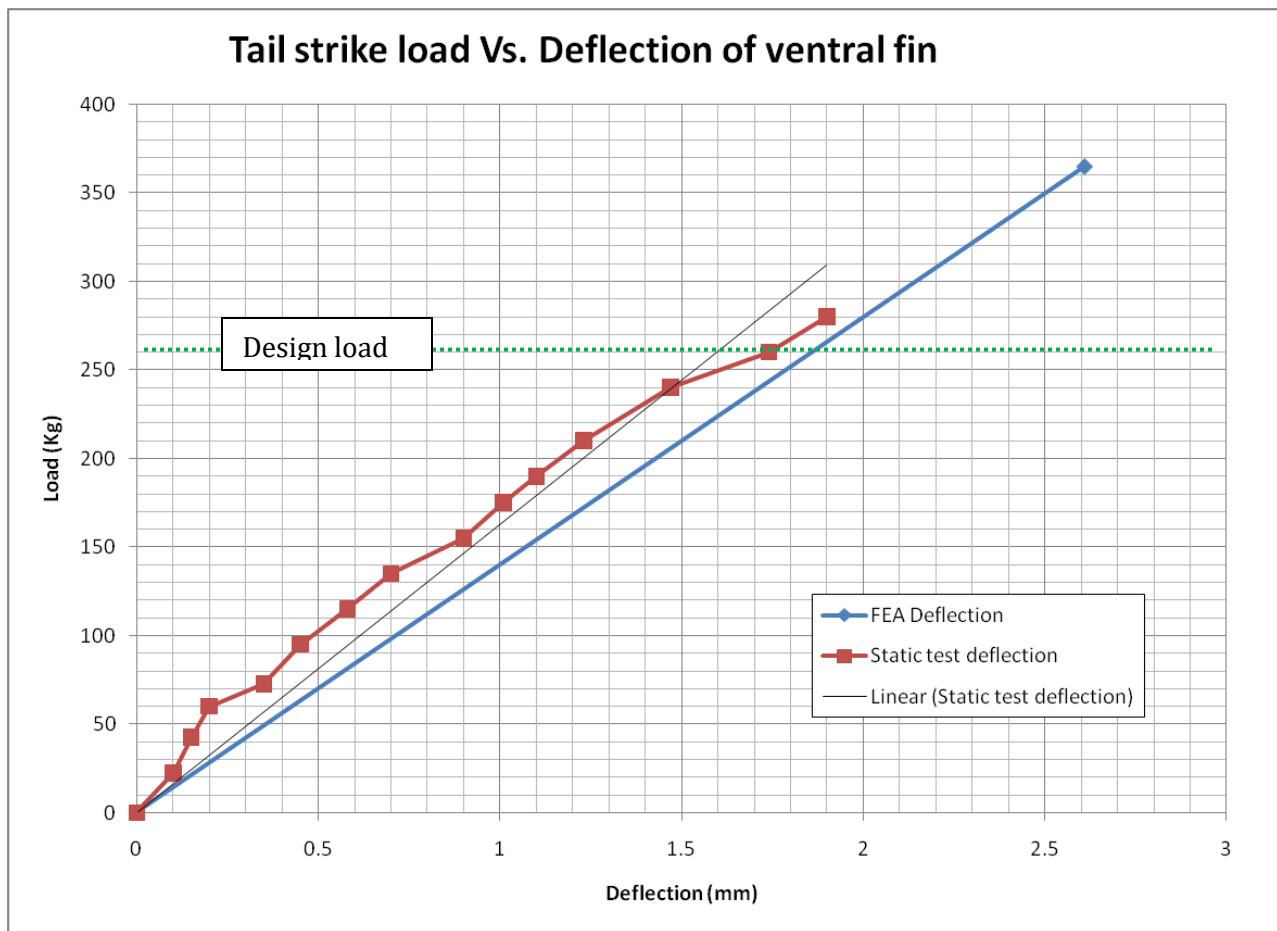
Figure 4-15: Results of static test compared to FEA: Tail strike load case

G-force load case

After the conclusion of this test, the ventral fin was inspected for any signs of damage. None was found. Also no audible signs of damage were heard during testing. Thus the ventral fin assembly has passed the test without any failure. For this specific test, the rear fastener set also had to be inspected and was found to be damage free.

With respect to Figure 4-16, the FEA is 18 % less stiff than the static test model. This test was done primarily to ensure the adequacy of the fasteners that attach the tail cone to the ventral fin. The deflection was measured on the mock-up tail cone and does not form part of the ventral fin design. Nonetheless, the same methodology was followed in the modelling of the mock tail cone and the comparison of the FEA and static test is shown in Figure 4-16.

In this test there were signs that the representative tail cone's side walls were buckling; this reduces the accuracy of the FEA. As with the aerodynamic load case, the material properties used in the FEA were determined at 55°C, whilst the test was done at room temperature. This should account for up to 13.8 % of the stiffness difference. This is a very close correlation between the FEA and all assumptions made in the material testing.
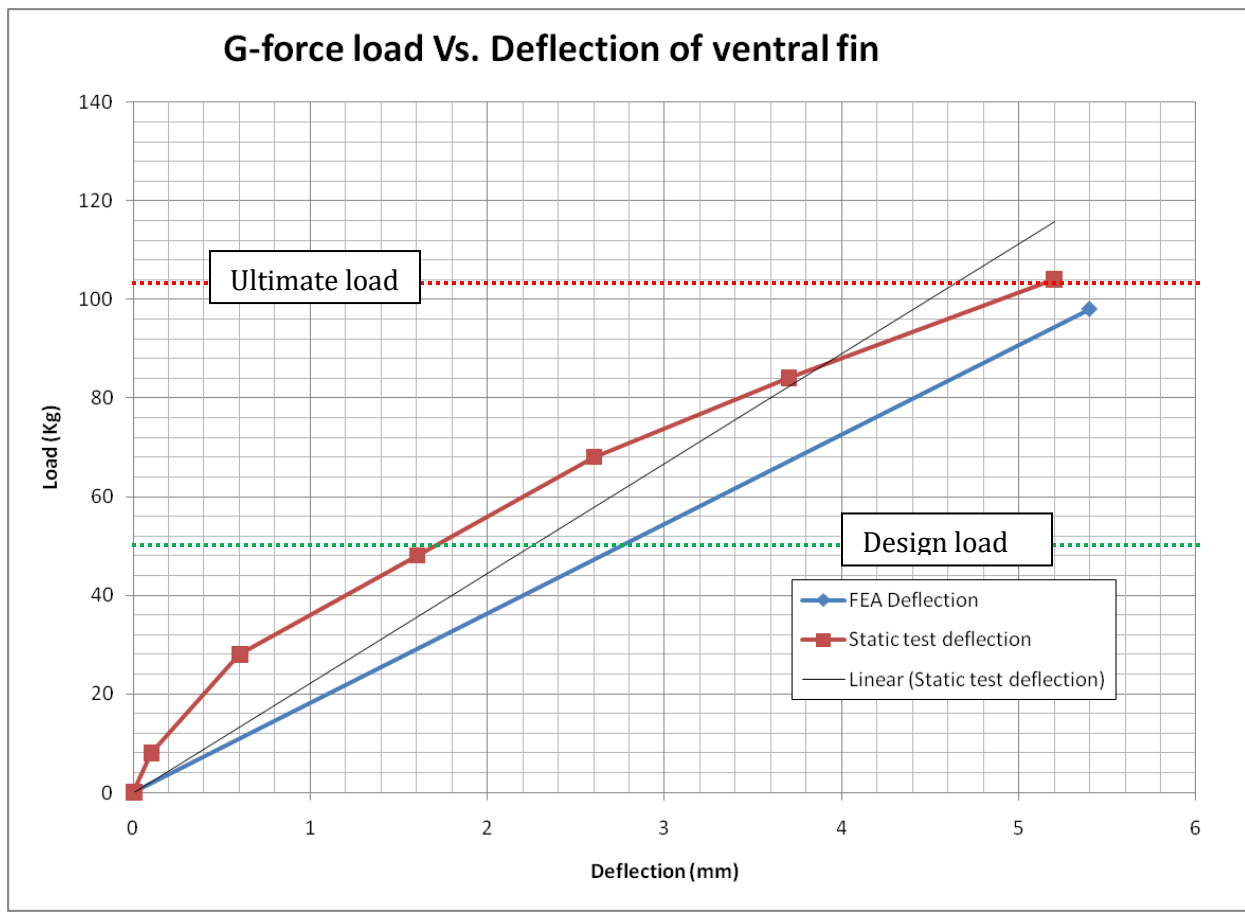
Figure 4-16: Results of static test compared to FEA: G-force load case

5 CONCLUSION AND RECOMMENDATIONS

In the final chapter of the dissertation, the conclusion will be discussed with regards to the design, manufacturing and testing of the ventral fin. Recommendations will also be made on problems encountered during this study and possible areas for further research.

The problem statement and outcomes discussed in Section 1.3 will be used as the basis of the conclusion discussion, with regards to the validation and verification of the ventral fin design methodology.

5.1 VENTRAL FIN OF AHRLAC XDM

The composite ventral fin of AHRLAC XDM was successfully designed using CATIA computer aided design software. This design was easy to manufacture and performed sufficiently in the load cases used to evaluate the performance of the fin. From the design, the behaviour of the fin could be accurately modelled using Patran/Nastran FEA software. This software could also accurately predict the strength of the assembly and ensure that the fin could withstand the expected service loads.

5.2 FINITE ELEMENT ANALYSIS – VERIFICATION

The FEA methods were shown to be sufficiently accurate to model the behaviour of the composite ventral fin under the three loading conditions of concern. The FEM was shown to be 42 %, 14 % and 18 % less stiff than the static tests in the aerodynamic, tail strike and G-force load cases, respectively. The main reason for the discrepancy in the aerodynamic load case, is that the load is introduced in the through thickness direction of the skin, which can cause large deflection of the skins and lead to the membrane effect. All static tests were done at room temperature while the FEA was done using material properties obtained at 55°C and could decrease the stiffness of the FEA by around 13.8 %.

The methodology followed in the FEA included the material testing and all the associated assumptions and test methods. This method of determining the input parameters for the composite analysis was also deemed sufficiently accurate for stiffness prediction and to illustrate resistance to failure, under load, of the composite ventral fin.

The FEA revealed that the ventral fin would be able to withstand the ultimate load case of the aerodynamic and G-force load cases. The fin was not loaded until failure, but after each ultimate load the fin showed no signs of damage or failure. Thus, the finite element method used was sufficiently accurate to predict that the fin would be able to withstand the loads, but no comment can be given on the accuracy of the failure predictions of the analysis.

5.3 Manufacturing – Validation part 1

The manufacturing of the ventral fin went as expected and was found to be satisfactory for the application of a prototype aircraft. The uncertainties due to the hand lamination and fibre placement were very limited, because of the great care exercised by the artisans during the process. The FEA, with its precise fibre directions, had a good correlation with the static tests, thus the manufacturing methods followed were deemed to be satisfactory in terms of component performance. The manufacturing process was very time consuming, but this is acceptable in the prototyping environment.

5.4 Static testing – Validation part 2

The testing values were close to the expected values obtained from the FEA, which indicates a close correlation between the two (Refer to Section 5.1.2). The tests were very basic in terms of the measuring methods and load application, but seemed to be accurate enough for this study's purposes.

5.5 Recommendations

The recommendations could be used to further develop the field of composite design, as well as material testing and characterizations.

5.5.1 Composite design

In this study, the assembly mass of the ventral fin was optimized by starting with the minimal part count to satisfy the design requirements, after which parts were added until the strength and stiffness requirements were met. There was no optimization of individual part lay-ups and thicknesses; there is scope to individually optimize each part within the assembly which would reduce the mass even further.

5.5.2 Material testing

For the fast prototyping requirements of this study, the test sample size used in the material testing phase was small. This leads to a relatively large scatter in the data, which in turn causes decreased limit stresses. These limit stresses used in the failure criteria could be increased if the sample size was to increase and could ultimately lead to thinner parts that would reduce the mass of the component.

The shear stress allowable was obtained at 5 % shear strain as per the ASTM test specification and leads to a conservative shear limit stress being used in the failure analysis. This allowable could also be increased through the addition of special equipment so that a more representative shear allowable test can be conducted.

5.5.3 COMPOSITE FINITE ELEMENT ANALYSIS

A linear static analysis was used in this study to reduce the FEA complexity and decrease the design time of the component in order to align it with the prototype environment. The decision was made to use a plane stress analysis as an acceptable practice when using "thin" skin composites. This leads to an acceptably close estimation of component stiffness if loads are kept in plane with respect to the laminates, but large underestimations can be expected when the loads are perpendicular to the composite laminate.

The FEA accuracy could be increased through further testing of the lamina in the through thickness direction and by removing the plane stress assumption. The use of a non-linear solver, to account for the membrane effect, would also greatly improve the accuracy of the FEA.

5.5.4 STATIC TESTING

The accuracy of the static testing could be improved by using electric measuring equipment to measure the displacement and to use hydraulic load cells to apply the load. This would decrease human error in taking measurements. The loading would be applied in a much smoother manner which would eliminate shock effects on the structure and also reduce the sought after static load introduction.

Strain gauges could be used in static testing to measure and compare the tested strain of the FEA values and in so doing, check the load paths of the structure.

In this study, the test ventral fin was loaded to ultimate load and not to failure, thus no comment can be given on the accuracy of the FEA failure prediction other than that the fin could withstand the ultimate loads in the aerodynamic and G-force load cases. Further testing could be done where the fin is loaded up to failure and then compared to the FEA,

5.6 CLOSURE

The goal of this study was to design and manufacture a composite ventral fin for the AHRLAC XDM prototype aircraft. There were numerous geometrical and stiffness requirements .The fin had to be able to withstand the loads that it would be expected to encounter in the service life of the aircraft.

This study resulted in a successful design methodology to accurately design a composite ventral fin which adequately fulfils the geometrical, stiffness and strength requirements.

REFERENCES

[1] Pierluigi Della Vecchia, Salvator Corcione and Fabrizio Nicolosi, "Design and aerodynamic analysis of a twin-engine commuter aircraft," *Aerospace Science and Technology* , vol. 40, no. 1-16, 2014.

[2] Andrea Goldstein, "The political economy of high-tech industries in developing countries: aerospace in Brazil, Indonesia and South Africa," *Cambridge Journal of Economics*, vol. 26, pp. 521-538, 2002.

[3] C. L. Benkard, "Learning and forgetting: the dynamics of aircraft production," *American Economic Review*, vol. 90, no. 4, 2000.

[4] W. T. Freeman, "The use of composites in aircraft primary structure," *Composites Engineering*, vol. 3, pp. 767-775, 1993.

[5] Greame James Kennedy, "Aerostructural analysis and design optimization of composite aircraft," Department of Applied Science and Engineering, University of Toronto, Thesis for Doctor of Philosophy 2012.

[6] S.T.Peters, *Handbook of Composites*, Second Edition ed.: Chapman & Hall, 1998.

[7] ASM International Handbook Committee, *ASM Handbook*., 2001, vol. 21: Composites.

[8] [Online]. http://www.recipe101.info/tag/ (Cited: 01 02 2015)

[9] Dr. Robert Reid, *Course on composite materials in aircraft structures*., 2009.

[10] F. Lin, X. Hu and W. Sun, "Computer-aided design and modeling of composite unit cells," *Composite Science and Technology*, vol. 61, pp. 289-299, 2001.

[11] A.A. Skordos, M.P.F. Sutcliffe and C. Monroy Aceves, "Design selection methodology for composite structures," *Materials and Design*, 2007.

[12] K.L. Loewenstein, "The Manufacturing Technology of Continuous Glass Fibers," *Platinum Metals,* no. 3rd revised, 1993.

[13] F.T. Wallenberger, *Advanced Inorganic Fibers Processes, Structures, Properties, Applications.*: Kluwer Academic Publishers, 1999.

[14] P.K. Gupta, "Glass Fibers for Composite Materials," *Fibre Reinforcements for Composite Materials*, 1988.

[15] C.Soutis, "Carbon fiber reinforced plastics in aircraft construction," *Materials Science and Engineering*, 2005.

[16] J. Awerback and H.T. Hahn, "Fatigue and Proof Testing of Unidirectional Graphite/ Epoxy Composites," *Fatigue of Filamentary Composite Materials*, 1977.

[17] L.A. Feldman, "High Temperature Creep Effects in Carbon Yarns and Composites," in *Proceedings of the 17th Biennial Conference on Carbon*, 1985.

[18] Robert M. Jones, *Mechanics of Composite Materials*, 2nd ed.: Taylor and Francis, 1999.

[19] Michael G. Bader, "Selection of composite materials and manufacturing routes for cost-effective performance," *Composites: Part A,* vol. 33, May 2002.

[20] C.Soutis, "Fibre reinforced composites in aircraft construction," *Progress in Aerospace Sciences*, 2005.

[21] Sanjay K. Mazumdar, *Composites Manufacturing: Materials, Product, and Process Engineering*.: CRC PRESS, 2002.

[22] Mathis Chlosta, "Feasibility study in fiber reinforced polymer cylindrical truss bridges for heavy traffic," Department of Design and Construction, Delft University of Technology, Master's Thesis 2012.

[23] D. V. Rosato, *Reinforced Plastics Handbook*.: Elsevier, 2004.

[24] ASTM, "Standard Specification for Glass Fiber Strands," ASTM D 578-98,.

[25] AN-COR DKG. [Online]. http://www.an-cor.com/ (Cited 11 12 2014)

[26] Molded Fiber Glass Companies. [Online]. http://www.moldedfiberglass.com (Cited 11 12 2014)

[27] Katarina Uusitalo, "Designing in Carbon Fibre Composites," Department of Product and Production Development, Chalmers University of Technology, Master of Science Thesis 2013.

[28] F. Campbell, *Structural Composite Materials*.: ASM International, 2010.

[29] P. K. Mallick, *Fiber-Reinforced Composite Materials, Manufacturing and Design*, 3rd ed.: CRC Press, 2007.

[30] N. Urban, H. Cheraghi and J. Sheikh-Ahmad, "Machining Damage in Edge Trimming of CFRP," *Materials and Manufacturing Processes*, vol. 27, 2012.

[31] J. Y. Sheikh-Ahmad, *Machining of Polymer Composites*.: Springer US, 2009.

[32] D. Hartmann, C. Schutte and W. Hintze, "Occurrence and propagation of delamination during the machining of carbon fibre reinforced plastics - An experimental study," *Composite Science and Technology*, vol. 71, 2011.

[33] X. Yang and S. A. Nassar, *Composite Materials and Joining Technologies for Composites*, D. Backman, G. Cloud E. Patterson, Ed. New York: Springer, 2013.

[34] U. Vaidya, *Composites for Automotive, Truck and Mass Transit: Materials, Design, Manufacturing*. Pennsylvania: DEStech Publications Inc., 2011.

[35] E. Bateh, J. Potter and R. Cole, *Composites book*., 1982.

[36] H. Saadatmanesh M. Tavakkolizadeh, "Galvanic Corrosion of Carbon and Steel in Aggressive Environments," *Journal of Composite for Construction*, vol. 5(2), 2001.

[37] R. Tognini, J. Mayer, S. Virtanen and Y. Mueller, "Anodized titanium and stainless steel in contact with CFRP: An electrochemical approach considering galvanic corrosion," *Journal of Biomedical Materials Research Part A*, no. 82A(4).

[38] R. Hill, *The Mathematical Theory of Plasticity*. London: Oxford University Press, 1950.

[39] Stephen W. Tsai, "Strength Theories of Filamentary Structures," in *Fundamental Aspects of Fiber Reinforced Plastic Composites*, Dayton, Ohio, 1966, pp. 3-11.

[40] Francis Samalot, Selvum Pillay, Gregg M. Janowski, George Husman, Klaus Gleich and Uday K. Vaidya, "Design and Manufacture of Woven Reinforced Glass/Polypropylene Composite for Mass Transit Floor Structure," *Journal of Composite Materials*, vol. 38, no. 1949, 2004.

[41] P. S. Nair K. K. Sairajan, "Design of low mass dimensionally stable composite base structure for a spacecraft," *Composites: Part B*, vol. 42, no. 280-288, 2010.

[42] Yongzhou Lin, Zhijian Zong, Guangyong Sun, Qing Li and Qiang Liu, "Lightweight design of carbon twill weave fabric composite body structure for electric vehicle," *Composite Structures*, vol. 97, no. 231-238, 2012.

[43] Rob Boom, Brijan Irion, Derk-Jan van Heerden, Pieter Kuiper, Hans de Wit and Yongxiang Yang, "Recycling of composite materials," *Chemical Engineering and Processing: Process Intensification*, vol. 51, Sep 2011.

[44] Remy Teuscher, Veronique Michaud, Christian Ludwig, Jan-Anders E. Manson and Robert A. Witik, "Carbon fibre reinforced composite waste: An enviromental assessment of recycling, energy recovery and landfilling," *Composites: Part A,* vol. 49, Feb 2013.

[45] J. Kok, W de Jesus, S. Vogel, G. Lundie, K. van Rijswijk and J. Pieterse, "Design and manufacture of composite aircraft fairings," in *ICCBN conferenece* , Durban, 2013.

[46] M. P. F. Sutcliffe, M. F. Ashby, A. A. Skordos, C. Rodriguez Roman and C. Monroy Aceves, "Design methodology for composite structures: A small low air-speed wind turbine blade case study," *Materials and Design*, vol. 36, no. 296-305, 2011.

[47] I. J. Fourie, "The design and development of a vehicle chassis for a Formla SAE competition car," University of North-West, Masters dissertation 2014.

[48] Lockheed - California Co, *Design Handbook*., 1983.

APPENDICES

APPENDIX A: HONEYCOMB CELLS

Hexagonal

Reinforced hexagonal

Overexpanded (OX) core

Flex-Core

Double Flex-Core

Tube-Core

Cross-Core

Square
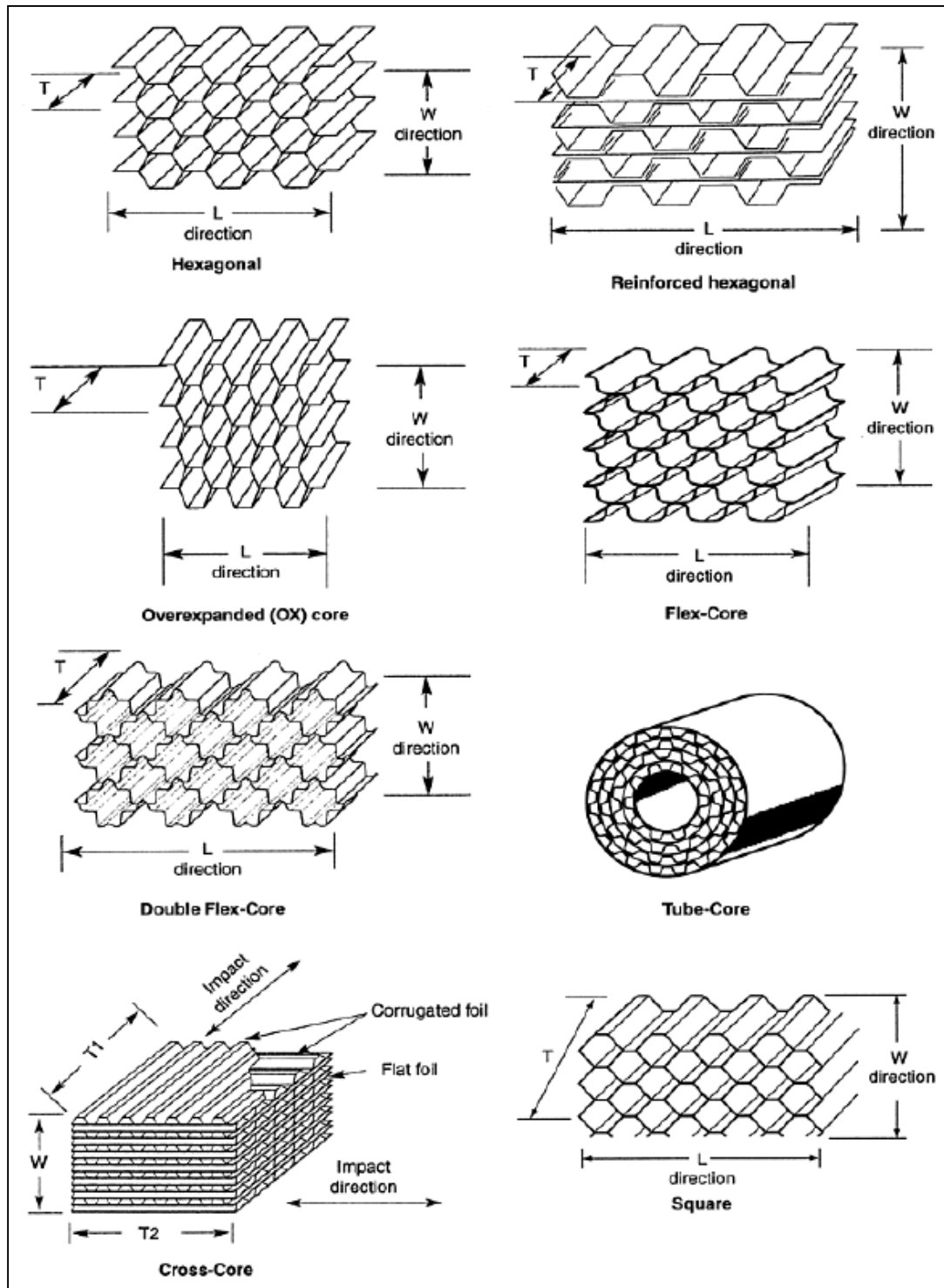
APPENDIX B: MICRO- AND MACROMECHANICS

MICROMECHANICS

The elastic properties of a **UD lamina** are calculated using data from the matrix and fibres as follows. This method is called the volume fraction method; it relates the amount of fibres and matrix present by fraction to the elastic properties.

$$E_1 = E_f V_f + E_m(1 - V_f) \qquad\qquad \text{Equation 1}$$

And

$$E_2 = \frac{E_f E_m}{V_f E_m + V_m E_f} \qquad\qquad \text{Equation 2}$$

With:

$$V_f = \frac{V_{fibers}}{V_{total}} \qquad\qquad \text{Equation 3}$$

And

E_1 =   Elastic modulus of lamina in the fibre direction

E_2 =   Elastic modulus of lamina in cross fibre direction

E_f =   Elastic modulus of fibres in longitudinal direction

E_m =   Elastic modulus of matrix

V_f =   Volume fraction of the fibres

V_{fibres} =   Volume of the fibres in the lamina

V_{total} =   Volume of total lamina

Equation 2 can be rewritten for the in-plane shear elastic properties as follows:

$$G_{12} = \frac{G_f G_m}{V_f G_m + V_m G_f}$$

Equation 4

With:

G_{12} =   In-plane shear modulus of lamina

G_f =   In-plane shear modulus of fibres

G_m =   Shear modulus of matrix

$$\nu_{12} = \nu_f V_f + \nu_m V_m$$

Equation 5

With:

ν_{12} =   Major Poisson's ratio of lamina

ν_f =   Major Poisson's ratio of fibres

ν_m =   Major Poisson's ratio of matrix

Equations 1 and 2 can be done semi empirically for **fabrics** using the rule of volume fractions. This is done as follows:

$$E_i = \eta_i E_f V_f + E_m V_m$$

Equation 6

With:

$$\eta_i = \frac{N_i}{N_j}$$

Equation 7

And:

E_i =   The Young's modulus of the lamina in the required direction *(i = 1 or 2)*

η_i =   The fraction of bias of the fabric (for balanced weave $\eta_1 = \eta_2 = 0.5$), *(i = 1 or 2)*

N_i =   The amount of filaments in each direction of the fabric *(i = 1 or 2)*

If we then assume in-plane stress, because of the "thin laminate" which means all out-of-plane stresses are zero:

- $\sigma_3 = 0$
- $\tau_{13} = \tau_{23} = 0$

With the above assumptions the stress-strain relationship becomes:

$$[\varepsilon]_{12} = [S]\,[\sigma]_{12} \qquad\qquad \textit{Equation 8}$$

$$\begin{bmatrix} \varepsilon_1 \\ \varepsilon_2 \\ \gamma_{12} \end{bmatrix} = \begin{bmatrix} \dfrac{1}{E_1} & -\dfrac{v_{12}}{E_1} & 0 \\ -\dfrac{v_{12}}{E_1} & \dfrac{1}{E_2} & 0 \\ 0 & 0 & \dfrac{1}{G_{12}} \end{bmatrix} \begin{bmatrix} \sigma_1 \\ \sigma_2 \\ \tau_{12} \end{bmatrix}$$

This can be rearranged as follows:

$$[\sigma]_{12} = [Q]\,[\varepsilon]_{12} \qquad\qquad \textit{Equation 9}$$

$$\begin{bmatrix} \sigma_1 \\ \sigma_2 \\ \tau_{12} \end{bmatrix} = \begin{bmatrix} \dfrac{E_1}{1 - v_{21}v_{12}} & \dfrac{v_{12}E_2}{1 - v_{12}v_{21}} & 0 \\ \dfrac{v_{12}E_2}{1 - v_{12}v_{21}} & \dfrac{E_2}{1 - v_{12}v_{21}} & 0 \\ 0 & 0 & G_{12} \end{bmatrix} \begin{bmatrix} \varepsilon_1 \\ \varepsilon_2 \\ \gamma_{12} \end{bmatrix}$$

With:

$[\varepsilon]$ = Strain matrix in lamina coordinate system (1, 2, 3)

$[\sigma]$ = Stress matrix in lamina coordinate system (1, 2, 3)

$[S]$ = Compliance matrix in lamina coordinate system (1, 2, 3)

$[Q]$ = Inverse compliance (reduced stiffness) matrix in lamina coordinate system (1, 2, 3)

Equation 8 and 9 are transformed into the laminate coordinate system by the following calculations and reference to the figure:
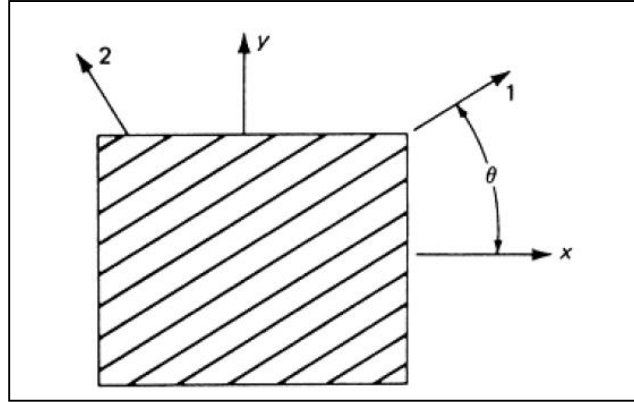
Transformation between lamina (principal) coordinate system and laminate (arbitrary) coordinate system

$$\begin{bmatrix} \sigma_1 \\ \sigma_2 \\ \tau_{12} \end{bmatrix} = [T] \begin{bmatrix} \sigma_x \\ \sigma_y \\ \tau_{xy} \end{bmatrix} \qquad \text{Equation 10}$$

$$\begin{bmatrix} \sigma_1 \\ \sigma_2 \\ \tau_{12} \end{bmatrix} = \begin{bmatrix} (\cos\theta)^2 & (\sin\theta)^2 & -2\sin\theta\cos\theta \\ (\sin\theta)^2 & (\cos\theta)^2 & 2\sin\theta\cos\theta \\ \sin\theta\cos\theta & -\sin\theta\cos\theta & (\cos\theta)^2 - (\sin\theta)^2 \end{bmatrix} \begin{bmatrix} \sigma_x \\ \sigma_y \\ \tau_{xy} \end{bmatrix}$$

With:

$[\sigma]_{12}$ =   Strain matrix in lamina (principal) coordinate system (1, 2, 3)

$[\sigma]_{xy}$ =   Stress matrix in laminate (arbitrary) coordinate system (x, y, z)

[T]   =   Transformation matrix

With the help of the transformation matrix the stress strain relationship can be written in the laminate or arbitrary coordinate system as follows:

$$[\varepsilon]_{xy} = \overline{[S]}\,[\sigma]_{xy} \qquad\qquad \textit{Equation 11}$$

And

$$[\sigma]_{xy} = \overline{[Q]}\,[\varepsilon]_{xy} \qquad\qquad \textit{Equation 12}$$

With:

$$\overline{[Q]} = [T][Q]\,[T']^{-1} \qquad\qquad \textit{Equation 13}$$

And:

$$[T'] = \begin{bmatrix} (\cos\theta)^2 & (\sin\theta)^2 & -\sin\theta\cos\theta \\ (\sin\theta)^2 & (\cos\theta)^2 & \sin\theta\cos\theta \\ 2\sin\theta\cos\theta & -2\sin\theta\cos\theta & (\cos\theta)^2 - (\sin\theta)^2 \end{bmatrix}$$

And:

$$\overline{[S]} = \overline{[Q]}^{-1} \qquad\qquad \textit{Equation 14}$$

With:

$[\varepsilon]_{xy}$ = Strain matrix in laminate (arbitrary) coordinate system (x, y, z)

$\overline{[S]}$ = Transformed compliance matrix

$\overline{[Q]}$ = Transformed Inverse compliance (reduced stiffness)

The apparent elastic properties of the laminate can be calculated as follows:

$$E_x = \frac{1}{\overline{S_{11}}}$$ *Equation 15*

$$E_y = \frac{1}{\overline{S_{22}}}$$ *Equation 16*

$$G_{xy} = \frac{1}{\overline{S_{66}}}$$ *Equation 17*

$$v_{xy} = -\frac{\overline{S_{12}}}{\overline{S_{11}}}$$ *Equation 18*

With:

E_x =   Apparent Young's modulus of laminate in X direction

E_y =   Apparent Young's modulus of laminate in Y direction

G_{xy} =   Apparent shear modulus of laminate in X direction

v_{xy} =   Apparent Poisson's ratio of laminate in X direction

Macromechanics are used to determine the laminate properties and the response of the laminate under loading conditions. This is also sometimes referred to classical laminate theory. The input required for this analysis is the lamina properties, which are determined using micromechanics. The roadmap of the composite analysis can be seen in Figure 2-23.
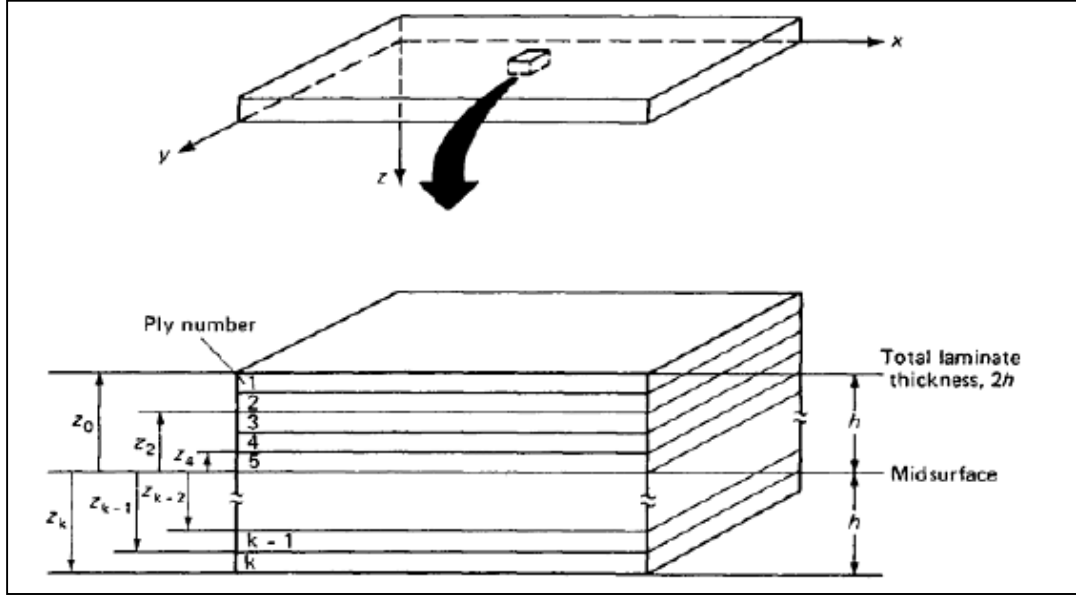
Laminate definitions for macromechanics [7]

$$\{\varepsilon_x\} = \left\{ \begin{array}{c} \dfrac{\partial u_x}{\partial x} \\ \dfrac{\partial u_y}{\partial y} \\ \dfrac{1}{2}\left(\dfrac{\partial u_x}{\partial y} + \dfrac{\partial u_y}{\partial x}\right) \end{array} \right\} = \{\varepsilon^0\} + z\{\kappa\} \qquad Equation\ 19$$

With:

$$\{\varepsilon^0\} = \left\{ \begin{array}{c} \dfrac{\partial u_x^0}{\partial x} \\ \dfrac{\partial u_y^0}{\partial y} \\ \left(\dfrac{\partial u_x^0}{\partial y} + \dfrac{\partial u_y^0}{\partial x}\right) \end{array} \right\} \qquad Equation\ 20$$

And,

$$\{\kappa\} = \begin{Bmatrix} \kappa_{xx} \\ \kappa_{yy} \\ 2\kappa_{xy} \end{Bmatrix} = \begin{Bmatrix} -\dfrac{\partial^2 u_z}{\partial x^2} \\ -\dfrac{\partial^2 u_z}{\partial y^2} \\ -2\dfrac{\partial^2 u_z}{\partial x \partial y} \end{Bmatrix}$$

Equation 21

$$(N) = \int_{-h}^{h} \{\sigma_x\} dz$$

$$(M) = \int_{-h}^{h} \{\sigma_x\} z dz$$
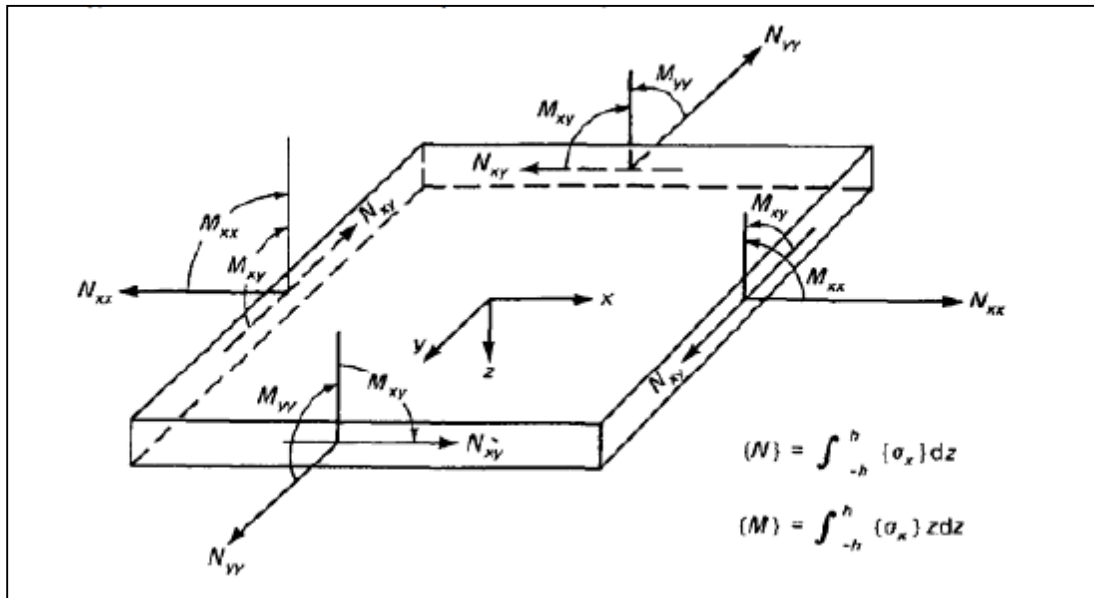
Laminate force, moment and shear definition used in macromechanics [7]

$$\begin{Bmatrix} N \\ M \end{Bmatrix} = \begin{bmatrix} A & B \\ B & D \end{bmatrix} \begin{Bmatrix} \varepsilon^0 \\ \kappa \end{Bmatrix}$$

Equation 22

With:

$$\{N\} = \begin{Bmatrix} N_{xx} \\ N_{yy} \\ N_{xy} \end{Bmatrix}$$

Equation 23

And

$$\{M\} = \begin{Bmatrix} M_{xx} \\ M_{yy} \\ M_{xy} \end{Bmatrix}$$

Equation 24

And

$$[A_{ij}] = \sum_{k=1}^{N}[\overline{Q_{iJ}}]_k (Z_k - Z_{k-1})$$ *Equation 25*

$$[B_{ij}] = \frac{1}{2}\sum_{k=1}^{N}[\overline{Q_{iJ}}]_k (Z_k^2 - Z_{k-1}^2)$$ *Equation 26*

$$[D_{ij}] = \frac{1}{3}\sum_{k=1}^{N}[\overline{Q_{iJ}}]_k (Z_k^3 - Z_{k-1}^3)$$ *Equation 27*

With the following matrix in the plain stress condition:

$$\begin{bmatrix} A & B \\ B & D \end{bmatrix} = \begin{bmatrix} A_{11} & A_{12} & A_{16} & B_{11} & B_{12} & B_{16} \\ A_{12} & A_{22} & A_{26} & B_{12} & B_{22} & B_{26} \\ A_{16} & A_{26} & A_{66} & B_{16} & B_{26} & B_{66} \\ B_{11} & B_{12} & B_{16} & D_{11} & D_{12} & D_{16} \\ B_{12} & B_{22} & B_{26} & D_{12} & D_{22} & D_{26} \\ B_{16} & B_{26} & B_{66} & D_{16} & D_{26} & D_{66} \end{bmatrix}$$ *Equation 28*

The matrix [A] is referred to as the extensional stiffness matrix. This matrix relates plane forces directly to strains in the same direction

- A_{11}, A_{22}, and A_{66} are direct stiffness terms for each x, y and z directions respectively.
- A_{12} is a Poisson's ratio type term which relates forces in one direction with strain in the direction perpendicular to the force.
- A_{16} and A_{26} are coupling terms that relate axial force with shear strains and vice versa. This implies that with an axial force shear strains will be induced.

The [B] matrix is referred to as the coupling matrix. It relates plane forces with curvatures and moments with plane strains. The different terms has the same effect as mentioned above with the plane forces and curvatures and moments with plane strains.

EPOLAM 2022

HIGH PERFORMANCE LAMINATING EPOXY RESIN
Tg 100°C

PHYSICAL PROPERTIES

	RESIN	HARDENER	MIXING
Mixing ratio by weight	100	40	
Mixing ratio by volume	100	50	
Physical appearance : liquid	Colourless	Colourless	Colourless
Brookfield viscosity at 25°C	1600 ± 200 mPa.s	40 ± 5 mPa.s	600 ± 100 mPa.s
Specific gravity at 25°C	1.17 ± 0.02	0.94 ± 0.02	1.10 ± 0.02
Pot-life (280 gr) at 25°C			1 hr 15 min. ± 5 min.

MECHANICAL AND THERMAL PROPERTIES

Final hardness *	(ISO 868)	D Shore	85 ± 2
Tg (DSC) *		°C	100
Flexural strength *	(ISO 178)	MPa	125 ± 10
Flexural modulus of elasticity *	(ISO 178)	MPa	3400 ± 200
Tensile strength *	(ISO 527)	MPa	58 ± 5
Demould time at room temperature		hr	24-36
Complete cure at room temperature		day	7

NB : The above values were obtained with an unmodified resin (no reinforcement).

The above properties, obtained using standardized specimens and in precise chemical crosslinking conditions, represent the optimum values for this system after thermal treatment and complete hardening.

EPOLAM 2022

**HIGH PERFORMANCES
LAMINATING EPOXY RESIN
Tg 100°C**

APPLICATIONS

This system is designed for the production of composite structures by impregnation hard layers, vacuum injection and low pressure injection methods as well as by filament winding.

PROPERTIES

Very low viscosity
Excellent fabric wetting
Good temperature resistance
Good mechanical properties

PROCESSING

After having prepared the mix according to the indicated ratio, carry out impregnation of the reinforcement materials (glass, aramid, carbon) using the different methods mentioned above. To obtain maximum heat resistance and mechanical properties, postcuring is necessary : after 24 hours at 20°C, stove for 4 hours at 50°C, 2 hr at 80°C then 2 hours at 100°C, with a temperature gradient of 20°C per hour between the above plateau values.

PRECAUTIONS

Normal health and safety precautions should be observed when handling these products :
. ensure good ventilation
. wear gloves and safety glasses
For further information, please consult the product safety data sheet.

STORAGE

Shelf life is 1 year in a dry place and in original unopened containers at a temperature between 15 and 25°C.

PACKAGING

RESIN

1 x   5.000 kg
1 x 20.000 kg

HARDENER

1 x   2.000 kg
1 x   8.000 kg

GUARANTEE

suter-kunststoffe ag
swiss-composite.ch
CH-3312 Fraubrunnen 031 763 60 60 Fax 031 763 60 61
www.swiss-composite.ch   info@swiss-composite.ch

interglas

GLASS FILAMENT FABRICS for PLASTICS REINFORCEMENT
PRODUCT SPECIFICATION

		Specification
Style Number	92125	MIL-Y-1140H
US Style		MIL-C-9084
WLB No.	8.4551.60	DIN 65066
British Standard		BS 3396

Finish/Designation	FK144

	Unit		Tolerance	Specification
Weave pattern		2 x 2 twill		DIN ISO 9354
Area weight	g / m²	280,0	± 5%	DIN EN 12127
Yarn	tex			DIN EN 12654
warp yarn		EC9-68x3 t0		
weft yarn		EC9-204		
Fibre count	1 / cm			DIN EN 1049
warp ends		7,0	± 5%	
weft picks		6,5	± 5%	
Temperature resistance 1)				
Continuous load	°C	260		
Short time resistance	°C	600		
Moisture content	%	< 0,2	± 1%	DIN EN 3616
Finish content	%	0,08 - 0,26	± 5%	DIN ISO 1887
				DIN EN 60
Thickness (approx. dry)	mm	0,35	± 5%	DIN ISO 4603/E
In laminate (43% Vol.)	mm	0,25	± 5%	

TS / 19.08.2010   Page 1 of 2

GLASS FILAMENT FABRICS for PLASTICS REINFORCEMENT
PRODUCT SPECIFICATION

	Unit	Standard	CS-ITG	Tolerance	Specification
Style Number		92125		/ FK144	
Tensile strength					DIN EN 2747
warp	MPa	335	430	± 10%	
weft	MPa	320		± 10%	
Young's-Modulus					
warp	GPa	19		± 10%	
weft	GPa	18		± 10%	
Compression strength					DIN 53454
warp	MPa	355		± 10%	DIN 65380
weft	MPa	340		± 10%	DIN prEN 2580
Compression-Modulus					
warp	GPa			± 10%	
weft	GPa			± 10%	
Interlaminar shear strength					DIN EN 2377
warp	MPa	50		± 10%	
weft	MPa	45		± 10%	
Flexural strength					DIN EN 2746
warp	MPa	495		± 10%	
weft	MPa	460		± 10%	
Flexural-Modulus					
warp	GPa	24		± 10%	
weft	GPa	24		± 10%	

Remarks

1) Temperature resistance for dry fabrics

APPENDIX E: AIREX C71.75 DATA SHEET

DATA SHEET
07.2011 (replaces 08.2010)

AIREX® BALTEK

AIREX® C71
Elevated Temperature Structural Foam

CHARACTERISTIC

- Outstanding strength and stiffness to weight ratio
- High temperature resistance
- Good impact strength
- High fatigue resistance
- Low resin absorption (fine cell structure)
- Good fire performance (self-extinguishing)
- High sound and thermal insulation
- Good styrene resistance

APPLICATION

- **Wind energy**
  Rotor blades, nacelles, turbine generator housings
- **Road and Rail**
  Roof panels, interiors, floors, doors, partition walls, side skirts, front-ends
- **Marine**
  Hulls, decks, bulkheads, superstructures, engine hatches
- **Aircraft**
  Interiors, radomes, galley carts, general aviation (sport aircraft) fuselage
- **Recreation**
  Skis, snowboards, surfboards, wakeboards, canoes, kayaks
- **Industrial**
  Tooling, tanks, ductwork, containers, covers

PROCESSING

- Contact molding (hand/spray)
- Resin injection (RTM)
- Adhesive bonding
- Pre-preg processing (up to 140 ℃, 285 ℉)
- Vacuum infusion
- Thermoforming

AIREX® C71 is a closed cell, cross-linked polymer foam especially formulated to maintain its stability also at higher processing or service temperatures.

It combines excellent stiffness and strength to weight ratios with superior toughness. It is non-friable, contains no CFC's, has negligible water absorption, and provides an excellent resistance to chemicals. The fine cell structure offers an excellent bonding surface.

Compatible with most resins and manufacturing processes AIREX® C71 is ideally suited as a core material for a wide variety of sandwich structures subjected to both static and dynamic loads, and exposed to elevated temperatures. Thanks to its unique lightness (properties vs. density) C71 is the material of choice for applications where lightweight is a priority.

www.corematerials.3AComposites.com – excellence in core solutions

3A COMPOSITES

Europe / Middle East / Africa:
Airex AG
Industrie Nord 26
5643 Sins, Switzerland
Tel +41 41 789 66 00
Fax +41 41 789 66 60
corematerials@3AComposites.com

North America / South America:
Baltek Inc.
P.O. Box 16148, High Point, NC 27261
Office/Plant: 5240 National Center Drive
Colfax, North Carolina 27235, USA
Tel +1 336 398 1900 / Fax +1 336 398 1901
corematerials.americas@3AComposites.com

Asia / Australia / New Zealand:
3A Composites (China) Ltd.
Shangfeng Road, 933, Building 6, Pudong
201201 Shanghai, China
Tel +86 21 585 86 006
Fax +86 21 338 27 298
corematerials.asia@3AComposites.com

AIREX® BALTEK®

Typical properties for AIREX® C71		Unit (metrical)	Value [1]	C71.55	C71.75
Density	ISO 845	kg/m³	Average *Typ. Range*	60 *54 - 69*	80 *72 - 92*
Compressive strength perpendicular to the plane	ISO 844	N/mm²	Average *Minimum*	0.95 *0.85*	1.5 *1.3*
Compressive modulus perpendicular to the plane	DIN 53421	N/mm²	Average *Minimum*	70 *60*	102 *85*
Tensile strength in the plane	ISO 527 1-2	N/mm²	Average *Minimum*	1.5 *1.0*	2.2 *1.4*
Tensile modulus in the plane	ISO 527 1-2	N/mm²	Average *Minimum*	42 *30*	60 *40*
Shear strength	ISO 1922	N/mm²	Average *Minimum*	0.93 *0.70*	1.35 *1.10*
Shear modulus	ASTM C393	N/mm²	Average *Minimum*	21.5 *18*	30 *25*
Shear elongation at break	ISO 1922	%	Average *Minimum*	25 *15*	32 *20*
Thermal conductivity at room temperature	ISO 8301	W/m.K	Average	0.031	0.036
Standard sheet	Width	mm ± 5		1120	1005
	Length	mm ± 5		2400	2150
	Thickness	mm ± 0.5		5 to 70	3 to 70
Color				light red	light yellow

Finishing Options, other dimensions and closer tolerances upon request

[1] Minimum values acc. DNV definition; test sample thickness 20 mm except tensile properties (10 mm) and compressive modulus (40 mm)

The data provided gives approximate values for the nominal density and DNV minimum values according to DNV type approval certificate. The information contained herein is believed to be correct and to correspond to the latest state of scientific and technical knowledge. However, no warranty is made, either expressed or implied, regarding its accuracy or the results to be obtained from the use of such information. No statement is intended or should be construed as a recommendation to infringe any existing patent.

AIREX C70 / C71

The information contained herein is to the best of our knowledge, believed to be correct and to correspond to the latest state of scientific and technical knowledge and experience. However, no warranty is made, either expressed or implied, regarding its accuracy or the results to be obtained from the use of such information.

Compressive strength at room temperature = 1

Legend:
- T92.130
- C70.075
- C71.075

X-axis: Temperature [°C]

Y-axis: relative compressive strength [-]

VENTRAL FIN SKIN ASSY

MATERIAL:
-INTERGLASS GLASS FIBER 92125
-SURFACE TISSUE
-EPOLAM 2022
-AIREX C71.75 (5mm)

BONDING:
-ALL BONDING DONE WITH RESIN
AND COTTON FLOCK

NOTES:
-ONLY RH FIN ASSY HAS CUT OUT
IN LH SKIN AND FORE RIB

ASSEMBLY:
1) SKINS
2) RIBS + CAP SPAR
3) BOND RIBS TO ONE SKIN
4) CLOSE SKINS

PART No.	NAME	EXP WEIGHT
1	RH SKIN	1960 g
2	FORE RIB	210 g
3	AFT RIB	120 g
4	SPAR	130 g
-	**TOTAL**	**4380 g**

Isometric view
Scale: 1:4

VENTRAL FIN SKIN (ALL SKINS EXCEPT RH FIN LH SKIN)

[0/90;±45;0/90;±45;±45;0/90;±45;0/90]

0°

90°

PLY DROP 1

PLY DROP 2

PLY DROP 2

PLY DROP 2

[0/90;±45]s

45° x 40mm

[0/90;±45;5mm CORE;±45;0/90]

A

B

C

D

E

F

G

Isometric view
Scale: 1:4

RH VENTRAL FIN LH SKIN

Isometric view
Scale: 1:4

VENTRAL FIN RIBS

SEC A-A:

[0/90;±45]3

[0/90;±45;5mm CORE;±45;±45;0/90]

CORE ENDS

0°

A

A

[0/90;±45;±45]s

0°
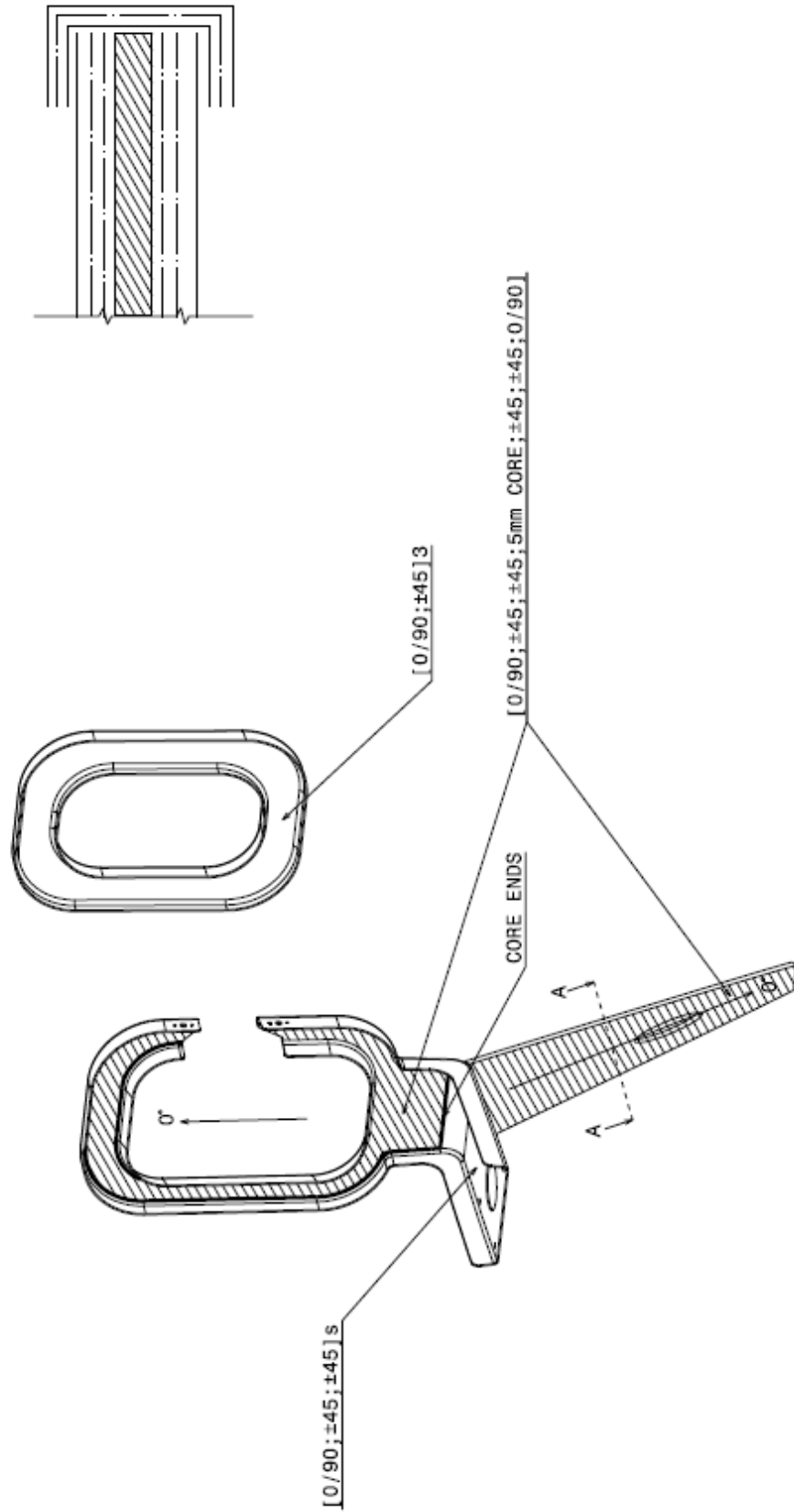
Isometric view
Scale: 1:4

PLY DROP 1

1) GF 0/90°
2) GF ±45°
3) GF 0/90°
4) GF ±45°
5) GF ±45°
6) GF ±45°
7) GF 0/90°
8) GF ±45°
9) GF 0/90°
10) GF SURFACE TISSUE

A

55

B

C 5

TOOL SIDE

PLY DROP 2

1) GF 0/90°
2) GF ±45°
3) GF 0/90°
4) GF ±45°
5) GF ±45°
6) GF ±45°
7) GF 0/90°
8) GF ±45°
9) GF 0/90°
10) GF SURFACE TISSUE

A, D

B, E

C, F

TOOL SIDE

TRAILING EDGE JOINT

MAX 30

TOOL SIDE

TOOL SIDE

COTTON FLOCK + RESIN

±45° GF 163 g/m²
0/90° GF 280 g/m²
±45° GF 280 g/m²

10 PLY JOIN DETAIL

5 PLY JOIN DETAIL

50

50

TOOL SIDE

TOOL SIDE
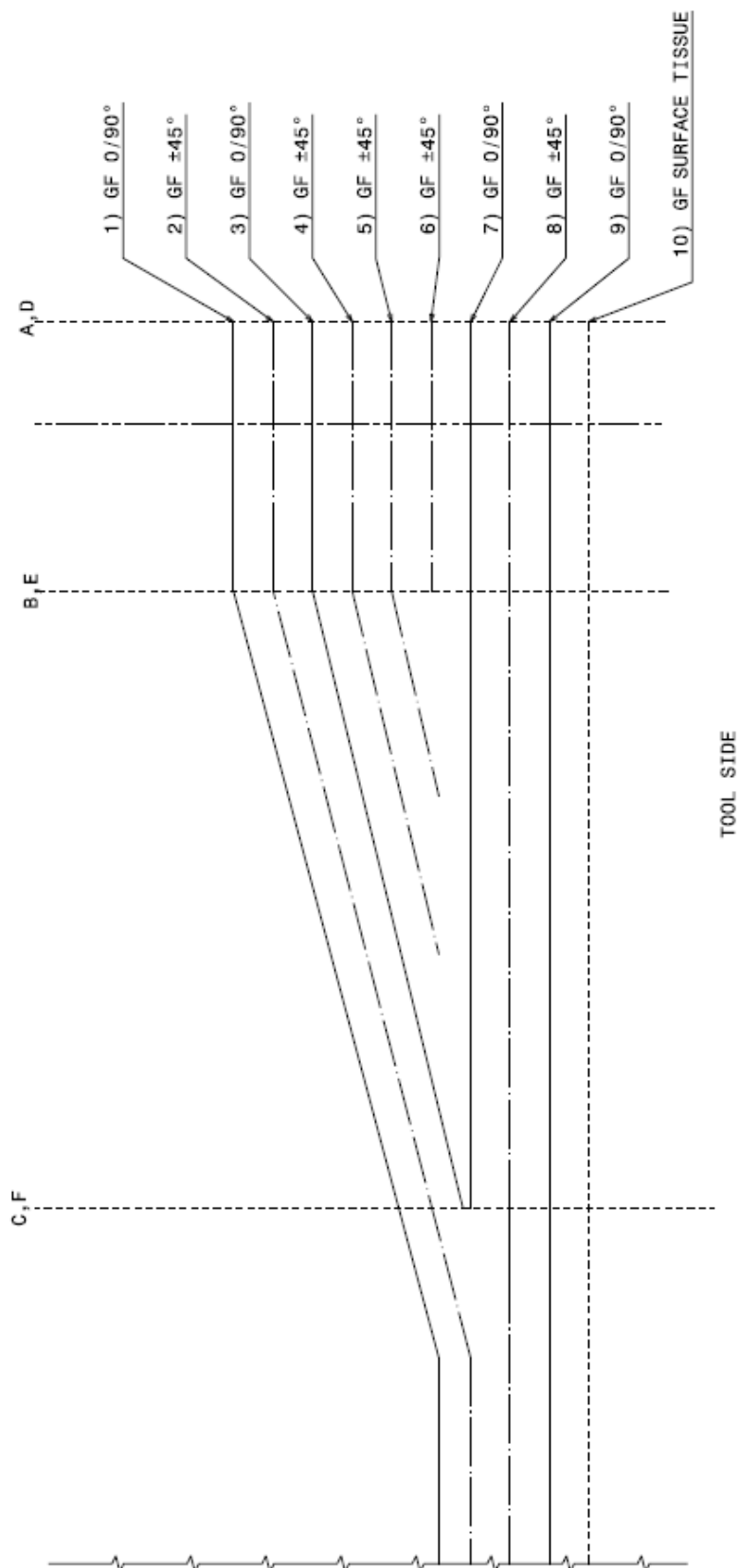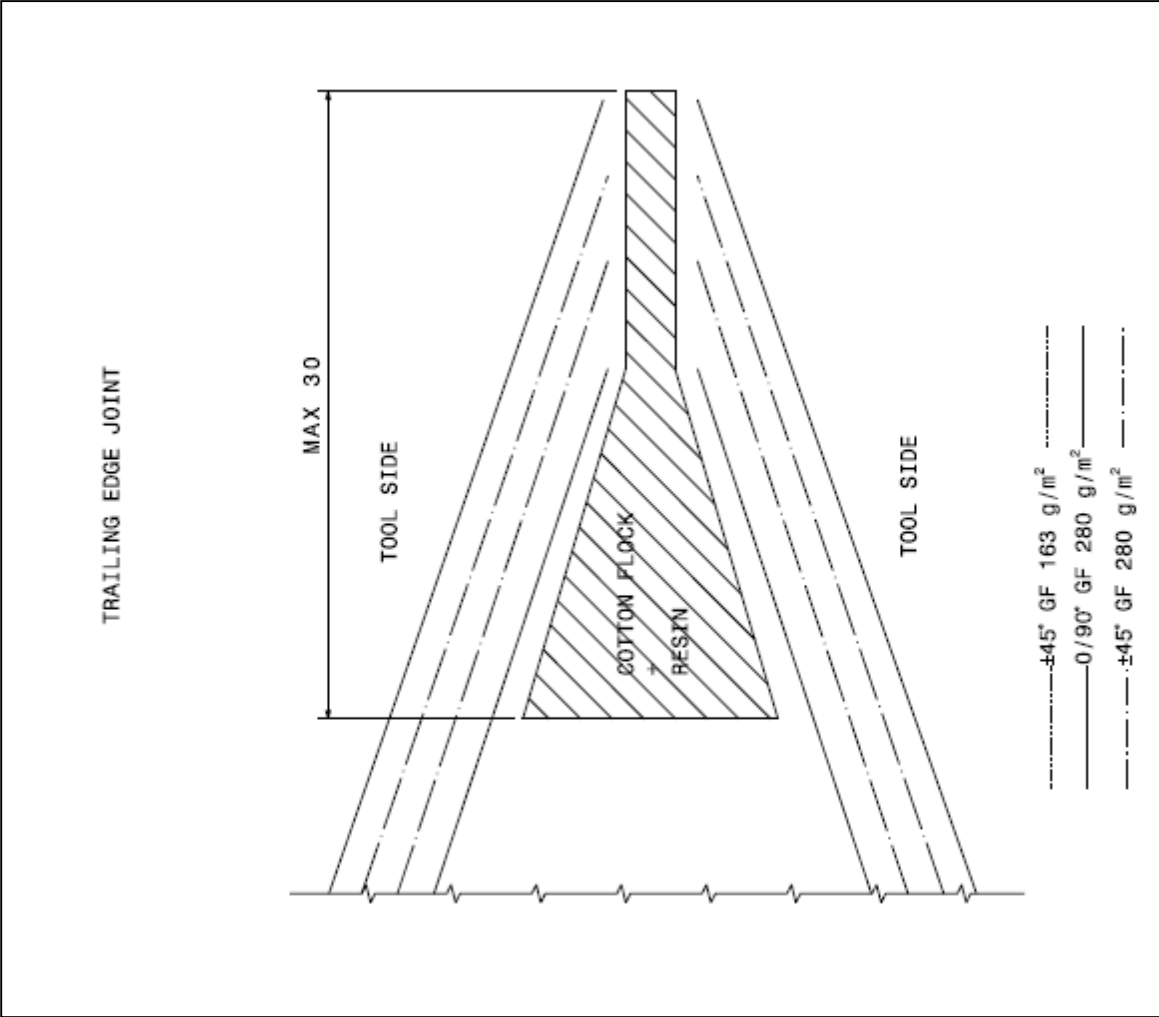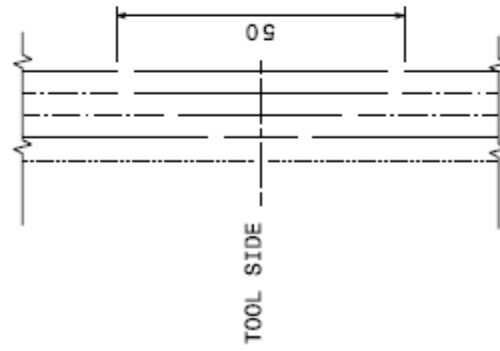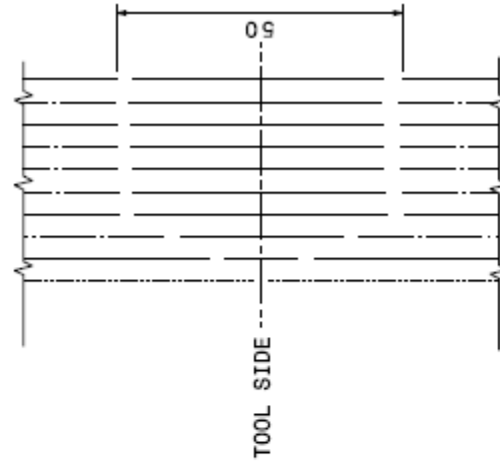
±45° GF 163 g/m²

0/90° GF 280 g/m²

±45° GF 280 g/m²

A - 25
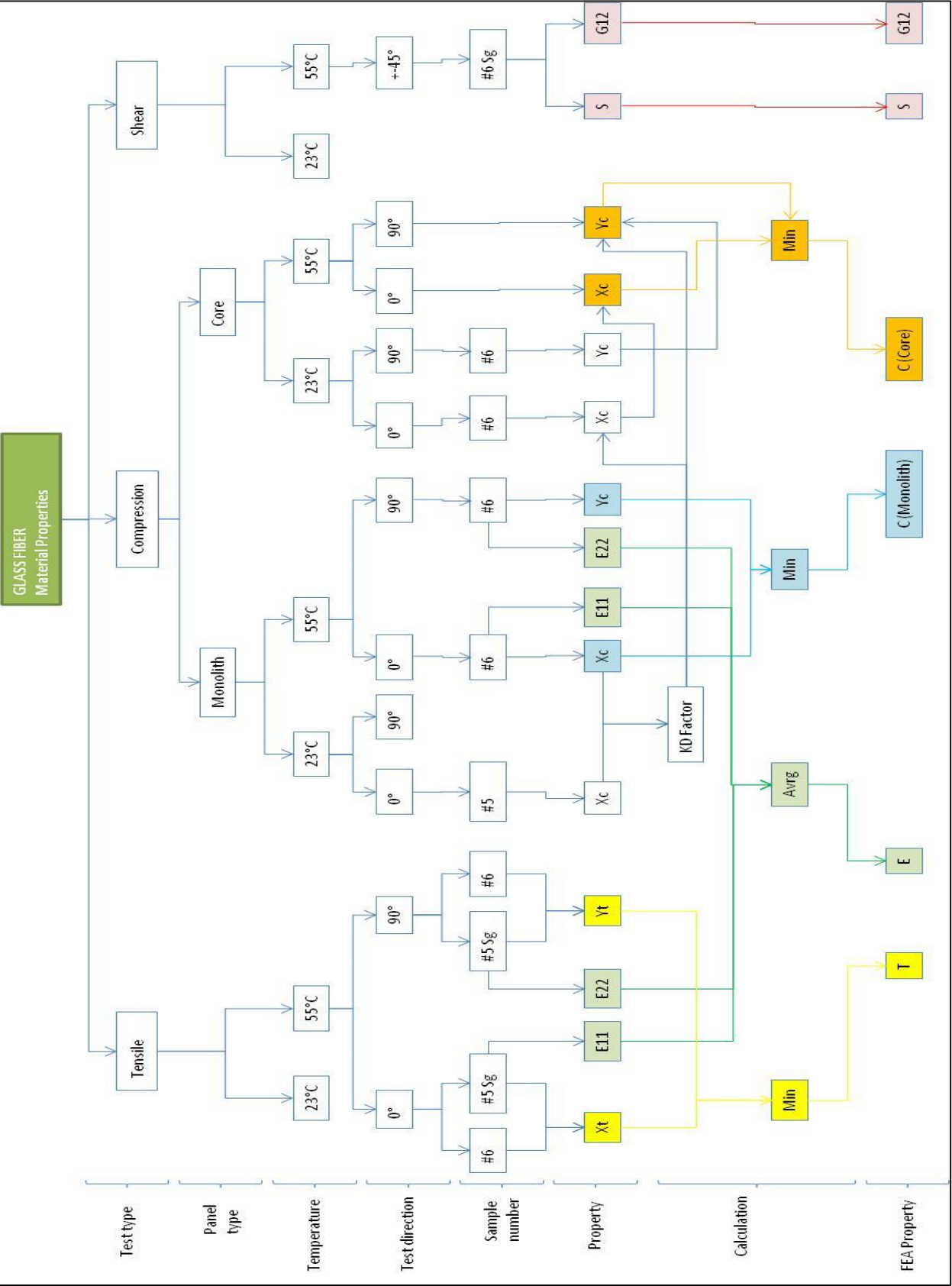
APPENDIX H: TEST DATA AND RESULTS

All allowable values were calculated via the following formula for B-basis value for a normal distribution:

$$B = \bar{x} - k_B(S.D)$$

Where,

B	=	the B-basis value allowable
$\bar{x}$	=	Average tests value
k_b	=	the tolerance limit factor for b values
S.D	=	the standard deviation

K$_B$ values can be found in the table below:

TABLE 8.5.10 *One-sided B-basis tolerance limit factors, k_B, for the normal distribution, continued on next page.*

N = 2 - 137

n	k$_B$	n	k$_B$	n	k$_B$	n	k$_B$
2	20.581	36	1.725	70	1.582	104	1.522
3	6.157	37	1.718	71	1.579	105	1.521
4	4.163	38	1.711	72	1.577	106	1.519
5	3.408	39	1.704	73	1.575	107	1.518
6	3.007	40	1.698	74	1.572	108	1.517
7	2.756	41	1.692	75	1.570	109	1.516
8	2.583	42	1.686	76	1.568	110	1.515
9	2.454	43	1.680	77	1.566	111	1.513
10	2.355	44	1.675	78	1.564	112	1.512
11	2.276	45	1.669	79	1.562	113	1.511
12	2.211	46	1.664	80	1.560	114	1.510
13	2.156	47	1.660	81	1.558	115	1.509
14	2.109	48	1.655	82	1.556	116	1.508
15	2.069	49	1.650	83	1.554	117	1.507
16	2.034	50	1.646	84	1.552	118	1.506
17	2.002	51	1.642	85	1.551	119	1.505
18	1.974	52	1.638	86	1.549	120	1.504
19	1.949	53	1.634	87	1.547	121	1.503
20	1.927	54	1.630	88	1.545	122	1.502
21	1.906	55	1.626	89	1.544	123	1.501
22	1.887	56	1.623	90	1.542	124	1.500
23	1.870	57	1.619	91	1.540	125	1.499
24	1.854	58	1.616	92	1.539	126	1.498
25	1.839	59	1.613	93	1.537	127	1.497
26	1.825	60	1.609	94	1.536	128	1.496
27	1.812	61	1.606	95	1.534	129	1.495
28	1.800	62	1.603	96	1.533	130	1.494
29	1.789	63	1.600	97	1.531	131	1.493
30	1.778	64	1.597	98	1.530	132	1.492
31	1.768	65	1.595	99	1.529	133	1.492
32	1.758	66	1.592	100	1.527	134	1.491
33	1.749	67	1.589	101	1.526	135	1.490
34	1.741	68	1.587	102	1.525	136	1.489
35	1.733	69	1.584	103	1.523	137	1.488

EQUIPMENT USED IN MATERIAL TESTING:

1. Instron 4505 tensile testing machine
    a. 50 kN load cells
    b. Climate chamber
    c. Tensile grips, 3 point bending fixture and compression fixtures
2. Strain gauges
    a. 350 Ω
    b. X – Y measuring directions
    c. Part Number: 1-XY36-6/350
3. Data logger with Wheatstone bridge

Instron 4505 tensile testing machine with climate chamber

TENSILE STRENGTH:

The tensile design strength value was obtained from tensile tests that were performed in accordance with the ASTM D3039 standard.

Temperature (°C)	Allowable tensile strength (σ, MPa) ("B" value)	
	Tension in 0° (Xt)	Tension in 90° (Yt)
55	247	290

22 Samples (8 Ply, t = 2 mm) were tested at 55°C in 0° and 90° directions, 10 with and 12 without strain gauges. These results show that the two principal material directions differ by only 14.7 % in tensile strength. Thus the assumption of two-dimensional orthotropic material is close and the weft direction is dominant. Taking the minimum of these two results, the tensile allowable that is to be used in FEA is:

$$\underline{X_t = Y_t = T = 247.57\ MPa}$$

Direction	0		Direction	90	
Temp	55		Temp	55	
Sample	Test#	Max Stress (MPa)	Sample	Test#	Max Stress (MPa)
1	TB0055	314.8	1	TB9055	290.522
2	TB0055	433.96	2	TB9055	393.122
3	TB0055	423.865	3	TB9055	404.124
4	TB0055	399.467	4	TB9055	384.163
5	TB0055	452.703	5	TB9055	339.349
6	TB0055	426.659	6	TB9055	422.405
7	TSG0055	335.135	7	TSG9055	351.315
8	TSG0055	344.098	8	TSG9055	373.991
9	TSG0055	307.945	9	TSG9055	377.901
10	TSG0055	320.451	10	TSG9055	372.246
11	TSG0055	337.95	11	TSG9055	364.913
	Avg	372.46		Avg	370.37
	SD	54.87		SD	35.16
	Kb	2.276		Kb	2.276
ALLOW	Xt	247.57	ALLOW	Yt	290.35

Maximum tensile stress tests of individual laminate samples

COMPRESSIVE STRENGTH:

Compressive testing was performed via two methods, namely: Compressive coupon testing to determine ultimate values for monolith panels and long beam bend tests for cored panels. Compressive coupon does not take skin crippling into consideration.

The compression coupon tests were done at 23°C and 55°C to determine a drop down factor in allowable. This was done because the long beam bend test could not be tested at 55°C, and the allowable was reduced by using the compressive coupon testing knock down value between 23°C and 55°C.

COMPRESSIVE MONOLITH STRENGTH:

A compressive design strength value was obtained from compressive tests that were performed in accordance with the ASTM D695 standard.

At Temperature (°C)	Allowable compressive strength via coupon testing (σ, MPa)	
	Compression in 0° (Xc)	Compression in 90° (Yc)
23	183	257*
55	160	225

Note: Value estimated by applying calculated knock down factor between Xc at 55°C and 23°C. Not a tested value.

12 Samples (8 Ply, t = 2 mm) were tested at 55°C in 0° and 90° directions. Four samples were ignored due to low ultimate strength values caused by incorrect failure mode, but the values were still higher that the final allowable.
Failure modes in the majority of the tests were due to split ends on the samples where there was tool contact, thus proving that the material can withstand higher compressive stresses when under pure compression.
The compressive strength differs by 28.8 % in the principal directions which is almost double that of the tensile difference. The weft is still the dominant direction. Taking the minimum of these two results, the compression stress allowable that is to be used for monolith panels in FEA is:

$$\underline{\textbf{\textit{X}}_c = \textbf{\textit{Y}}_c = \textbf{\textit{C}}^{mono} = 160.79 \textbf{\textit{MPa}}}$$

Coupon test			Coupon test			Coupon test		
Direction	0		Direction	90		Direction	0	
Temp	55		Temp	55		Temp	23	
Sample	Test#	Max Stress (MPa)	Sample	Test#	Max Stress (MPa)	Sample	Test#	Max Stress (MPa)
1	C0055	197.013	1	C9055	319.783	1	C0023	315.9
2	C0055	263.313	2	C9055	326.242	2	C0023	256.3
3	C0055	293.439	3	C9055	295.917	3	C0023	266.1
4	C0055	248.514	4	C9055	285.178	4	C0023	306.7
5	C0055	202.631	5	C9055	233.364	5	C0023	333.3
6	C0055	311.256	6	C9055	207.531			
	Avg	279.13		Avg	306.78		Avg	295.66
	SD	28.43		SD	19.43		SD	33.06
	Kb	4.163		Kb	4.163		Kb	3.408
ALLOW	Xc	160.79	ALLOW	Yc	225.90	ALLOW	Yc	183.00

Maximum compressive stress tests of individual monolith laminate samples

COMPRESSIVE CORE STRENGTH:

A second compressive design strength value was obtained from long beam bend tests, which were performed in accordance with the ASTM D393 standard.

At Temperature (°C)	Allowable compressive strength via long beam bend test (σ, MPa) ("B" value)	
	Compression in 0° (Xc)	compression in 90° (Yc)
23	161.60	158.12
55	141.98*	138.93*

value estimations were applied by using the knock down factor calculated from the Xc 23°C and 55°C compressive coupon results. Values not tested

12 Samples were tested at 23°C, with quarter span load introduction, in 0° and 90° directions. Tests consisted out of 8 mm thick Airex C71 closed cell foam with two layers of glass/epoxy resin on both sides. These results were used in combination with the knock down factor determined from the compression coupon tests between 23°C and 55°C to determine the allowable.

Failure occurred where the loads were introduced. Contact point radius on the jig is 12.7 mm. Using the minimum of these two results, the compression stress allowable that is to be used for cored panels in FEA is:

$$\underline{X_C = Y_C = C^{core} = 138.93 \ MPa}$$

Long beam bend			Long beam bend		
Direction	0		Direction	90	
Temp	23		Temp	23	
Sample	Test#	Max Stress (MPa)	Sample	Test#	Max Stress (MPa)
1	LBBT2300	170.837	1	LBBT2390	169.571
2	LBBT2300	180.787	2	LBBT2390	164.496
3	LBBT2300	175.297	3	LBBT2390	175.960
4	LBBT2300	172.357	4	LBBT2390	174.867
5	LBBT2300	170.989	5	LBBT2390	170.339
6	LBBT2300	170.778	6	LBBT2390	169.037
	Avg	173.508		Avg	170.712
	SD	3.961		SD	4.188
	Kb	3.007		Kb	3.007
ALLOW	Xc	161.60	ALLOW	Yc	158.12

Maximum compressive stress tests of individual sandwich panel samples
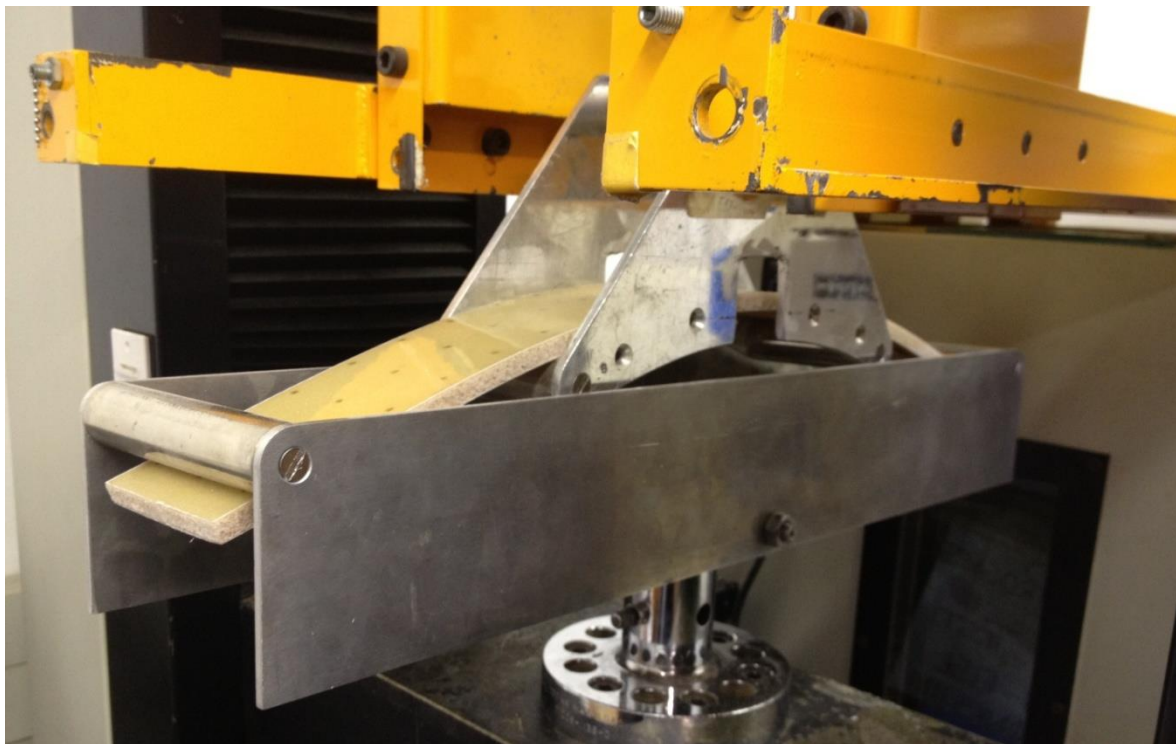
Long beam bend test in progress

IN-PLANE SHEAR STRENGTH:

The shear design strength value was obtained from in-plane shear tests in accordance with the ASTM D3518 and ASTM D3039 standards.

Temperature (°C)	Allowable Shear strength (τ, MPa) (@ 5 % ϵ_{xy}) ("B" value)
55	33.93

6 Samples (8 Ply, t = 2 mm) were tested at 55°C in a 45° direction. Strain gauges were used to determine ϵ_x and ϵ_y. The max shear stress was determined at 5 % shear strain, which yields a very conservative value. The shear stress allowable that is to be used for cored panels in FEA is:

S = 33.93 MPa

Dir		45
Temp		55
		@ 5% shear strain
Sample	Test#	txy (MPa)
1	ISP0055	37.816
2	ISP0055	38.769
3	ISP0055	39.368
4	ISP0055	36.779
5	ISP0055	35.908
6	ISP0055	38.558
	Avg	37.87
	SD	1.31
	Kb	3.007
	S	33.93

Maximum shear stress tests of individual laminate samples

MODULUS:

The modulus values were obtained from combining strain gauge data, with the tensile tester load cell data.

In the tensile modulus testing there is a 111% increase in standard deviation between 90° and 0° directions respectively. The 2nd sample of the 0° tensile testing has the lowest E value of 15861 MPa, this is test sample could have had a slightly loose or misaligned strain gauge. If this sample is ignored the difference in standard deviation would be 20%. The tensile modulus testing standard deviation is heavy dependant on the quality of the strain gauge bonding their angular accuracy.

Temperature (°C)	Modulus (MPa)		Poisson's ratio (ν)
	Young's modulus (E)	Shear modulus (G) (≤0.26 % ϵ_{xy})	
55	17837.7	3060.83	0.108

TENSILE				TENSILE			
Dir	0			Dir	90		
Temp	55			Temp	55		
Sample	Test#	Ext (MPa)	v	Sample	Test#	Eyt (MPa)	v
1	TSG0055	17704	0.132	1	TSG9055	16114	0.07716
2	TSG0055	15861	0.143	2	TSG9055	16069	0.113
3	TSG0055	17944	0.129	3	TSG9055	16060	0.07142
4	TSG0055	18242	0.118	4	TSG9055	16814	0.09446
5	TSG0055	16965	0.1	5	TSG9055	16980	0.10639
	Avg	17343.20	0.12		Avg	16407.40	0.09
	SD	953.80	0.02		SD	451.24	0.02

Tensile modulus of individual laminate samples

In the compression modulus testing there is a 560% increase in standard deviation between 90° and 0° directions respectively. The 1st and 6th sample of the 0° compression testing has the lowest E values of 17891 MPa and 14114 MPa respectively, these test samples could have had an imperfection or the compression edge could have had a geometrical deviation that would have resulted in an unwanted load introduction. If these samples are ignored the difference in standard deviation would be 31%. The compression modulus testing standard deviation is heavy dependant on the quality of the sample edge quality.

COMPRESSION		
Dir	0	
Temp	55	
Sample	Test#	Exc (MPa)
1	C0055	17891
2	C0055	19209
3	C0055	19243
4	C0055	18891
5	C0055	19462
6	C0055	14114
	Avg	18135.00
	SD	2046.54

COMPRESSION		
Dir	90	
Temp	55	
Sample	Test#	Exc (MPa)
1	C9055	19501
2	C9055	19743
3	C9055	19557
4	C9055	19667
5	C9055	18871
6	C9055	19452
	Avg	19465.17
	SD	310.11

Table 23: Compressive modulus of individual laminate samples

The determining of the shear modulus is a difficult value to plot due to the small linear region of the stress strain curve. The shear modulus was calculated at ±0.2 % ϵ_{xy} and less. The shear modulus will not be valid when exceeding this value. The average Young's modulus was determined by incorporating all tensile and compression values into the calculations, and is applicable up to max load.

SHEAR		
Dir	45	
Temp	55	
Sample	Test#	G(MPa)
1	ISP0055	3001
2	ISP0055	3096
3	ISP0055	3136
4	ISP0055	2968
5	ISP0055	3062
6	ISP0055	3102
	Avg	3060.83
	SD	64.47

Shear modulus of individual laminate samples
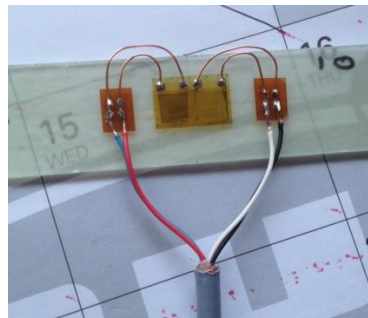
Strain gauge mounted on a typical test sample

FASTENER PULL THROUGH:

The strength value was obtained from fastener pull through tests that were performed in accordance with the ASTM D7332 standard.

All pull through test samples consisted out off a 0°/90°, 45° quasi isotropic lay-up.

Tests were performed at 23°C and 55°C. The allowable was calculated at 55°C via testing of 13 samples.

Fastener configuration			Ply qty	Temperature (°C)	Edge Distance (xD)	Allowable load @ Initial failure (kN)
Screw	Washer	Anchor nuts				
NAS1153E4	NAS1169 C10L	MS21059-L3	10	55	2.0xD	1.82
NAS1153E4	NAS1169 C10L	MS21059-L3	9	55	2.0xD	1.63*

Note: Value estimated by using 10 ply test results and interpolating to 9 ply. Not a tested value.

Bolt tension	
PTSC551020	
55degC	
2.0D	
10 ply	0/90 ; 45
Sample	initial failure (kN)
1	2.103
2	2.127
3	1.983
4	2.054
5	2.029
6	1.936
7	1.965
8	1.924
Mean	2.015
STD Dev	0.076
Kb	2.583
Allowable	1.820

a) Fastener pull through test results of individual samples. b) Typical fastener pull through sample

FASTENER SHEAR OUT:

The strength value was obtained from fastener shear resistance tests that were performed in accordance with the ASTM D7248 standard.

All fastener shear out test samples consisted of a 0°/90°, 45° quasi isotropic lay-up.

Fastener configuration			Ply qty	Temperature (°C)	Edge Distance (xD)	Allowable load (kN)
Screw	Washer	Anchor nuts				
NAS1153E4	NAS1169 C10L	MS21059-L3	8	55	2.0xD	3.61
NAS1153E4	NAS1169 C10L	MS21059-L3	9	55	2.0xD	4.34*

Note: Value estimated by using 8 ply test results and interpolating to 9 ply. Not a tested value.

Tests were performed at 23°C and 55°C. The allowables were calculated at 55°C via testing of 26 samples.

Bolt Shear	
SRSC550820_H	
	55degC
	2.0D
8 ply	0/90 ; 45
Sample	Max Load (kN)
1	3.868
2	4.054
3	4.006
4	4.335
5	4.126
6	4.064
Mean	4.076
STD Dev	0.154
Kb	3.007
Allowable	3.613

a) Fastener shear out test results of individual samples. b) Typical fastener shear out sample